2021

MicroRNA in the Mammalian Growth Plate: Matrix Vesicles and 1α,25-Dihydroxyvitamin D3

Niels C. Asmussen
Virginia Commonwealth University

MicroRNA in the Mammalian Growth Plate: Matrix Vesicles and 1α,25-Dihydroxyvitamin D3

A dissertation submitted in partial fulfillment of the requirements for the degree of Doctor of Philosophy in Integrative Life Science at Virginia Commonwealth University.

Niels C. Asmussen

MicroRNA in the Mammalian Growth Plate: Matrix Vesicles and 1α,25-Dihydroxyvitamin D3

Approved by:

Dr. Barbara D. Boyan, Advisor
Department of Biomedical Engineering
Virginia Commonwealth University

Dr. Zvi Schwartz
Department of Biomedical Engineering
Virginia Commonwealth University

Dr. Henry J. Donahue
Department of Biomedical Engineering
Virginia Commonwealth University

Dr. Tarynn Witten
Department of Computer Science
Virginia Commonwealth University

Dr. Preetam Ghosh
Department of Computer Science
Virginia Commonwealth University

Date Approved: May 12, 2022

Table of Contents

Acknowledgements

I would like to thank Dr. Boyan and Dr. Schwartz for the opportunity to join this lab, the willingness to train me in molecular biology, and the patience to help me improve my presentations. I am grateful for the opportunity to work in a lab where I have been encouraged to move back and forth between computational and bench work and thank you for not only providing the space to do that but also challenging me throughout.

I would like to thank Dr. Cohen for his guidance, availability to help out regardless of the time, and for letting me assist with surgeries. I have learned an immense amount during my time here and couldn't have done it without your help. I don't know how this lab would function without you.

I would like to thank my committee members, Dr. Donahue, Dr. Ghosh, and Dr. Witten for their advice and thoughtful questions over the course of this work.

I would like to thank Kayla for taking the time to work through problems with me and teach me how to put a presentation together. You helped make the lab a welcoming and enjoyable place to be and I enjoyed our many problem solving conversations. Johnny and Smita for keeping the cells alive and the lab functioning. To Red, Anne, and everyone else in lab, you all made for a great working environment and an even better time at all the conferences over the years.

I would like to thank my parents – Hannelore & Paul – for their support and belief over this long process. I would also like to thank all of my friends who have been there during this adventure and listened to me vent or deal with frustrating moments. Special thanks to Lindsey who has encouraged me throughout the entire journey and always provided me with some of the best perspective for my struggles. You even clued me in on where to apply to next and I couldn't be more grateful.

List of Abbreviations

$1\alpha,25(OH)_2D_3$	1α,25-dihydroxyvitamin D3
$24R,25(OH)_2D_3$	24R,25-dihydroxyvitamin D3
$25OHD_3$	25-hydroxyvitamin D3
ALP	Alkaline phosphatase activity
ATP	Adenosine triphosphate
BAX	Apoptosis regulator BAX
Bcl2	BCL2 apoptosis regulator
BMP	Bone morphogenetic protein
COMP	Cartilage oligomeric matrix protein
DNA	Deoxyribonucleic acid
ECM	extracellular matrix
EdU	5-Ethynyl-2′-deoxyuridine
ELISA	Enzyme-linked immunosorbent assay
FGF	Fibroblast growth factor
GC	Growth zone
HUVEC	Human umbilical vein endothelial cells
HDAC4	Histone deacetylase 4
Ihh	Indian hedgehog protein
MFE	Minimum free energy
MMP	Matrix metalloproteinase
MSC	Mesenchymal stem cell
MTT	3-(4,5-dimethylthiazol-2-yl)-2,5-diphenyltetrazolium bromide
MV	Matrix vesicle
OCN	Osteocalcin
OPG	Osteoprotegerin
p53	Tumor protein P53
PCR	Polymerase chain reaction
PDIA3	Protein disulfide isomerase family A member 3
PHOSPHO1	Phosphoethanolamine/phosphocholine phosphatase
PKCα	Protein kinase C alpha
PKCζ	Protein kinase C zeta
PLA2	Phospholipase A2
PPi	Pyrophosphates

PTHrP	Parathyroid hormone-related protein
RANKL	Receptor activator of NF-κB ligand
RC	Resting zone
RISC	RNA-induced silencing complex
RNA	Ribonucleic acid
RT-qPCR	Reverse transcription quantitative polymerase chain reaction
Runx2	RUNX family transcription factor 2
sGAG	Sulfated glycosaminoglycans
Sox9	SRY-Box transcription factor 9
TGF-β	Transforming growth factor beta
TNAP	Tissue non-specific alkaline phosphatase
TUNEL	Terminal deoxynucleotidyl transferase dUTP nick end labeling
UTR	Untranslated region
VDR	Vitamin D receptor
VEGF	Vascular endothelial growth factor

Abstract

Growth plate chondrocytes are the driving force of long bone elongation and they accomplish this vital task, in part, by producing, remodeling, and finally mineralizing the cartilage tissue that makes up the growth plate. This mineralized tissue is turned over again as bone forming cells invade and began the process of turning mineralized cartilage into bone. Chondrocytes undergo a distinct series of observable phases as they move through this process transitioning from a stage of proliferation to one of hypertrophy and finally capillary invasion. Chondrocytes produce matrix vesicles (MVs) that they release into the growth plate and that attach to collagen in the extracellular matrix (ECM). These MVs are involved in chondrocyte regulation, tissue remodeling, and matrix mineralization.

This entire process is highly regulated by various factors and hormones. 1α,25-dihydroxyvitamin D3 [1α,25$(OH)_2D_3$] is a well-studied hormone with known regulation of both chondrocytes and MVs. With the recent discovery of selectively exported microRNA in growth plate MVs there is the possibility of an additional regulator of growth plate maturation. The ***central hypothesis*** of this work was that MV microRNA are able to regulate growth plate chondrocytes and that the production and packaging of MV microRNA is regulated by 1α,25$(OH)_2D_3$.

Specific aim 1 determined whether microRNA were selectively exported in MVs, if those microRNA remain protected within the MVs, if certain microRNA are found in *ex-vivo* tissue, and the ability of specific microRNA to regulate growth plate chondrocytes. ***Specific aim 2*** determined the regulatory potential of 1α,25$(OH)_2D_3$ on microRNA production and packaging into MVs and the known mRNA and pathways targeted by the exported microRNA that were differentially expressed following 1α,25$(OH)_2D_3$ treatment as well as the impact of 1α,25$(OH)_2D_3$ on MV endocytosis and the release of microRNA from MVs. ***Specific aim 3*** examined the transcriptome following specific microRNA transfections and adapted an approach to target the interactions between specific tagged microRNA and the corresponding mRNA followed by RNAseq of the mRNA for the purpose of pathway analysis.

Summary

This thesis aimed to further elucidate the role of extracellular MV microRNA found in the mammalian growth plate. This was done by examining the ability of specific MV microRNA to regulate growth plate chondrocytes and investigating multiple aspects of the MV microRNA lifecycle including regulation during production and packaging, the release within the ECM, MV endocytosis, and what mRNA and pathways the MV microRNA are regulating within chondrocytes. The work was carried out both *in vitro* using a wide-ranging array of assays and visualization tools and *in silico* analyzing small RNA sequencing and RNA probe multiplex data. Work began with the bioinformatic analysis of existing small RNAseq data followed by the *in vitro* examination of chondrocytes responding to microRNA transfection. Expanding on this we began investigating the role that 1α,25$(OH)_2D_3$ plays with respect to the packaging and release of MV microRNA. Finally, we examined the direct regulation that these microRNAs exert on the cells.

RNAseq data examining the population of small RNA molecules found in resting zone (RC) and growth zone (GC) chondrocytes and the MVs that they produce were analyzed to examine zonal regulation and compile a list of specific microRNAs for detailed *in vitro* investigation. MicroRNA were found to make up zone-specific populations in the RC and GC cells and MVs; moreover, a subpopulation of select microRNA were exported within MVs into the ECM. When comparing the chondrocytes from the two zones and MVs from the two zones a far larger number of microRNA differed between the MVs than between the chondrocytes. Four microRNA were selected, three being disproportionately found in the MVs while one microRNA was present at relatively high levels in all groups. These microRNA were transfected into chondrocytes and a wide host of phenotypic changes and activity were measured to assess effects on proliferation, apoptosis, ECM components, factor production, and enzyme activity. Of the four select microRNA under investigation two stood out (22-3p and 122-5p) for their impact on the proliferation, ECM composition, and factor production of both RC and GC chondrocytes as well as the angiogenic activity of HUVEC cells. Attempts were made to localize and validate specific microRNA in *ex vivo*

tissue slices to pinpoint their location but due to collagen's autofluoresence and insufficient microscope resolution, the results were inconclusive. Further validation of the specific microRNAs was successfully carried out using RT-qPCR and the NanoString's nCounter system on *ex vivo* tissue samples. Combining the bioinformatic analysis that microRNA is being selectively exported from the cells (to such a degree that some microRNA had no copies remaining behind in the cell population) and the phenotypic response from chondrocytes to these exported microRNA, we have compelling evidence that the microRNAs are being packaged within MVs for a regulatory purpose. Remaining unanswered is how these microRNAs make their way back into the cells and whether they fall under the control of known growth plate regulators.

With the regulatory role of microRNA in the MVs established we wanted to see if $1\alpha,25(OH)_2D_3$ was involved in aspects of the MV microRNA lifecycle. We decided to examine the role of $1\alpha,25(OH)_2D_3$ in regulating the production and/or packaging of microRNA by GC chondrocytes, if it released microRNA from the MVs, and if it aided MV or microRNA endocytosis. GC chondrocytes were treated with $1\alpha,25(OH)_2D_3$ for 24 hours and the small RNA in the cells and MVs were sequenced. We were surprised to find very little change between the cell populations with virtually all of the differential expression taking place in the MVs. The chondrocytes exported a select population of microRNA in MVs, confirming previous observations, with an apparent coordinated regulation of microRNA production and packaging taking place in response to $1\alpha,25(OH)_2D_3$ treatment. This resulted in markedly different MV microRNA populations but virtually identical cell microRNA populations. The differentially expressed microRNAs in the MV population as compared to the parent cells were searched for known connections to musculoskeletal pathways, mRNAs, and tissues. The majority of microRNA were at most only associated with musculoskeletal related tissues and had no mRNA or pathway information indicating a large area of further investigation.

In order to look at various aspects of the MV microRNA lifecycle we began by examining the ability of $1\alpha,25(OH)_2D_3$ to release microRNA from the MVs as it is known to initiate breakdown of the MV's phospholipid membrane. Surprisingly the microRNA was not released free into

solution as they remained protected from RNase activity indicating either the presence of a protective carrier protein or lipid microcompartment or that a subpopulation of MVs houses the microRNA. This result was unexpected but provides further emphasis for the likelihood of the MV microRNA being a regulatory factor in the growth plate as the microRNA remain protected from the near ubiquitous presence of RNase within tissues.

We decided to further examine potential paths of microRNA reentry into cells by staining MVs with a lipophilic dye, incubating them with GC chondrocytes with either vehicle or 1α,25$(OH)_2D_3$ treatment, applying a nuclear counter stain to the cells, and imaging them in order to quantify how many cells were in the process of endocytosing stained MVs. When six or more distinct green dots, indicating MVs, were observed on a cell it was considered positively stained. Percent of positively stained chondrocytes increased with 1α,25$(OH)_2D_3$ treatment. This indicates an increase in the binding of MVs to chondrocytes due to either or both responding to 1α,25$(OH)_2D_3$ by increasing their binding potential or possibly the creation of MV fragments that are produced as MVs respond to 1α,25$(OH)_2D_3$ by breaking down their lipid membrane leaving an increased number of stained vesicle fragments for binding. In either scenario an increase in chondrocyte to MV exposure appears to occur and given that the microRNA may well be bound to the inner leaflet of the MVs even a population of MV fragments could be delivering a regulatory message to the chondrocytes.

With most of the selectively exported microRNA having only bioinformatically predicted activity and no detailed knowledge of their specific action in growth plate chondrocytes we looked into an approach to determine the target mRNAs for certain microRNA in our specific cells. We transfected biotin tagged microRNA mimics into cells and then used streptavidin coated magnetic beads to pull down the tagged microRNA and any attached RNA. The beads were then extensively washed and the RNA isolated for long read sequencing on a benchtop sequencer. Resulting fastq files were filtered and aligned to the rat cDNA transcriptome and gene IDs were determined. Differential expression analysis was conducted between each microRNA group and the negative control group and it was found that the majority of differentially expressed mRNA

were not shared between the five comparisons and largely unique for each microRNA under examination. The binding energies of the microRNA against the 3` UTR of the up-regulated genes were calculated and found to be on the higher end but well within commonly accepted values for microRNA to mRNA binding energies. An introductory pathway analysis of the differentially expressed mRNA was conducted to begin to examine what phenotypic effects might be resulting from these microRNA.

Specific Aims

RNA molecules were initially discovered in MVs in 1969 though believed at the time to most likely be an artifact.[1] Their presence was confirmed in 2016 at which time small RNA molecules, specifically microRNA, had been discovered and the technology to sequence and analyze the RNA was widely available.[2] The purpose of these MV microRNA in the growth plate and their ability to regulate the chondrocytes was unclear.

1α,25$(OH)_2D_3$ is a well-known regulator of growth zone chondrocytes and the mineralization process that occurs in the growth plate.[3] This regulation occurs through interactions with the chondrocytes and the MVs as both have receptors for 1α,25$(OH)_2D_3$.[4] In addition to responding to 1α,25$(OH)_2D_3$, GC chondrocytes are able to metabolize 25-hydroxyvitamin D3 (25OHD_3) to 1α,25$(OH)_2D_3$ on their own.[5,6] MVs respond to 1α,25$(OH)_2D_3$ by releasing enzymes that are able to activate latent TGF-β in the ECM that, in turn, regulates chondrocyte 1α,25$(OH)_2D_3$ production.[7,8] 1α,25$(OH)_2D_3$ is also able to regulate aspects of the production of MVs and initiate MV breakdown once they are in the ECM.[7]

From this standpoint a working hypothesis was put together:

> *The specifically packaged microRNAs in matrix vesicles regulate the maturation of chondrocytes in the growth plate. Packaging and release of microRNA is a well-regulated process controlled by hormones and local factors, specifically 1α,25-dihydroxyvitamin D3.*

Previous work in our lab had sequenced RNA from growth plate chondrocytes and MVs and found selective packaging of microRNA in MVs.[2] Additionally, the MVs provided protection to the small RNAs from RNase activity when in solution. The selective export in MVs and a protective lipid membrane suggested the potential for MV microRNA to regulate growth plate chondrocytes.

Aim 1:

> *Determine the role of matrix vesicle microRNAs in the growth and differentiation of resting zone and growth zone chondrocytes.*

This was accomplished by determining that a zonal production of microRNA occurs in the growth plate with RC and GC chondrocytes and MVs each containing a distinct population of microRNA. Both RC and GC zones export a selective population of microRNA into MVs and these microRNAs are protected in suspension from RNase treatment. This work was published in collaboration with Dr. Zhao Lin and is reprinted here in the section “MicroRNA Contents in Matrix Vesicles Produced by Growth Plate Chondrocytes are Cell Maturation Dependent”. My bioinformatic analysis is found in the first six tables of the paper and in figures three and five. Following this, we analyzed the small RNA sequence data from growth plate chondrocytes and MVs and selected three microRNA that were selectively exported in MVs and had a minimal presence within chondrocytes and one microRNA that made up a relatively large portion of both chondrocyte and MV microRNA populations. These four microRNA were transfected into RC and GC chondrocytes and phenotypic changes investigated through a variety of assays.[9] We examined effects on proliferation (DNA content and EdU incorporation), apoptosis (p53, Bax/Bcl, and TUNEL), ECM composition (sulfated glycosaminoglycans [sGAG], collagen types I, II, and X, and cartilage oligomeric matrix protein [COMP]), production of factors and proteins (BMP2, FGF2, IHH, OCN, OPG, RANKL, PTHrP, Runx2, Sox9, TGF-β1, and VEGF-A), alkaline phosphatase specific activity, and metabolism in cultures of growth plate chondrocytes and assessed angiogenic activity in cultures of HUVEC cells. GC chondrocytes were transfected with microRNA mimics, a corresponding microRNA inhibitor, and both together to validate target specificity of the microRNA mimic and see if adding an inhibitor would begin to alleviate the effect of the microRNA mimic. We analyzed *ex vivo* growth plate tissue in order to verify the presence of our target microRNAs. This was accomplished by carefully isolating RC and GC regions of the growth plate, removing all tissue and isolating the RNA. The RNA was analyzed using a multiplex microRNA probe assay and RT-qPCR. These results were published in 2021 and are reprinted here in the section “Specific MicroRNAs Found in Extracellular Matrix Vesicles Regulate Proliferation and Differentiation in Growth Plate Chondrocytes”.

Aim 2:

Determine the effect of 1α,25-dihydroxyvitamin D_3 on the composition of microRNAs in matrix vesicles and whether 1α,25-dihydroxyvitamin D_3 plays a role in the release of microRNAs by matrix vesicles into the extracellular matrix.

GC chondrocytes were treated with 1α,25$(OH)_2D_3$ for 24 hours and the cells and MVs isolated. The RNA was extracted from the isolations and submitted for small RNAseq. The sequencing data were aligned and the reads analyzed for differential expression between the various groups and the differentially expressed microRNA submitted for pathway and target analysis. Isolated MVs were treated with 1α,25$(OH)_2D_3$ in the presence and absence of RNase for three hours and the RNA isolated and analyzed for degradation. To assess endocytosis isolated MVs were stained with a lipophilic membrane fluorophore, treated with vehicle or 1α,25$(OH)_2D_3$ and incubated with chondrocytes for 24 hours. The chondrocytes were treated with a nuclear counterstain and fixed before imaging on a confocal microscope to determine the percent of chondrocytes with bound MVs. These results are under review and are printed here in the section "1α,25$(OH)_2D_3$ Regulation of MV MicroRNA".

Aim 3:

Ascertain mRNA targets of select microRNA and the pathways linking microRNA regulation to phenotypic changes.

Specific biotin tagged microRNA mimics were transfected into chondrocytes and incubated for 48 hours. The chondrocytes were then lysed and RNA isolated using streptavidin tagged magnetic beads. The isolated RNA was sequenced in house on a benchtop long read sequencer. The resulting reads were aligned against the rat transcriptome and analyzed for differential expression against the NC group. Up and down-regulated differentially expressed genes between each of the five comparisons were examined for overlap and the 3` UTR downloaded in order to predict the microRNA to mRNA binding energies. Differentially expressed up-regulated genes were used for pathway analysis.

Background

Growth Plate

Mammalian bone growth is driven by two types of ossification. Endochondral ossification is responsible for long bone growth while intramembranous ossification primarily produces the flat bones found in the skull.[10] Both processes stem from mesenchymal tissue with endochondral ossification building upon a cartilaginous intermediate template – the growth plate – that is mineralized and then replaced with bone.[11] In long bones and in the cartilage at the costochondral junction of the ribs, the growth plate has a linear morphology and can be divided into different zones populated by chondrocytes with distinct phenotypical characteristics. Chondrocytes mature as they move through the growth plate forming into organized columns of cells as they progress, passing from the resting or reserve zone through the proliferative zone, the prehypertrophic zone, the hypertrophic zone and finally into the zone of calcification, which is accompanied by capillary invasion.[12]

The linearity of the growth plate enables separation of the regions by sharp dissection. Cells in the RC, located at the epiphyseal end of the growth plate in long bones, are less differentiated and produce an ECM that is enriched in collagen type II and sGAG.[13,14] The GC region contains cells in the lower proliferative cell zone, prehypertrophic chondrocytes, and the upper hypertrophic cell zone, in which cells are undergoing terminal differentiation.[15] GC chondrocytes can be characterized by increased levels of collagen type X, ALP, VEGF and RANKL.[13,16–18] At the edge of the hypertrophic zone the vasculature begins to invade from the bordering metaphysis marking the end of the growth plate.[19] This process of maturation is precisely regulated by a complex interplay of growth factors, cytokines, and hormones, including two metabolites of vitamin D, 1α,25$(OH)_2D_3$ and 24R,25$(OH)_2D_3$.[20–22]

One role of the growth plate is to provide a mechanism for tissue growth prior to mineralized bone formation.[23] RC chondrocytes are surrounded by a proteoglycan-rich, non-mineralized ECM.[7,24] A subset of these cells align into columns and undergo a series of

doublings, thereby increasing the overall length of the tissue. In the post-proliferative growth plate, GC chondrocytes prepare the proteoglycan and type II collagen rich ECM for mineralization.[25] This is a complex process requiring selective removal of proteoglycan aggregates, which inhibit mineral formation via stearic hindrance as well as by limiting available Ca^{++} via interaction with negatively charged sGAG.[17] Chondrocytes manage the process by synthesizing appropriate ECM proteins and by releasing enzymes targeted to the specific removal of calcification inhibitors, as well as by the release of cell zone-specific MVs.[25,26]

Matrix Vesicles

MVs have been isolated from the ECM of growth plate cartilage, as well as from other calcifying tissues, including primary bone, fracture callus, and dentin.[27,28] MVs were first observed via electron microscopy and found to be focal points for the calcification process and have since been found to play an active role in matrix turnover and chondrocyte regulation.[29] They have also been found at the epithelial/mesenchymal interface of calcifying neoplasias and more recently, similar extracellular microsomes have been found associated with metastatic cancers[30,31]

In the growth plate, MVs are small (50 – 150 nm in diameter) lipid bound organelles anchored to collagen within the ECM.[19,32,33] They are produced by the chondrocytes but are distinct from them with respect to their membrane phospholipid composition.[34,35] Their payload consists of minerals, enzymes, factors, and microRNAs with distinct packaging dependent on where in the growth plate they are produced.[2,9,36,37] MVs are enriched in acidic phospholipids, particularly phosphatidylserine and phosphatidylinositol, which have been associated with initial sites of Ca^{++} hydroxyapatite formation in tissues not previously calcified, such as the growth plate and fracture callus.[38,39] MVs found in the ECM contain selectively enriched complements of enzymes (e.g. TNAP, carbonic anhydrase, pyrophosphatase, PHOSPHO1, MMPs and their inhibitors, etc.), as well as growth factors (e.g. BMP, VEGF), and other proteins including osteopontin, all of which contribute to the mineralization process and subsequent bone formation.[34,40–44] TNAP is an enzyme associated with calcification and considered a defining

characteristic of MVs.[43] TNAP is anchored to the outer leaflet of the matrix vesicle membrane via glycosylphosphatidylinositol.[45] Specific activity of this enzyme in matrix vesicles is greater than twice that of the plasma membrane of the cells from which they were derived.[46]

MVs play an integral role in the mineralization process as centers for the start of hydroxyapatite mineralization.[27,34,47,48] Initiation of calcification is generally considered to take place in two distinct phases. As part of phase 1, 1α,25$(OH)_2D_3$ activates PDIA3 in MVs, which stimulates PLA2 activity resulting in formation of lysophospholipids that stimulate PKCα activity and destabilization of the MV membrane.[49] As the ATP content of the MV is depleted, the concentration of Ca^{++} increases and Ca^{++} binds to phosphatidylserine forming calcium-phospholipid-phosphate complexes, leading to the start of hydroxyapatite crystal formation on the inner leaflet of the MV membrane.[19,50] Phase 2 involves MV membrane breakdown and exposure of hydroxyapatite to extracellular Ca^{++} and inorganic phosphate, resulting in crystal growth in the ECM.[30,47] MV phosphatases play an important role in this process by hydrolyzing ATP, producing PPi. Pyrophosphatases in the MV hydrolyze PPi, releasing inorganic phosphate thereby increasing the concentration of inorganic phosphate.[51] MV TNAP also acts on other phosphorylated proteins and lipids in the ECM.[28] Mutations in the TNAP gene result in hypomineralization in mice and the accumulation of pyrophosphates has been demonstrated to reduce *in vitro* mineralization.[52–54]

Studies comparing MVs produced by RC chondrocytes and those produced by GC chondrocytes show that they differ markedly.[55] They possess a different membrane phospholipid composition; their alkaline phosphatase activity differs; and their matrix metalloproteinase content differs. Whereas RC MVs contain primarily neutral metalloproteinases, GC MVs are enriched in acidic metalloproteinases.[7] This implies that production of the microsomes is under genomic regulation, but once in the matrix, control of their function must involve non-genomic mechanisms, as they lack the machinery necessary for gene transcription and protein synthesis.

The importance of MVs to bone formation and cartilage maturation has become clearer as our understanding of their regulatory potential expands. Over the years, researchers have characterized MVs in increasing detail, focusing primarily on their role in calcification.[27] MVs were found to contain genomic data in 1969 although it was not clear that the detected RNA had a function or if it was potentially remnants from the cell that were unintentionally incorporated during MV formation.[1] Small RNAs, including microRNA, have now been successfully sequenced from MVs.[2] Their lifecycle and exact role in the growth plate is a central focus of this work.

1α,25-dihydroxyvitamin D3

In vitro and *in vivo* studies in our lab have shown that vitamin D metabolites play a significant role in the formation, content, and fate of MVs.[56] Two metabolites of vitamin D, 1α,25$(OH)_2D_3$ and 24R,25$(OH)_2D_3$ have different effects on MV composition that are specific to the parent chondrocyte's maturation zones in the growth plate.[7] RC cells respond primarily to 24R,25$(OH)_2D_3$, producing MVs that are enriched in neutral MMPs.[22] In contrast, GC chondrocytes respond primarily to 1α,25$(OH)_2D_3$ and produce MVs that are enriched in acidic MMPs.

MVs produced by both cell types possess receptors for 1α,25$(OH)_2D_3$, including the canonical VDR and the membrane-associated receptor, PDIA3.[57,58] 1α,25$(OH)_2D_3$ acts on GC chondrocyte plasma membrane associated PDIA3 to stimulate PKCα activity.[59] Although the receptor for 24R,25$(OH)_2D_3$ is not yet known, this vitamin D metabolite also regulates PKC, but only in RC cells and MVs.

The mechanisms by which these metabolites exert their modulation of MV PKCα is not yet well understood but it appears to involve differential regulation of PLA2. The phospholipid composition of the MV membrane differs, which may also play a role; PKCα is both Ca^{++} and lipid dependent.[7] Particularly intriguing is the observation that both metabolites regulate MV production in their respective target cells and stimulate inclusion of PKCζ.[59] PKCζ is not a Ca^{++}-dependent protein kinase, but why this isoform should be specifically incorporated is not yet

known.[60] In the end 1α,25$(OH)_2D_3$ elicits an increase in PKC activity in GC chondrocytes and a reduction in GC MVs while 24R,25$(OH)_2D_3$ produces an increase in PKC activity in RC chondrocytes and a reduction in RC MVs.[60]

Chondrocytes are able to produce vitamin D metabolites under the regulation of growth factors and hormones and secrete them into the ECM where they take part in regulating MVs.[5,6,8] This suggests that control of ECM events by 1α,25$(OH)_2D_3$ and 24R,25$(OH)_2D_3$ produced locally is important to the overall management of growth plate development. Studies examining regulation of TGF-β1 demonstrate this. Chondrocytes produce a number of TGF-β related proteins, a superfamily that includes TGF-βs and BMPs as subfamilies.[61,62] Synthesis and storage of TGF-β1 as latent TGF-β1 in the ECM is differentially regulated by the metabolites on their target cells [8,63]. Activation of latent TGF-β1 stored in the ECM is regulated by MV MMP3 and activation of latent TGF-β2 is regulated by MV MMP2, but this requires the direct action of 1α,25$(OH)_2D_3$ on the MV membrane, resulting in formation of lysophospholipid and release of the enzymes.[7,64] Active TGF-β1 binds to cellular membrane receptors, initiating a signaling cascade,[62] that has a range of effects depending on the TGF-β1 concentration and the cell type involved. TGF-β1 is able to regulate the enzymes involved in the metabolism of 25OHD_3 in RC and GC cells as well as the maturation of growth plate chondrocytes.[7]

MicroRNAs stored in the MVs may be released into the ECM by a similar mechanism. Lysophospholipids, produced by the action of PLA2 following binding of 1α,25$(OH)_2D_3$ to PDIA3 in the MV membrane, are naturally occurring detergents that have been shown to be able to both activate TGF-β1 and release MMP-3.[65] Their detergent properties weaken the MV membrane, resulting in the uptake of water and ultimately MV breakdown. Alternatively, released lysophospholipids may modify the ECM, increasing access to MV enzymes.[7]

microRNA

MicroRNA are roughly 22 nucleotide long single-stranded non-coding RNA molecules that play a role in the regulation of gene expression as part of the RISC.[66] RISC down-regulates the transcription of specific messenger RNA or downright degrades them dependent on the level of

complementarity the loaded microRNA strand has with the individual mRNA.[67,68] The scope of microRNA's role in regulating gene expression is still being elucidated although microRNAs are being discovered in more and more places with some estimates claiming that microRNAs may regulate over 1/3 of human genes.[2,69–72] microRNAs are understood to typically bind to the three prime untranslated region (3′-UTR) of the mRNA strand (plants appear to disregard this trend) using only a 6 to 8 base 'seed region' of the 22 base long miRNA.[72] microRNAs are typically not restrained to an individual mRNA and multiple microRNAs can often regulate individual mRNAs.[68]

MicroRNAs are able to impact the expression rates of mRNA within the cell and as a result they are able to impact the expression of transcription factors within a cell. Modifying the translation rates of transcription factors enables microRNAs to have a wide array of downstream effects within the cell including the up or down-regulation of other microRNAs leading to the potential for a type of microRNA network to exist within the cell.[73]

Selected microRNAs have been found to be concentrated within MVs[2]. Moreover, the MV microRNA profile depends on the growth plate zone from which the parent chondrocytes have been isolated. microRNAs 451-5p, 223-3p and 122-5p exhibit fold change increases in MVs ranging from 25 to over 2,000 times what is observed in their respective parent cells, suggesting a selective export and a role in growth plate regulation. These microRNAs have been examined in other tissues. microRNA 451 reduces proliferation in human osteosarcoma cells; microRNA 223 reduces inflammation-based activation of macrophages; and microRNA 122 is a well-known suppressor of hepatocellular carcinoma.[74–76] Effects of these microRNAs on chondrocytes and the mineralization process are likely going to be somewhat unique as microRNAs typically are able to impact the expression of multiple genes and the pathways impacted depend on the state of the transcriptome. The differential content of the MVs reflects other differences in MV composition (enzymes, lipid composition, membrane enzymes), which are also dependent on the region of the growth plate where the MVs are produced.[7]

Demonstration of MV microRNA composition is facilitated by the methods used to isolate them. Whether isolating them from growth plate cartilage or from cultures of growth plate chondrocytes, the process involves enzymatic digestion of the ECM, removal of cells and cell fragments by differential centrifugation, and collection of the MVs from differential ultracentrifugation of the trypsin digested ECM supernatant.[77] Efficiency of the isolation can be verified by the enrichment of TNAP in the MV fraction compared to the cell plasma membrane,[34,78] as well as absence of marker enzymes for various cell organelles.

A wide selection of microRNA target prediction tools is available, many with easy-to-use web interfaces.[79–83] The tools are typically relying on a predictive algorithm to examine the microRNA to mRNA binding within the 3` UTR of the mRNA and trying to predict what type of stem and loop secondary structures will be present. These algorithms typically search for the most energy advantageous location within the 3` UTR for a specific microRNA and use that MFE value to predict the likelihood of mRNA regulation by the specific microRNA.[84–87] The combination of algorithmic predictions and published research data results in putative lists of target mRNA that number in the hundreds to thousands. Going from these lists to affected pathways would require knowing the cell's active transcriptome, factoring in the potential for network, or secondary, microRNA effects and linking the resulting mRNA to active pathways within the cell. Much of this information is not readily available for a given cell type and would need to be confirmed by subsequent experimentation.

Differential Expression

Differential expression analysis is the standard first step when examining sequencing datasets. Library preparation, polymerase chain reaction (PCR) bias, sample source, among others, are all potential contributors to variation in read counts between samples.[88] This is typically addressed using the normalization procedure included in the differential expression software package (e.g. edgeR and DESeq2). DESeq2 was used for the analyses performed in these studies and DESeq2's median of ratios normalization procedure was implemented. Isolations from cells had a 100 to 250 fold increase in total RNA when compared to the

corresponding MVs. This large variation in RNA has the potential to bias the differential expression analysis and skew the final results. A novel normalization procedure for this type of data with very divergent samples could have broad usefulness for this and other studies. We examined the six most exported microRNA in the initial study and verified the RNAseq results with RT-qPCR. The confirmation of highly exported microRNA in MV samples that have comparatively low starting quantities of total RNA using RT-qPCR provides reassurance that the RNAseq analyses are valid.

MicroRNA Contents in Matrix Vesicles Produced by Growth Plate Chondrocytes are Cell Maturation Dependent

Lin, Z., McClure, M.J., Zhao, J. *et al.* MicroRNA Contents in Matrix Vesicles Produced by Growth Plate Chondrocytes are Cell Maturation Dependent. *Sci Rep* **8**, 3609 (2018).

Abstract

Chondrocytes at different maturation states in the growth plate produce MVs, membrane organelles found in the extracellular matrix, with a wide range of contents, such as matrix processing enzymes and receptors for hormones. We have shown that MVs harvested from GC chondrocyte cultures contain abundant small RNAs, including miRNAs. Here, we determined whether RNA also exists in MVs produced by less mature RC chondrocytes and, if so, whether it differs from the RNA in MVs produced by GC cells. Our results showed that RNA, small RNA specifically, was present in RC-MVs, and it was well-protected from RNase by the phospholipid membrane. A group of miRNAs was enriched in RC-MVs compared RC-cells, suggesting that miRNAs are selectively packaged into MVs. High throughput array and RNA sequencing showed that ~39% miRNAs were differentially expressed between RC-MVs and GC-MVs. Individual RT-qPCR also confirmed that miR-122-5p and miR-150-5p were expressed at significantly higher levels in RC-MVs compared to GC-MVs. This study showed that growth plate chondrocytes at different differentiation stages produce different MVs with different miRNA contents, further supporting extracellular vesicle miRNAs play a role as “matrisomes” that mediate the cell–cell communication in cartilage and bone development.

Introduction

Endochondral bone formation consists of a developmental cascade of chondrocyte maturation that is well-regulated in temporal and spatial dimensions.[89] This is reflected in a zonal change in cell morphology and function from resting to proliferative, prehypertrophic and hypertrophic chondrocytes followed by calcification of the extracellular matrix, vasculogenesis, and bone formation on the calcified cartilage scaffold. Central to the process of growth plate development is the role of small membrane-bound extracellular microvesicles, called matrix vesicles.[90] MVs are enriched in alkaline phosphatase specific activity compared to the plasma membrane and the first calcium phosphate crystals are observed on the inner leaflet of the MV membrane. Depending on the state of chondrocyte maturation within the growth plate, MVs have a different phospholipid composition[91] and are selectively packed with different matrix

metalloproteinases[35,44,92], alkaline phosphatase activity[91,93–95], growth factors[40], and receptors for hormones[46,96,97], suggesting they function as regulators of the endochondral bone formation environment[34,43,98].

We have established a cell culture model to study the phenotypic transition of chondrocytes from the RC to the prehypertrophic/upper hypertrophic zone (GC), in which these two cell types are cultured separately after discarding the intervening proliferative cell zone.[91] Characterization of these two distinct cell populations has shown that they are different in morphology[91], proliferation rate[91], extracellular matrix components[91], basal cation flux and membrane fluidity[99–101], membrane phospholipid composition[91,101], basal production of prostaglandin E2[102] and production of vitamin D metabolites 1,25-dihydroxyvitamin D3 [1,25(OH)2D3] and 24,25-dihydroxyvitamin D3 [24,25(OH)2D3][6].

In addition, RC and GC chondrocytes exhibit marked differences in their response to vitamin D metabolites and growth factors[46,59,92]. Whereas RC cells respond primarily to 24 R,25(OH)2D3, GC chondrocytes respond primarily to 1α,25(OH)2D3. Testosterone stimulates alkaline phosphatase specific activity in GC cells, with no effects on RC cells[103]; TGF-β1 induces a dose-dependent increase in proliferation of RC cells, but this effect was not seen in GC cells[104]. Interestingly, even though RC chondrocytes will form nodules in long-term culture, these cells do not mineralize their matrix. However, BMP2 or 24 R,25(OH)2D3 treatment of RC cells induces a phenotypic shift into GC chondrocytes[105], which are able to calcify their extracellular matrix.

Both types of chondrocytes produce MVs, but with distinctly different properties. MVs produced by GC cells possess greater specific activities of alkaline phosphatase (the MV marker enzyme)[91] and phospholipase A2 than do MVs produced by RC cells[101]. RC MVs contain neutral metalloproteinases, whereas MVs produced by GC chondrocytes contain acidic matrix metalloproteinases[35,92,102,106]. RC MVs also have different phospholipid profiles, membrane fluidities and membrane receptors compared to MVs produced by GC cells[46,91,96,101]. PKC activity in RC-MVs is regulated by 24 R,25(OH)2D3; however, it is stimulated by 1α,25(OH)2D3

in GC-MVs[107,108]. RC-MVs are usually not able to calcify, however, mineralization occurs in GC-MVs[109,110]. Taken together, these findings suggest that chondrocytes at different maturation status in the growth plate produce different MVs with different contents, which modulate their different local environment and satisfy different metabolic needs.

Recent studies show that microRNAs (miRNA), which are short (20–22-nucleotide), endogenous, single-stranded, non-coding RNA molecules that regulate gene expression at the post-transcriptional level[67], are involved in endochondral bone formation[111]. miR-145 was downregulated during TGFβ3-induced chondrogenic differentiation of MSCs, and targeted Sox9 mRNA transcripts[112]. miR-140 was expressed in cartilage during embryonic development, contributes to craniofacial development, and regulated HDAC4, but there was no evidence to indicate its involvement in postnatal tissue[113]. miR-1 was shown to be specifically expressed in the hypertrophic zone in postnatal growth plate, and repressed HDAC4[114]. These studies substantiate the hypothesis that specific miRNA regulate growth plate cartilage.

miRNA is packaged in membrane bound vesicles termed endosomes, which are found in biofluids such as blood, plasma, urine and saliva, as well as culture medium[115]. Emerging as novel mediators in cell-cell communications, extracellular miRNA is involved in various physiological and pathological processes[116]. Recently, our lab showed that small RNA, and miRNA in particular, is highly enriched in matrix vesicles produced by GC chondrocytes[2]. Moreover, our results indicate that a group of miRNAs is selectively packed into these MVs, suggesting that MVs function as “matrisomes,” providing a mechanism for information transfer in the non-vascularized growth plate. However, it is not known whether small RNA also exists in MVs produced by RC chondrocytes and, if so, whether there is difference in their miRNA composition. The purpose of this study was to determine the presence of RNA in RC-MVs, and then use PCR array and next generation sequencing to identify their miRNA profile. We also compared the RC-MV miRNAs to those present in GC-MVs.

Results

Characterization of RC-MVs.

Nanosight analysis showed that MVs isolated from RC chondrocyte cultures were approximately 100 nm in diameter (Fig. 1.1 A). These vesicles demonstrated a more than 2-fold increase in alkaline phosphatase specific activity compared to the RC plasma membrane, which is a marker for MVs (Table 1.1). In addition, activity in RC-MVs was lower than in MVs from GC chondrocyte cultures (Fig. 1.1 B), which exhibited a 6-fold enrichment over plasma membrane activity (Fig. 1.1 C), being consistent with our previous observations[91].

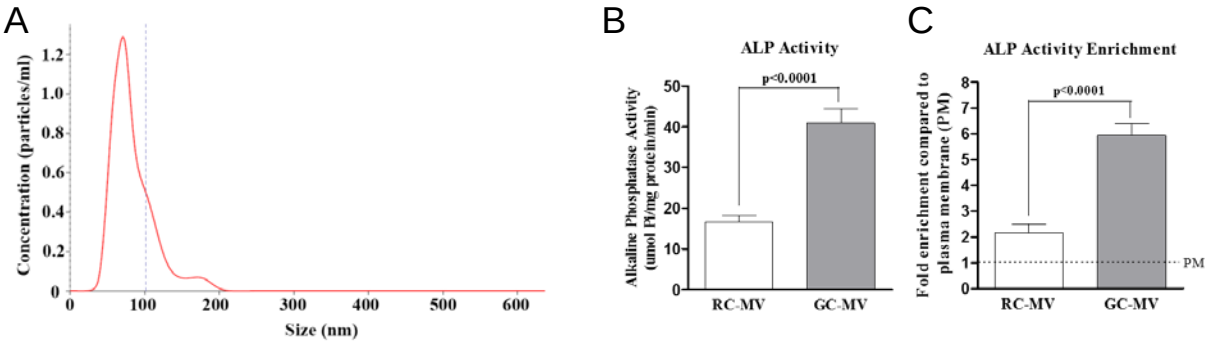

Figure 1.1 Characterization of RC-MVs. (**A**) Nanosight was used to measure the size of RC-MVs, which showed an average diameter around 80 nm. (**B**) Alkaline phosphatase (ALP) specific activity was compared between RC-MVs and GC-MVs. GC cells produced MVs with higher ALP specific activity than RC cells (n = 5 or 6). (**C**) In RC cell cultures, less ALP activity enrichment was seen in MVs compared to that in GC cell cultures (n = 5 or 6). PM=plasma membrane.

	ALP activity (μmol Pi/mg protein/ min) (mean ± s.e.m.)	Fold enrichment
Total cell lysate	$4.04 \pm 0.45^{c,d}$	1
Mitochondria	4.67 ± 2.58^{d}	1.16
Plasma membrane	$8.00 \pm 1.00^{d,e}$	1.98
MVs	$16.65 \pm 3.79^{a,b,c,e}$	4.12
Pellet from culture medium	$2.33 \pm 0.43^{c,d}$	0.57

Table 1.1 Alkaline phosphatase (ALP) specific activity of MVs from resting zone chondrocytes. Note: $^{a}p < 0.05$ compared with total cell lysate; $^{b}p < 0.05$ compared with mitochondria; $^{c}p < 0.05$ compared with plasma membrane; $^{d}p < 0.05$ compared with MVs; $^{e}p < 0.05$ compared with pellet from culture medium; n = 5 or 6. All the comparisons were done within the same cell type. ($^{a–e}$Based on one way ANOVA). The enrichment folds compared with total cell lysate are presented on the right.

Small RNA is selectively packaged in matrix vesicles produced by resting zone chondrocytes.

RC cells had both large ribosomal RNA (28 s and 18 s) and small RNA, while MVs produced by these cells only exhibited small RNA that was less than 200 nt (Fig. 1.2 A). This was confirmed by Bioanalyzer (Fig. 1.2 B). These RNAs were packed inside MVs and were protected from enzymatic digestion by RNase. RNase treatment did not decrease the yield of RNA extracted from MVs (Fig. 1.2 C). If the membrane was intact, RNase did not digest the MV RNA (Fig. 1.2 D). However, when Triton X-100 was added to disrupt the membrane, RNase completely digested

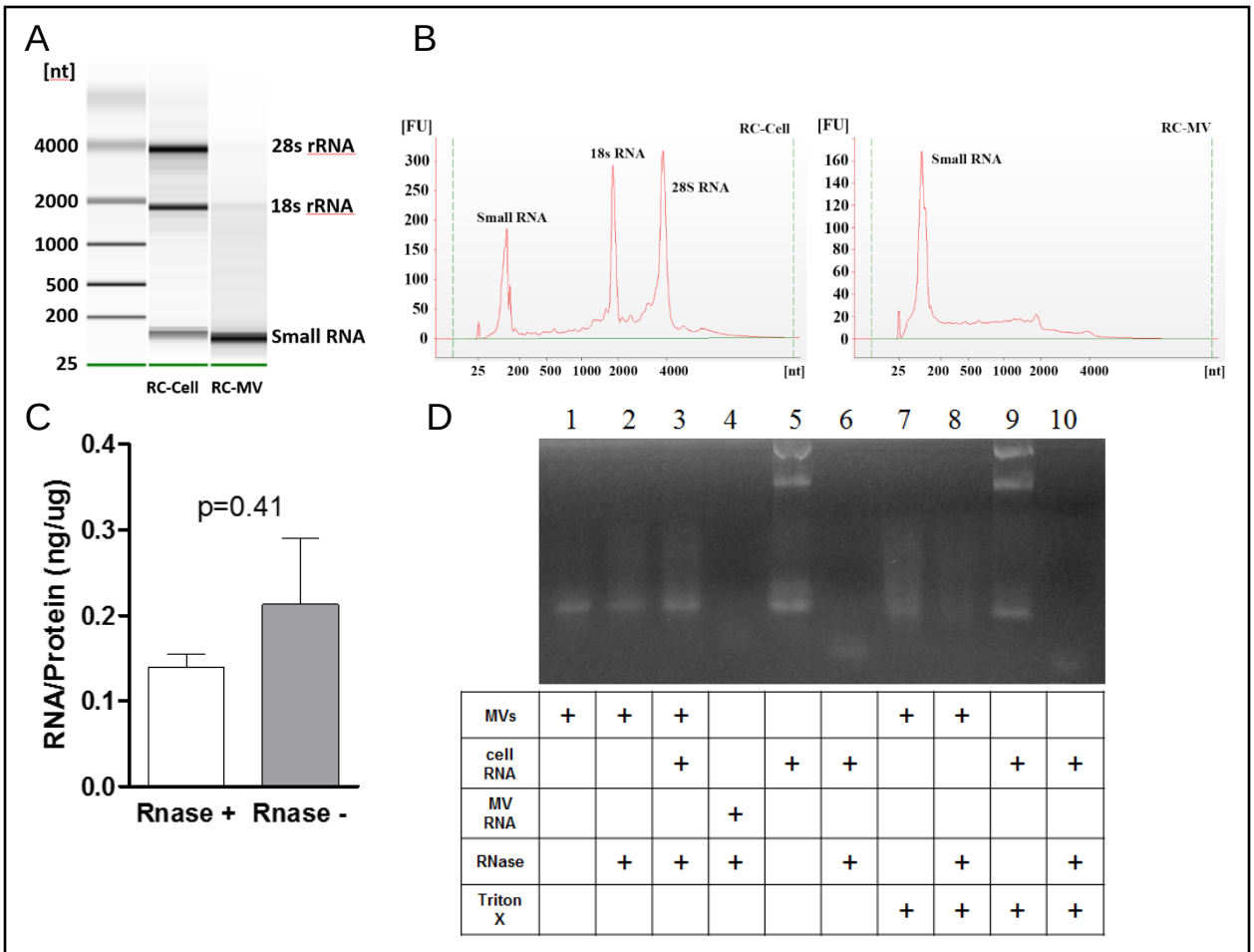

Figure 1.2 RNA exists in RC-MVs. (**A**) MV RNA was compared to cell RNA. In a 2% agarose gel, RC-MV RNA was heterogeneous in size but contained little or no large ribosomal RNA species (18S- and 28S-rRNA) compared to parent cells. Enriched small RNAs were observed in MVs. (**B**) A similar pattern was observed in the Bioanalyzer. (**C**) RC-MVs were treated by RNase A before RNA extraction by TRIzol. No significant differences in the RNA:protein ratios of MVs with or without RNase pretreatment (n = 6) were observed. (**D**) RNase was not able to digest the RNA component in MVs. However, it was able to digest the total cell RNA. When the MVs were pre-treated with the membrane detergent Triton X-100, RNA degradation was observed, suggesting that RNA in RC-MVs is protected by the intact lipid membrane.

the RNA in the MV suspension. These results suggested that the RNA in the MVs was protected by the phospholipid bilayer membrane.

Selective miRNAs are enriched in RC-MVs.

We used a PCR array to determine the miRNA profile of RC-MVs, and compared that to the total cell miRNA profile. A distinct pattern was seen in RC-MVs with a selective group of miRNAs that were highly enriched (Table 1.2). In this data set, 13 miRNAs were only detected in RC-MVs but not RC-cells; 10 other miRNAs were found to have at least more than 2-fold enrichment in RC-MVs, which included miR-150-5p, miR-126a-3p, and miR-129-2-3p. Conversely, miRNA expression levels within the cells that were elevated compared to MVs included miR-29b-3p, miR-503-5p, and miR-27a-3p. We also obtained a global view of RC-MV small RNA using high throughput, unbiased RNA-Seq and compared the results to parent chondrocytes (Fig. 1.3 A). The annotated small RNAs in RC-MVs included rRNA (20.55%), transfer RNA (12.01%), miRNAs (6.08%), and non-coding RNA like snoRNA, Y_RNA, etc (9.57%). In contrast, chondrocytes had significantly more miRNAs (10.54%).

When the RC-MV miRNA pool was examined more closely, we determined that it was dominated by a small number of miRNAs. The most abundant miRNA in RC-MVs was miR-22-3p, which accounted for 20.27% of the total miRNA reads, followed by miR-21-5p (17.21%) and miR-143-3p (11.77%). The top 3 most abundant miRNAs occupied over 50% of the miRNA pool (Table 1.3), which was similar to that of the parent cell miRNA pool (Table 1.4). However, we also found distinct differences in the miRNA profile between RC-MVs and RC-cells (Fig. 1.3 B). 139 (32.1%) miRNAs were found to be enriched in MVs by at least two-fold. The top 20 most RC-MV enriched miRNAs (compared to RC-cells) identified from RNA sequencing are listed in Table 5. We validated these findings using real time PCR.

miRNA unique in RC-MVs	miRNAs shared in RC-MVs and RC-cells		miRNA unique in RC-MVs
miRNA	miRNAs	Fold_change	miRNA
rno-miR-451-5p	***rno-miR-150-5p***	**10.23**	rno-miR-27a-3p
rno-miR-223-3p	***rno-miR-126a-3p***	**6.73**	rno-miR-219-5p
rno-miR-142-3p	*rno-miR-129-2-3p*	4.61	rno-miR-190a-5p
rno-miR-122-5p	*rno-miR-10a-5p*	3.45	rno-miR-147
rno-miR-139-5p	*rno-miR-125a-3p*	2.75	rno-miR-325-3p
rno-miR-339-5p	*rno-miR-490-3p*	2.16	rno-miR-499-5p
rno-miR-142-5p	*rno-miR-186-5p*	2.14	rno-miR-598-3p
rno-miR-144-3p	*rno-miR-196b-5p*	2.12	rno-miR-196a-5p
rno-miR-211-5p	*rno-miR-34b-3p*	2.11	rno-miR-298-5p
rno-miR-133a-3p	*rno-miR-132-3p*	2.04	rno-miR-181d-5p
rno-miR-133b-3p	rno-miR-136-5p	−2.07	rno-miR-540-5p
rno-miR-200c-3p	rno-miR-218a-5p	−2.15	rno-miR-203a-3p
rno-miR-330-5p	rno-miR-324-5p	−2.15	rno-miR-130b-3p
	rno-miR-193-3p	−2.18	rno-miR-384-5p
	rno-let-7i-5p	−2.38	rno-miR-384-3p
	rno-miR-29c-3p	−2.40	rno-miR-296-5p
	rno-miR-301a-3p	−2.51	rno-miR-135a-5p
	rno-miR-210-3p	−2.52	rno-miR-187-3p
	rno-miR-376a-3p	−2.54	rno-miR-291a-5p
	rno-miR-195-5p	−2.58	rno-miR-181c-5p
	rno-miR-34c-5p	−2.71	rno-miR-342-5p
	rno-miR-32-5p	−4.21	
	rno-miR-503-5p	−4.59	
	rno-miR-29b-3p	−5.65	
	rno-miR-33-5p	−5.80	
	rno-miR-34b-5p	−6.35	

Table 1.2 miRNAs with different expression levels between RC-MVs and RC-cells in miRNA PCR array. Note: miRNAs that were only detected in MVs from resting zone chondrocytes were shown in the left column. miRNAs that were only detected in the resting zone chondrocytes were shown in the right column. miRNAs that were detected both in resting zone MVs and cells, but with at least a 2-fold change and $p < 0.05$ were shown in the middle column. miRNAs that are in Italic area: highly enriched in RC MVs. miRNAs that in underline area: mostly remained in RC cells. miRNAs highlighted in bold italic were selected for further validation by RT-PCR.

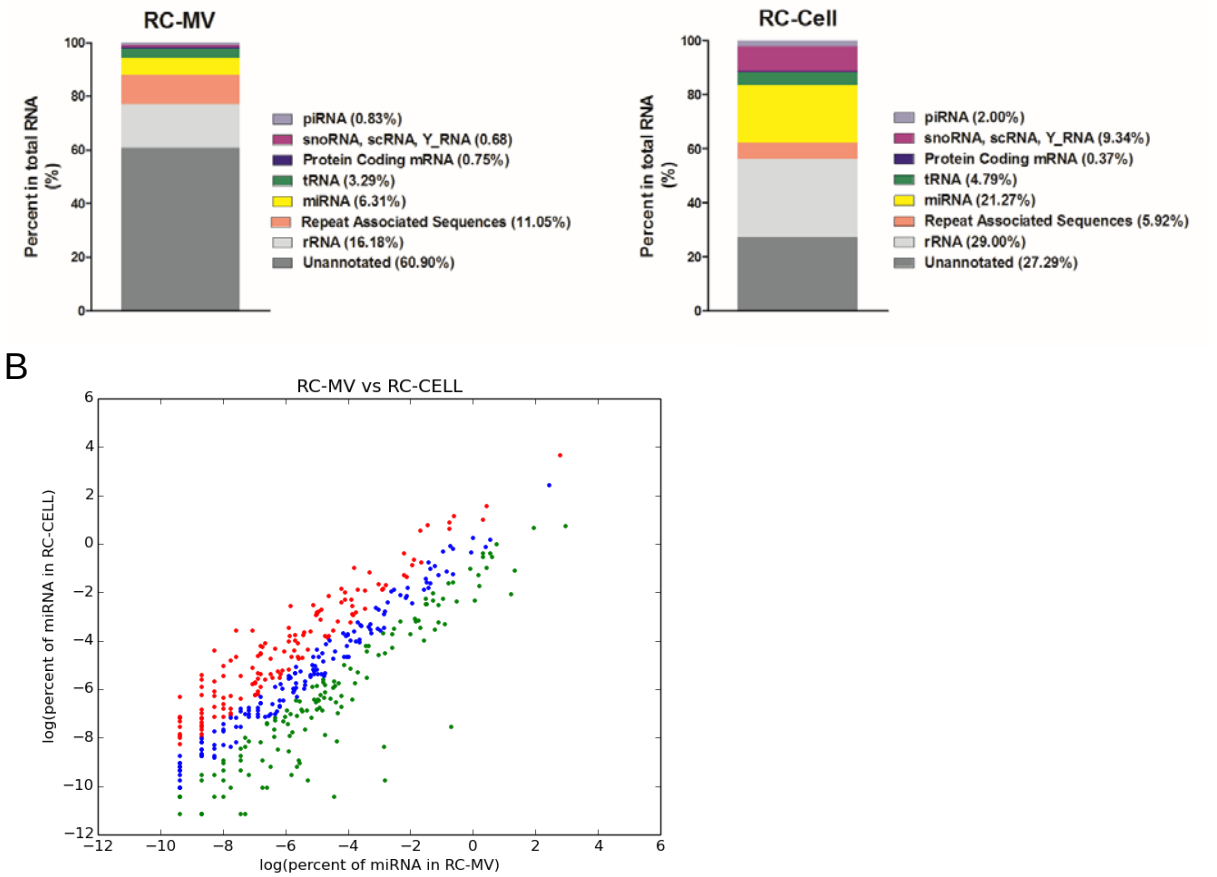

Figure 1.3 The profiles of small RNAs in RC-MVs and parent cells. (**A**) Complex populations of coding and non-coding small RNAs were found in RC-MVs in proportions that were distinct from those in the RC cells. (**B**) miRNAs in RC-MVs and RC-cells identified by RNA-seq were plotted. Red dots represent miRNAs with at least a 2-fold expression level increase in MVs than those in cells. Green dots represent miRNAs with more than a 2-fold expression level increase in cells than that in MVs. Blue indicates the overlap between these two groups. A large number of miRNAs were differentially expressed between RC-MVs and RC-cells.

6 RC-MV miRNAs (miR-451-5p, miR-223-3p, miR-122-5p, miR-142-3p, miR-150-5p, miR-126a-3p) were selected because they were only detected or were highly enriched in RC-MV based on the PCR-array (Table 1.2, highlighted in bold). We confirmed that these miRNAs were expressed at significantly higher levels in RC-MV compared to RC-Cell (Fig. 1.4), suggesting that the packaging of miRNAs into resting zone chondrocyte matrix vesicles is a selective process.

miRNA	% in RC-MVs
rno-miR-22-3p	20.27
rno-miR-21-5p	17.21
rno-miR-143-3p	11.77
rno-miR-127-3p	6.84
rno-miR-320-3p	3.50
rno-miR-134-5p	3.43
rno-miR-541-5p	1.93
rno-let-7c-5p	1.88
rno-miR-152-3p	1.77
rno-let-7b-5p	1.62
rno-let-7i-5p	1.54
rno-miR-381-3p	1.50
rno-miR-100-5p	1.49
rno-miR-99b-5p	1.36
rno-miR-370-3p	1.27
rno-miR-181a-5p	1.26
rno-miR-341	1.22
rno-miR-148a-5p	1.12
rno-miR-125b-5p	1.03
rno-miR-140-3p	0.95

Table 1.3 Top 20 most abundant miRNAs in RC-MV

miRNA	% in RC-Cells
rno-miR-21-5p	42.70
rno-miR-143-3p	11.21
rno-let-7i-5p	5.00
rno-miR-27b-3p	3.11
rno-miR-148a-3p	2.67
rno-let-7f-5p	2.35
rno-miR-22-3p	2.23
rno-miR-199a-5p	2.07
rno-miR-127-3p	1.73
rno-miR-199a-3p	1.46
rno-miR-125b-5p	1.34
rno-let-7c-5p	1.34
rno-miR-24-3p	0.96
rno-miR-100-5p	0.91
rno-miR-26a-5p	0.91
rno-miR-30a-5p	0.79
rno-miR-379-5p	0.77
rno-miR-152-3p	0.75
rno-let-7g-5p	0.73
rno-miR-99b-5p	0.67

Table 1.4 Top 20 most abundant miRNAs in RC-cells.

miRNA	% in RC-MVs	% in RC-Cells	Fold enrichment in MVs
rno-miR-122-5p	4.01E − 01	4.91E − 04	816.82
rno-miR-451-5p	6.14E − 02	7.67E − 05	800.54
rno-miR-144-3p	1.30E − 02	3.07E − 05	423.20
rno-miR-23a-5p	6.40E − 03	1.23E − 04	52.16
rno-miR-320-3p	3.50E + 00	1.29E − 01	27.10
rno-miR-490-3p	9.02E − 03	3.84E − 04	23.51
rno-miR-615	1.57E − 02	1.23E − 03	12.78
rno-miR-296-3p	1.75E − 02	1.41E − 03	12.39
rno-miR-365-5p	1.33E − 02	1.12E − 03	11.92
rno-miR-134-5p	3.43E + 00	2.88E − 01	11.90
rno-miR-664-2-5p	1.37E − 02	1.18E − 03	11.60
rno-miR-770-3p	8.78E − 02	8.15E − 03	10.78
rno-miR-148a-5p	1.12E + 00	1.04E − 01	10.76
rno-miR-129-5p	1.91E − 01	1.97E − 02	9.72
rno-miR-22-3p	2.03E + 01	2.23E + 00	9.10
rno-miR-666-5p	1.14E − 02	1.30E − 03	8.71
rno-miR-219a-1-3p	7.85E − 03	9.82E − 04	7.99
rno-miR-423-5p	3.24E − 01	4.09E − 02	7.94
rno-miR-760-3p	2.24E − 02	2.98E − 03	7.51
rno-miR-127-5p	5.82E − 01	8.26E − 02	7.05

Table 1.4 Top 20 selectively packaged miRNAs in MVs in RNA sequencing.

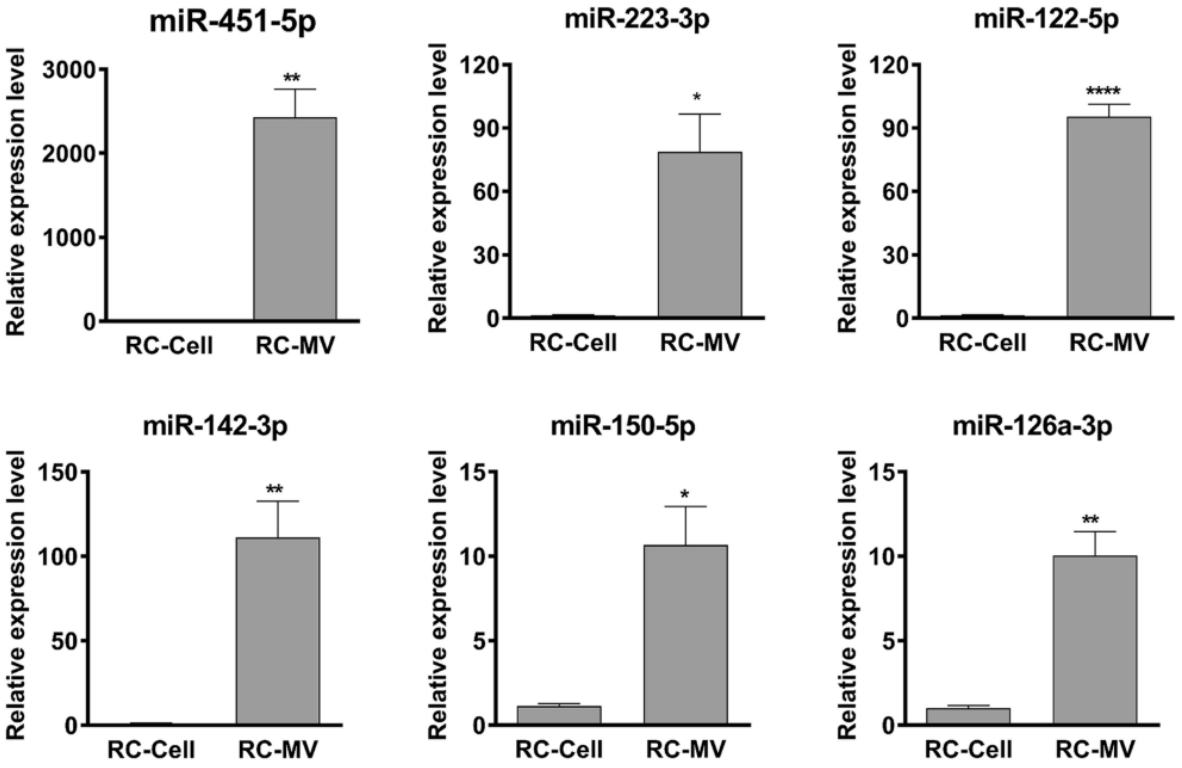

Figure 1.4 Validation of the miRNA enriched in RC-MVs compared with parent cells. Six miRNAs (miR-451-5p, miR-223-3p, miR-122-5p, miR-142-3p, miR-150-5p, miR-126a-3p) were selected for RT-qPCR assays. Consistent with previous array results, the expression of all these miRNAs were significantly higher in MVs compared to cells. These results suggest that certain miRNAs are selectively exported into MVs. *$p < 0.05$ in t-test. **$p < 0.01$ in t-test. ****$p < 0.0001$ in t-test ($n = 3$).

Functional annotation of RC-MV enriched miRNAs.

miRNAs function by binding to target mRNAs and inhibiting their translation or promoting degradation. We identified the target genes of the top most enriched miRNA in RC-MVs and analyze the signaling pathways that are potentially involved. Based on results from KEGG signaling pathway analysis, key functions of target genes included roles in stem cell regulation, Hippo signaling, Wnt signaling, Rap1 signaling, ErbB signaling, focal adhesion, and cell cycle, many of which have been shown to be involved in chondrocyte proliferation and differentiation (Table 1.6).

KEGG pathway	*P* value
Axon guidance	2.30E − 13
Signaling pathways regulating pluripotency of stem cells	6.70E − 13
Hippo signaling pathway	2.60E − 12
Wnt signaling pathway	3.20E − 09
Focal adhesion	6.80E − 09
MAPK signaling pathway	1.30E − 08
Thyroid hormone signaling pathway	3.50E − 08
PI3K-Akt signaling pathway	1.40E − 07
Rap1 signaling pathway	1.60E − 07
TGF-beta signaling pathway	3.00E − 07
cAMP signaling pathway	7.40E − 07
ErbB signaling pathway	8.20E − 07
cGMP-PKG signaling pathway	2.30E − 06
Calcium signaling pathway	2.50E − 06
Endocytosis	3.50E − 06
Oxytocin signaling pathway	3.60E − 06
Neurotrophin signaling pathway	4.30E − 06
Ras signaling pathway	5.90E − 06
Circadian entrainment	7.80E − 06
Insulin resistance	1.40E − 05
Dorso-ventral axis formation	1.70E − 05

Table 1.6 KEGG pathways targeted by the top 10 RC-MV enriched miRNAs.

MV miRNA component is dependent on the cell maturation status.

We have previously shown distinct differences in MVs that can be ascribed to the level of chondrocyte maturation. We recently reported that GC-MVs were packed with selective miRNAs. Based on these studies, we hypothesized that miRNAs were selectively packed into RC and GC MVs. To investigate unique maturation-dependent differences, we compared the PCR array results of RC-MVs to those of GC-MVs. In the 182 miRNAs detected, 10 miRNAs were identified in GC-MVs and 7 were found in RC-MVs (Fig. 1.5 A). 35 miRNAs were differently expressed between RC-MVs and GC-MVs with at least a more than 2-fold difference (increase or decrease) (Table 1.7). We also identified a group of miRNAs that showed different expression levels between RC cells and GC cells (Table 1.8). Using principle component analysis, we observed differences between RC-MVs (purple dots, top left) and GC-MVs (green dots, bottom left) (Fig. 1.5 B). While 39% of miRNAs showed differential expression level with more than 2-fold difference between RC-MVs (green dots, circled) and GC-MVs (red dots, circled), we observed a unique separation between these miRNA (Fig. 1.5 C), further supporting our hypothesis. Therefore, the

selective packaging of miRNAs into MVs exhibits spatial and maturation dependence. Interestingly, less miRNAs were found differentially expressed between RC-cells and GC-cells than between RC-MVs and GC-MVs (Fig. 1.5 C), suggesting more heterogeneous miRNA profiles exist in the extracellular vesicles than that in the cytoplasm. It is worth mentioning that the difference between RC-MVs and GC-MVs was less dramatic than between RC-MVs and RC-cells or between GC-MVs and GC-cell, since the distance at the x-axis represents the most prominent difference followed by the distance at the y-axis. This indicates that the difference between MVs and the cells that produce them is more significant than that between two cell maturation statuses (RC vs. GC) (Fig. 1.5 C).

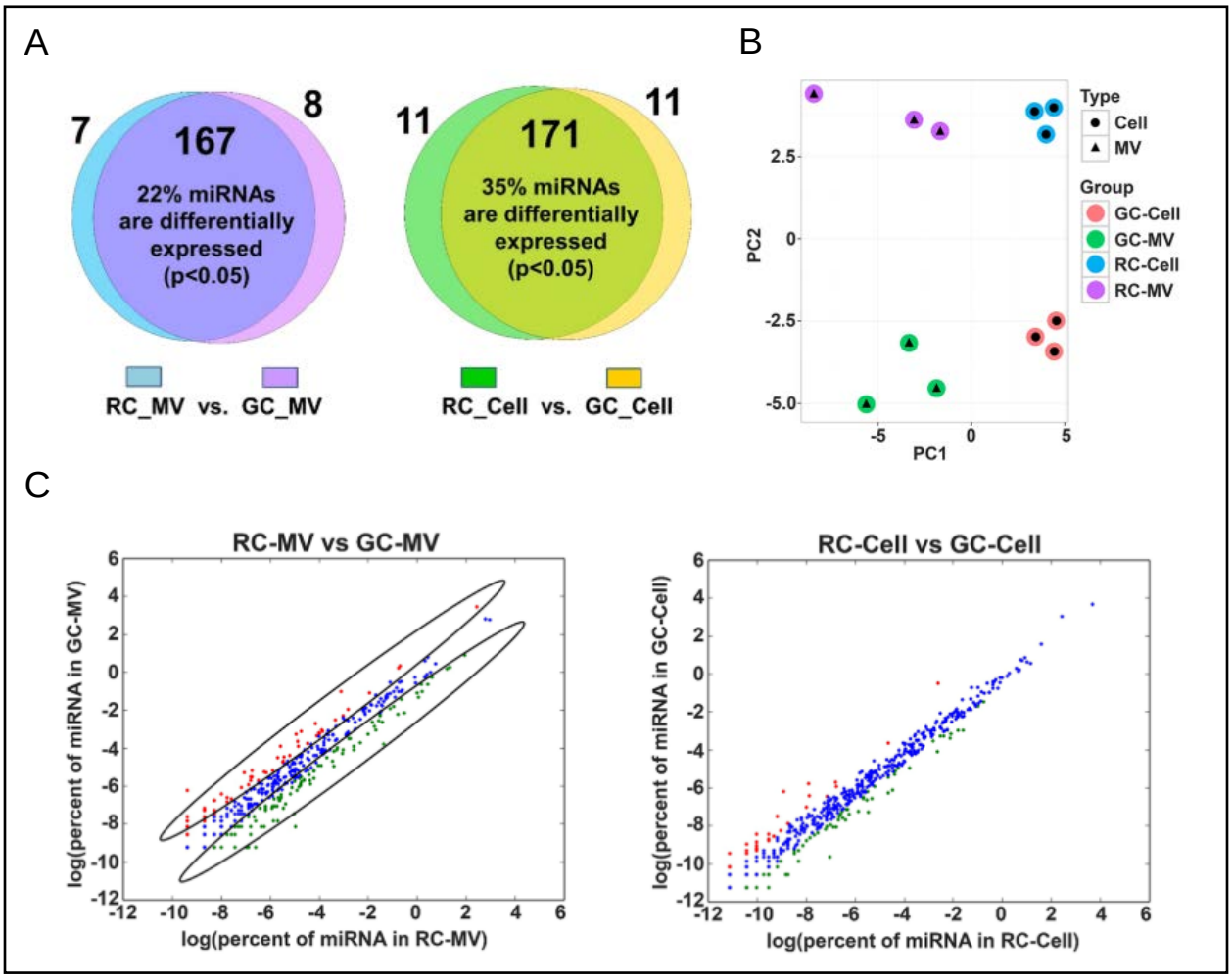

Figure 1.5 Distinct differences in the miRNAs between RC-MVs and GC-MVs. (**A**) Different miRNAs patterns were identified from PCR-array between two maturation status of chondrocytes, both in MVs and the parent cells. (**B**) Principal component analysis (PCA) of the miRNA PCR-array data for all the four different types of samples: RC-MVs, RC-cells, GC-MVs and GC-cells. The differences among these samples were clear, as larger difference showed on the x-axis direction compared to that on the y-axis. This suggests that the differences between MVs and cells were larger than between two different cell maturation stages. (**C**) Left panel: miRNAs in RC-MVs and GC-MVs identified by RNA-seq were plotted. Red dots represent miRNAs with at least a 2-fold expression level increase in GC-MVs than in RC-MVs. Green dots represent miRNAs with a more than 2-fold expression level increase in RC-MVs than in GC-MVs. Blue indicates the overlap between these two groups. A large number of miRNAs were differentially expressed between RC-MVs and GC-MVs. Right panel: similar comparison was done between RC-cells and GC-cells. Interestingly, the difference between RC-cells and GC-cells was not as large as that was seen between RC-MVs and GC-MVs.

To further validate our observations in miRNA PCR-array and RNA-Seq, we selected a set of miRNAs that are highly expressed in RC-MVs and performed RT-qPCR to compare their expression levels between RC-MVs and GC-MVs. Although we did not observe significant differences in some of the selected miRNAs such as miR126a-3p and miR-451-5p, higher expression levels of miR-122-5p and miR-150-5p were consistently seen in RC-MVs compared with GC-MVs (Fig. 1.6). This further suggests that cells at different maturation status produced different matrix vesicles with different miRNA contents.

Discussion

In this study, we demonstrate that RNA exists in MVs produced by costochondral growth plate resting zone cartilage cells. This RNA is packaged by the cells within the extracellular matrisomes and is protected by the MV membrane. RNase treatment of intact RC MVs didn't digest their RNA component, however significant degradation occurred after the membrane was disrupted by Triton X-100. Moreover, a set of miRNAs was specifically enriched in the MVs, further supporting the hypothesis that their inclusion involves a regulated process.

miRNA unique in RC-MVs	miRNAs shared in RC-MVs and GC-MVs		miRNA unique in GC-MVs
miRNA	miRNAs	Fold_change	miRNA
rno-miR-380-5p	**rno-miR-503-5p**	**8.73**	rno-miR-325-3p
rno-miR-200c-3p	**rno-miR-672-5p**	**4.31**	rno-miR-326-3p
rno-miR-874-3p	**rno-miR-450a-5p**	**3.85**	rno-miR-219-5p
rno-miR-339-3p	**rno-miR-204-5p**	**3.10**	rno-miR-298-5p
rno-miR-340-3p	**rno-miR-322-5p**	**2.78**	rno-miR-130b-3p
rno-miR-186-5p	**rno-miR-668**	**2.78**	rno-miR-760-3p
rno-miR-212-3p	**rno-miR-362-5p**	**2.37**	rno-miR-598-3p
	rno-miR-125a-3p	**2.37**	rno-miR-181c-5p
	rno-miR-329-3p	**2.29**	rno-miR-592
	rno-miR-181b-5p	**2.14**	rno-miR-499-5p
	rno-miR-130a-3p	−2.01	
	rno-miR-129-5p	−2.05	
	rno-miR-20a-5p	−2.11	
	rno-miR-133a-3p	−2.17	
	rno-miR-365-3p	−2.29	
	rno-miR-18a-5p	−2.30	
	rno-miR-143-3p	−2.39	
	rno-miR-150-5p	−2.40	
	rno-miR-195-5p	−2.48	
	rno-miR-451-5p	−2.55	
	rno-miR-497-5p	−2.57	
	rno-miR-223-3p	−2.57	
	rno-miR-582-5p	−2.60	
	rno-miR-132-3p	−2.63	
	rno-miR-133b-3p	−2.65	
	rno-miR-29b-3p	−2.74	
	rno-miR-192-5p	−2.76	
	rno-miR-126a-3p	−2.81	
	rno-miR-210-3p	−2.83	
	rno-miR-122-5p	−2.88	
	rno-miR-142-5p	−3.07	
	rno-miR-142-3p	−3.57	
	rno-miR-139-5p	−3.69	
	rno-miR-144-3p	−4.78	
	rno-miR-10a-5p	−5.93	

Table 1.7 miRNAs with different expression levels between RC-MVs and GC-MVs in miRNA PCR array. Note: miRNAs that were only detected in MVs from RC were shown in the left column. miRNAs that were only detected in MVs from GC were shown in the right column. miRNAs that were detected in MVs from both RC and GC cells, but with at least a 2-fold change and $p < 0.05$ were shown in the middle column. miRNAs that are bold area: highly enriched in RC-MVs. miRNAs that in underline area: mostly enriched in GC-MVs.

miRNA unique in RC-cells	miRNAs shared in RC-cells and GC-cells		miRNA unique in GC-cells
miRNA	miRNAs	Fold_change	miRNA
rno-miR-203a-3p	**rno-miR-503-5p**	**4.62**	rno-miR-339-5p
rno-miR-384-5p	**rno-miR-204-5p**	**4.31**	rno-miR-139-5p
rno-miR-135a-5p	**rno-miR-380-5p**	**3.64**	rno-miR-211-5p
rno-miR-335	**rno-miR-450a-5p**	**3.60**	rno-miR-760-3p
rno-miR-384-3p	**rno-miR-322-5p**	**3.07**	rno-miR-592
rno-miR-291a-5p	**rno-miR-542-5p**	**2.69**	rno-miR-142-3p
rno-miR-27a-3p	**rno-miR-376c-3p**	**2.02**	rno-miR-330-5p
rno-miR-147	rno-miR-143-3p	−2.21	rno-miR-182
rno-miR-339-3p	rno-miR-449a-5p	−2.27	rno-miR-326-3p
rno-miR-484	rno-miR-17-5p	−2.27	rno-miR-141-3p
	rno-miR-497-5p	−2.38	rno-miR-206-3p
	rno-miR-132-3p	−2.54	
	rno-miR-296-5p	−2.69	
	rno-miR-196b-5p	−2.73	
	rno-miR-582-5p	−4.06	
	rno-miR-298-5p	−4.85	
	rno-miR-10a-5p	−10.69	

Table 1.8 miRNAs with different expression levels between RC-cells and GC-cells in miRNA PCR array. Note: miRNAs that were only detected in RC cells were shown in the left column. miRNAs that were only detected in GC cells were shown in the right column. miRNAs that were detected in cells from both RC and GC, but with at least a 2-fold change and $p < 0.05$ were shown in the middle column. miRNAs that are in bold area: highly enriched in RC-cells. miRNAs that in underline area: mostly enriched in GC-cells.

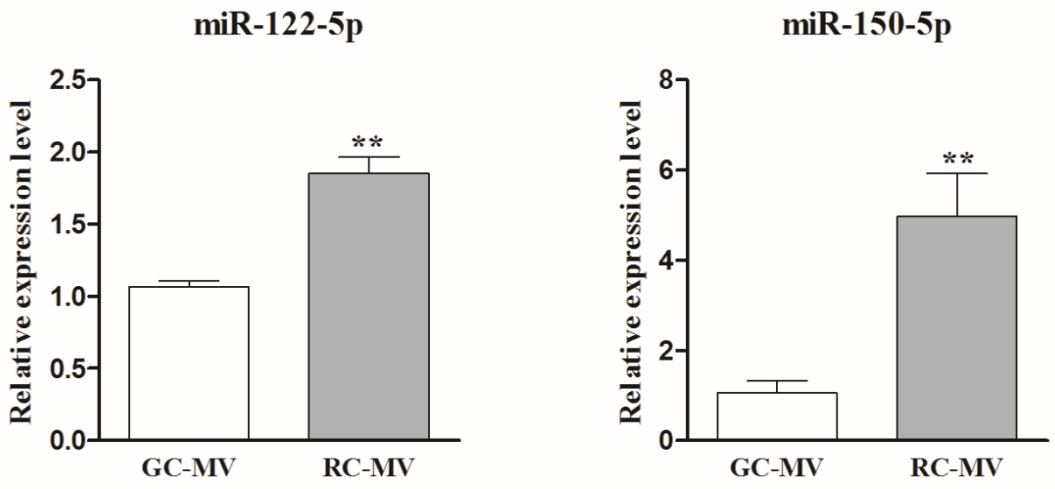

Figure 1.6 RT-qPCR was used to further validate the differences in miRNA expression between RC-MVs and GC-MVs. miR-122-5p and miR-150-5p had significantly higher expression levels in RC-MVs than GC-MVs, suggesting the miRNAs contents in MVs are associated with the cell maturation status. **$p < 0.01$ in t-test. ($n = 6$).

A variety of RNA species were found in RC-MVs, similar to RNA species found in MVs produced by GC chondrocytes[2]. The majority of the RNA pool in RC-MVs was rRNA and tRNA. It is still not clear the biological meaning of these RNAs in the regulation of extracellular matrix and cell behavior. Recently, it was reported that tRNAs can be cleaved into small fragments that

can also function as miRNAs[117]. Despite these similarities, however, PCR array and RNA-Seq showed that a large group of miRNAs was differentially expressed in MVs from RC and GC cells. Individual RT-PCR confirmed that there were significant differences in some miRNAs, such as miR-122-5p and miR-150-5p.

Chondrocytes at different maturation states in the growth plate not only produce zone-specific extracellular matrix[91,118–120], but as noted above, their matrix vesicles differ in phospholipid profile[91], enzyme content[35,91,92], and response to hormones[46,102,108]. Our results add to this by demonstrating maturation-dependent differences in miRNA composition. This suggests that MV miRNAs may be involved in the regulation of zone-specific phenotypic behavior of the cells. Our previous observation that release of matrix vesicle contents is mediated by regulated secretion of 1α,25$(OH)_2D_3$ and 24R,25$(OH)_2D_3$ and their interaction with the MV membrane[7,8,92,121], provides a mechanism for modulating the bioavailability of the miRNAs during endochondral development.

The relative differences between miRNA in RC and GC cells and the differences between RC-cells and RC-MVs or GC-cells and GC-MVs were greater than the differences between RC-MVs and GC-MVs. Chondrocytes in the resting zone of the growth plate will eventually express a growth zone phenotype, so it is likely that the phenotypic shift involves only a subset of components. MV species are heterogeneous[122], so it is also possible that not all MVs are uniformly modulated during growth plate development.

Further investigation is needed to determine whether there are general properties that define matrisomes or if they are tissue or cell specific. Others have reported the presence of RNA in the extracellular matrix of mineralizing tissues[1], and miRNAs have been found in dermis, bladder and small intestinal submucosa, which are associated with extracellular matrix-bound nanovesicles[123]. Compared to other extracellular vesicles such as exosomes, MVs are unique in many ways. MVs have a strong affinity to collagen and stay in the extracellular matrix, while exosomes are released into the culture media[2,91]. The biogenesis mechanisms of MVs and exosomes are different as well. MVs are formed by a cell “budding” mechanism, but exosomes

are formed through membrane invagination[124]. MVs released by resting zone and growth zone chondrocytes also express higher alkaline phosphatase activity than the plasma membrane and compared to membrane vesicles they secrete into the medium[91]. Furthermore, the heterogeneity of matrix vesicles produced by chondrocytes[122], indicates that they may perform multiple functions in the extracellular matrix. A recent study also found that mesenchymal stem cells secret at least three different types of microvescicles with different RNA material[125], raising the possibility that miRNAs may be differentially packaged in subsets of matrisomes and exosomes to modulate specific cell functions.

Extracellular miRNAs, exosomal miRNAs in particular, have been shown to play an important role in cell–cell communication in physiological and pathological processes[116]. Similarly, MV miRNAs may also function as a modulator during chondrogenesis by transferring to other cells in the local environment in an autocrine or paracrine manner, and thereby, regulating their gene expression and biological behavior. Functional analysis suggests that MV miRNAs are associated with stem cell regulation. miR-122-5p, which has been related to liver function and HCV infection[126], was more highly expressed in RC-MVs than GC-MVS. Others have shown that miR-122-5p targets the IGF-1R signaling pathway, which is a major player in the musculoskeletal system[127]. Our preliminary data showed that overexpression of miR-122-5p enhanced chondrocyte proliferation and maintained the stemness of these cells (data not shown). miR-150-5p, which is also higher in RC-MVs was reported to target matrix metalloproteinases[128,129]. Therefore, RC-MV enriched miRNAs may help maintain the local environment needed for RC cells to maintain a stronger proliferative capability than GC cells.

In conclusion, we demonstrated that RNA is present in MVs derived from resting zone chondrocytes, and selective miRNAs are enriched. We also observed that miRNAs are differentially expressed between RC-MVs and GC-MVs, although these differences are not as prominent as those between RC-MVs and RC-cells. Our results further suggest the importance of extracellular matrix RNA during chondrogenesis and endochondral bone formation.

Methods

Chondrocyte cultures.

Chondrocytes were isolated by enzymatic digestion of the costochondral cartilage of 125 g male Sprague Dawley rats and cultured as described by Boyan et al. previously[91]. All procedures conducted on animals followed a protocol approved by the Institutional Animal Care and Use Committee (IACUC) at Virginia Commonwealth University, and all experiments were performed in accordance with relevant guidelines and regulations. Rib cages were removed and placed in Dulbecco's modified Eagle's medium (DMEM, Life Technologies). The resting zone and growth zone cartilage was carefully dissected out, sliced, and incubated in 1% trypsin (Life Technologies) for 1 hour and 0.02% collagenase for 3 hours. After filtering by 40-micro nylon mesh, cells were collected by centrifugation, resuspended in DMEM, and plated at a density of 25,000 cells/cm^2. Fetal bovine serum (FBS, Life Technologies) was centrifuged at 184,000 × g for 4 h to remove the bovine serum exosomes. Chondrocytes were incubated in DMEM containing 10% exosome-free FBS, 1% penicillin/streptomycin and 50 mg/ml ascorbic acid (Sigma-Aldrich). Cell culture medium was changed 24 hours after plating and then at 72-hour intervals. At confluence (5–7 days), cells were subcultured using the same plating densities and allowed to return to confluence. All experiments used confluent cells in their fourth passage.

MV isolation and characterization.

MVs were isolated from chondrocyte cultures by differential centrifugation of the trypsin digested cell layer, as described in detail previously[91]. Briefly, after trypsinization (0.25% Trypsin-EDTA, Life Technologies) for 10 min, 1 × DPBS containing 10% exosome-free FBS was added to stop the reaction. The MVs were isolated by sequential centrifugation at 500 g for 5 min, 21,000 g for 20 min, and 184,000 g for 70 min. The MV pellets were washed with 0.9% NaCl and recentrifuged at 184,000 g for 70 min. The same centrifugation protocol was used to pellet the microvesicles in cell culture media. Alkaline phosphatase specific activity was measured and normalized to protein content. In addition, to validate that MVs were isolated but not plasma membrane debris, plasma membranes were isolated from the cell pellet as described previously

and alkaline phosphatase activity determined. Alkaline phosphatase specific activity was enriched in MVs at least 2 folds compared to plasma membrane, which was consistent with our previous studies. The original MVs solution was diluted 200 times for nanoparticle tracking analysis (Nanosight, Malvern, UK).

RNA extraction and detection.

RNA was isolated from MVs or cells using TRizol (Life Technologies). RNA was eluted with RNase-free water and quantified by NanoDrop spectrophotometer (Thermo Scientific). For agarose gels, 100 ng RNA was run and visualized on a 2.2% agarose gel FashGelTM System (Lonza). Bioanalyzer analyses were performed using 300 ng RNA with an RNA 600 Nano Kit (Agilent) and an Agilent 2100 Bioanalyzer (Agilent) according to manufacturer's protocol. To confirm that RNA was inside and not outside the MVs, the vesicles were treated with RNase A (10 mg/ml, Qiagen) before RNA extraction as described previously[2]. MVs were also incubated with 0.05% Triton-X 100 in order to break down the membrane in some experiments.

miRNA PCR profiling in MVs.

cDNA library preparation and miRNA profiling were performed in MV and cell RNA from RC and GC chondrocytes as described previously[2]. The microRNA PCR array (miRCURY LNA Universal RT microRNA PCR array) included 223 rat miRNAs. Details in data normalization and analysis were provided in supplementary materials.

Reverse transcription and quantitative real-time PCR (RT-qPCR).

50 ng RNA was reverse transcribed to cDNA with miScript II RT kit (Qiagen), followed by real-time qPCR using the StepOnePlus Real-time PCR System and miScript SYBR Green PCR Kit (Qiagen). Fluorescence values were quantified as starting quantities using known dilutions of standard control. The reverse primer was the universal primer in the kit. The sequences for the forward primers were synthesized by Eurofins MWG Operon: rno-miR-451-5p: AAACCGTTACCATTACTGAGTT; rno-miR-223-3p: TGTCAGTTTGTCAAATACCC; rno-miR-122-5p: TGGAGTGTGACAATGGTGTT; rno-miR-142-3p: TGTAGTGTTTCCTACTTTATGGA;

rno-miR-150-5p: TCTCCCAACCCTTGTACCAGT; rno-miR-126a-3p: TCGTACCGTGAGTAATAATGCG; rno-miR-652-3p: AATGGCGCCACTAGGGTT.

RNA sequencing (RNA-Seq).

RNA was isolated from MVs or cells using TRizol. Next generation sequencing was performed in an Illumina HiSeq. 2500 (Illumina, San Diego, CA). Data normalization and analysis were conducted with the miARma-Seq tool (see supplemental materials). Briefly, sequence quality was assessed with FASTQC; sequence reads were aligned with Bowtie2 to the NCBI Rattus norvegicus annotation release 105 (Rnor_6.0). The resulting bam files were used by miARma-Seq for tabulating discovered miRNA. Reads were also aligned to Rfam 12.3 with Bowtie2 for categorization of RNA reads. To quantify the differential expression of miRNA between samples, the count of each miRNA was normalized as the percent of all discovered miRNAs in that sample. The fold-change was calculated as the percent expression of MV miRNA/Cell miRNA. KEGG Pathway enrichment analyses were performed based on the target genes of selected miRNAs.

Statistical analysis.

Alkaline phosphatase specific activity is presented as mean ± standard error of the mean (SEM) for 6 independent MV samples per variable. RT-qPCR is presented as mean ± SEM for 3 independent samples per variable. Data were examined by ANOVA with post-hoc Bonferroni's modification of Student's t-test. A p value of less than 0.05 was considered statistically significant. Statistical analyses for miRNA array and RNA-Seq data were performed according to our previous protocol[2].

Data availability statement.

The datasets generated during the current study have been submitted to NCBI GEO database (GSE106348).

Supplementary materials

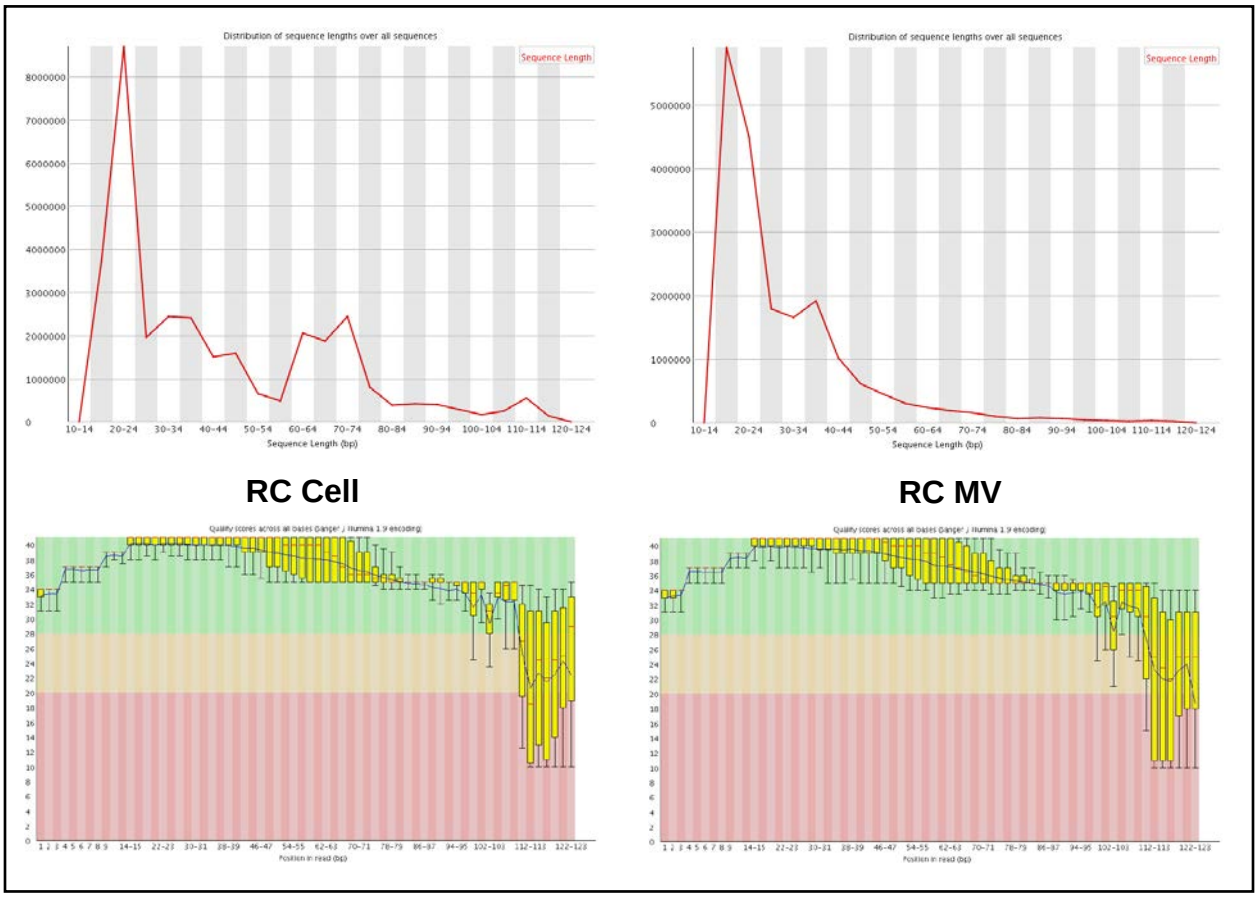

Next generation RNA sequencing

RNA was isolated from MVs or cells using TRizol. Next generation sequencing was performed in an Illumina HiSeq 2500 (Illumina, San Diego, CA). Data normalization and analysis were conducted with the miARma-Seq too (Andres-Leon, E. et al, 2016). Briefly, sequence quality was assessed with FASTQC; sequence reads were aligned with Bowtie2 to the NCBI Rattus norvegicus annotation release 105 (Rnor_6.0). The resulting bam files were used by miARma-Seq for tabulating discovered miRNA. Reads were also aligned to Rfam 12.3 with Bowtie2 for categorization of RNA reads. To quantify the differential expression of miRNA between samples, the count of each miRNA was normalized as the percent of all discovered miRNAs in that sample. The fold-change was calculated as the percent expression of MV miRNA/Cell miRNA. KEGG Pathway enrichment analyses were performed based on the target genes of selected miRNAs.

Specific MicroRNAs Found in Extracellular Matrix Vesicles Regulate Proliferation and Differentiation in Growth Plate Chondrocytes

Asmussen, N.C., Cohen, D.J., Lin, Z. *et al.* Specific MicroRNAs Found in Extracellular Matrix Vesicles Regulate Proliferation and Differentiation in Growth Plate Chondrocytes. *Calcif Tissue Int* **109,** 455–468 (2021).

Abstract

MVs are extracellular organelles produced by growth plate cartilage cells in a zone-specific manner. MVs are similar in size to exosomes, but they are tethered to the ECM via integrins. Originally associated with matrix calcification, studies now show that they contain matrix processing enzymes and microRNA that are specific to their zone of maturation. MVs produced by costochondral cartilage RC chondrocytes are enriched in microRNA 503-5p whereas those produced by GC chondrocytes are enriched in microRNA 122-5p. MVs are packaged by chondrocytes under hormonal and factor regulation and release of their contents into the ECM is also under hormonal control, suggesting that their microRNA might have a regulatory role in growth plate proliferation and maturation. To test this, we selected a subset of these enriched microRNAs and transfected synthetic mimics back into RC and GC cells. Transfecting growth plate chondrocytes with select microRNA produced a broad range of phenotypic responses indicating that MV-based microRNAs are involved in the regulation of these cells. Specifically, microRNA 122-5p drives both RC and GC cells towards a proliferative phenotype, stabilizes the matrix and inhibits differentiation whereas microRNA 22-3p exerts control over regulatory factor production. This study demonstrates the strong regulatory capability possessed by unique MV enriched microRNAs on growth plate chondrocytes and their potential for use as therapeutic agents.

Introduction

MVs are small membrane bound organelles present in the ECM of mammalian growth plates, as well as other calcifying tissues including dentine, metastatic cancers, and blood vessels.[30,31] Like exosomes, they range in size from roughly 50 to 150 nm. Whereas exosomes are found in biological fluids, MVs are tethered to the ECM via integrins.[43,130] Long associated with matrix calcification,[29,34,131] studies show that MVs also play a role in growth plate regulation.[34,36] Their importance in the avascular growth plate is related to their contents, which vary with the zone of chondrocyte maturation. MVs produced by RC cartilage cells are

enriched in neutral metalloproteinases needed for maintenance of a proteoglycan rich matrix.[36,37,132] In contrast, MVs produced by GC cartilage cells contain acid metalloproteinases, which are involved in matrix degradation prior to matrix calcification.[35–37]

Recently, studies have demonstrated that microRNAs are selectively packaged inside these MVs in both the RC and GC regions of the costochondral cartilage growth plate, with 37% of the MV microRNA significantly increased or decreased compared to cell microRNA.[2,55] Further examination showed that 22% of the microRNA in RC MVs are differentially expressed when compared to GC MVs.[55] This suggests that MV microRNA may also function in the regulation of growth plate chondrocyte proliferation, differentiation and maturation.

The costochondral cartilage growth plate provides an excellent model for assessing the role of individual microRNA in this process. Growth plate chondrocytes express phenotypic changes as they mature with corresponding alterations in the composition of the ECM. Within the costochondral cartilage growth plate the RC encompasses the reservoir of immature chondrocytes and the upper proliferative zone. Cells in the lower proliferating zone, pre and upper hypertrophic zones are referred to as GC chondrocytes. RC and GC chondrocytes can be successfully cultured and retain unique phenotypes through four passages as well as exhibiting zone-specific responses to regulatory factors and hormones.[8,91,133,134]

Various factors are involved in growth plate regulation. We selected a handful of the key regulators, described here in greater detail, to investigate if their production is affected by select microRNA transfection. Ihh and PTHrP are two factors that form a feedback loop regulating the proliferation and differentiation of chondrocytes at various stages of the growth plate.[135–137] Resting chondrocytes at the periarticular end of the fetal lone bone growth plate express PTHrP that, in turn, maintains chondrocytes in a proliferative state, delaying their differentiation to hypertrophic cells.[11,138] As chondrocytes move far enough away from the PTHrP production they stop proliferating and begin to express Ihh, marking the transition within the growth plate from proliferating to hypertrophic chondrocytes.[11,136] This Ihh diffuses through the growth plate and stimulates continued PTHrP production in the resting chondrocytes. This feedback loop

functions to regulate the distance between PTHrP and Ihh expressing zones, providing sufficient space for the proliferating chondrocytes.[137]

Additional factors are known to play important roles in regulating the growth plate. TGF-β1 stimulates bone marrow stromal cell differentiation and regulates chondrocyte maturation.[139] VEGF is produced by hypertrophic chondrocytes and is involved in the vascular invasion that occurs in the late hypertrophic region.[16,137,140] Sox9 is an early transcription factor active during chondrocyte differentiation and required for the expression of specific matrix proteins.[141,142] RUNX2 is involved in late stage chondrocyte differentiation and needed for the expression of numerous proteins.[143]

This study examines the role that MV microRNA may be playing in the regulation of growth plate chondrocytes. We hypothesize that the microRNAs exported with the highest fold change by GC chondrocytes likely play distinct roles in proliferation, differentiation, factor production and ECM composition of cells in the upper growth plate as well as the zone of maturation. Accordingly, we report on the effect that a select subgroup of GC MV microRNAs have on both RC and GC chondrocytes.

Results

Where an effect from treatment was observed it is in relation to the negative control (NC) microRNA group. Unlike the no treatment (NT) group, NC received transfection reagents and a scrambled vector microRNA.

MicroRNA Expression

Comparing the differentially expressed microRNAs in GC MVs vs. cells using a stacked bar chart we were able to identify the microRNAs exhibiting the largest fold change (Fig. 2.1 A). We selected microRNA 22-3p as a positive control due to its abundance in the cell fraction (2.2%) compared to the top three MV microRNA (≤ 0.0005 %) and its similar expression profile in RC samples (Fig. 2.1 B). We selected the three microRNA (122-5p, 223-3p and 451-5p) having log2 fold change values below -10 (Fig. 2.1 C).

Nanostring analysis using a panel of rat microRNA showed that microRNA 22-3p was present in high proportion for both RC and GC sections. MicroRNA 122-5p and 223-3p were not above background levels in either RC or GC samples and microRNA 451-5p was only found above background in the GC samples (Fig. 2.1 D). MicroRNA not above background levels are those that are at or below the threshold levels determined by the system for each sample.

A

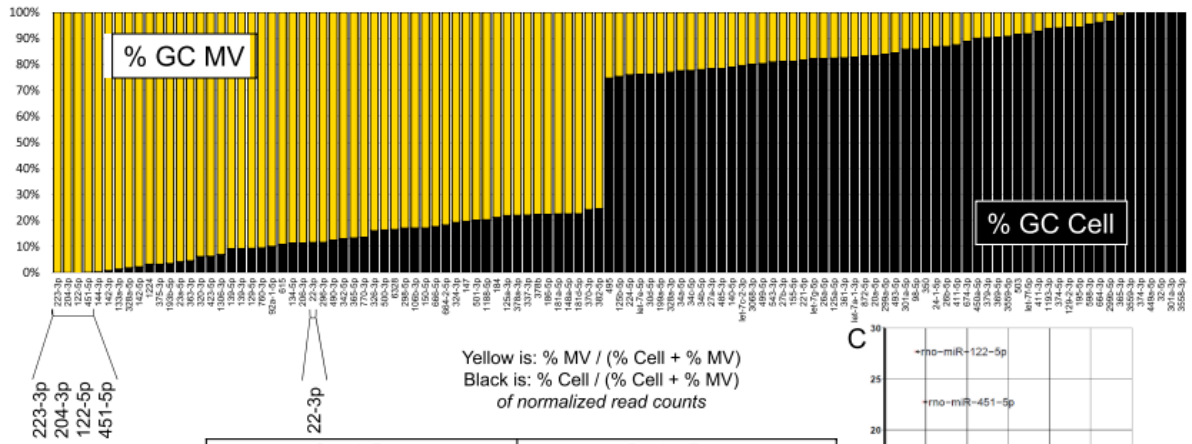

B

	Growth Zone			Resting Zone		
	Cell %	MV %	MV / Cell log2 FC	Cell %	MV %	MV / Cell log2 FC
rno-miR-223-3p	$0.0x10^{+0}$	$1.2x10^{-2}$	-11.9	$1.5x10^{-5}$	$4.3x10^{-3}$	-7.9
rno-miR-122-5p	$4.6x10^{-4}$	$1.1x10^{+0}$	-11.2	$4.9x10^{-4}$	$4.0x10^{-1}$	-9.7
rno-miR-451-5p	$1.1x10^{-4}$	$1.4x10^{-1}$	-10.3	$7.7x10^{-5}$	$6.1x10^{-2}$	-9.6
rno-miR-22-3p	$2.2x10^{+0}$	$1.7x10^{+1}$	-2.9	$2.2x10^{+0}$	$2.0x10^{+1}$	-3.2

C

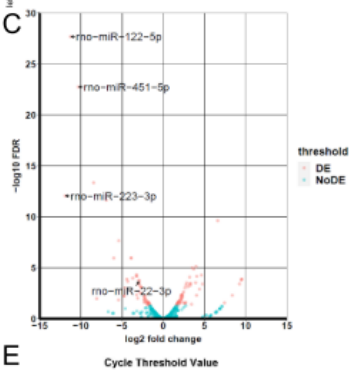

D

Probe Name	% Samples above Threshold	GC Samples			RC Samples		
		%	%	%	%	%	%
rno-miR-22	100.00	4.89	5.64	4.91	14.81	8.94	9.82
rno-miR-122	0.00	0.03	0.03	0.03	0.03	0.04	0.03
rno-miR-223	0.00	0.03	0.03	0.03	0.03	0.04	0.03
rno-miR-451	50.00	0.06	0.08	0.06	0.03	0.04	0.03
Threshold Levels		0.03	0.03	0.03	0.03	0.04	0.03

E

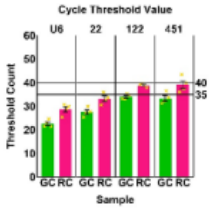

Figure 2.1 MicroRNA expression of resting zone (RC) and growth zone (GC) cells. (**A**) Differentially expressed microRNAs (FDR < 0.05) found in MVs as compared to cell isolate. (**B**) Expression of select four microRNA in RC and GC samples based on normalized read counts from EdgeR. (**C**) Volcano plot of microRNA in GC cells compared to MVs, red denotes differentially expressed microRNA with FDR < 0.05, teal are not differentially expressed. (**D**) Nanostring analysis of RC and GC ex-vivo tissue samples, minimum threshold levels determined by Nanostring system. (**E**) MicroRNA RT-qPCR cycle threshold values for RC and GC ex-vivo tissue samples. Mean ± SE.

MicroRNA RT-qPCR on RC and GC tissue samples had CT values below 35 for snRNA U6 and microRNA 22-3p. MicroRNA 122-5p and 451-5p groups had three out of four GC samples below 35, all RC samples were between 35 and 40 but one in 451-5p group that was above 40

(Fig. 2.1 E). For microRNA 122-5p the standard curve stopped amplifying at 0.06 ng/μL and for microRNA 451-5p amplification was no longer detected at 0.02 ng/μL with a total cycle count of 60. Examining the melt curves for all eight groups shows tight clustering and a peak appearing within or near to the expected T_m range of 74.5-76˚C for these primers (Supplemental Fig. 2.1).

Response of GC Chondrocytes

Chondrocyte Proliferation and Apoptosis

MicroRNA 122-5p increased total DNA at 24 and 48 hours while microRNA 451-5p decreased it. MicroRNA 22-3p and 223-3p had no effect at 24 hours whereas at 48 hours microRNA 22-3p decreased and microRNA 223-3p increased total DNA (Fig. 2.2 A,B). We normalized microRNA treatments to controls for 12 separate experiments and observed a consistent increase in DNA production as a result of microRNA 122-5p while being unaffected by microRNA 22-3p, 223-3p or 451-5p (Fig. 2.2 C). We examined proliferation rates using EdU incorporation at 24 and 48 hours. MicroRNA 122-5p and 451-5p increased the proliferation rate at 24 hours while all four microRNAs increased proliferation at 48 hours (Fig. 2.2 D,E). We examined whether the acute impact of microRNA 122-5p on proliferation was present at earlier time points. MicroRNA 122-5p increased proliferation at 0, 12 and 24 hours compared to NC after which it fell below NC for 36 and 48 hours (Fig. 2.2 F). Examining metabolic activity, there was increased MTT reduction in GC cells transfected with microRNA 122-5p at 48 hours (Fig. 2.2 G).

None of the select microRNA appeared to induce cellular apoptosis. No change was observed between NC and any of the microRNAs with TUNEL (DNA fragmentation) (Fig. 2.2 H), Bax / Bcl2 levels (Fig. 2.2 I) or p53 levels (Fig. 2.2 J).

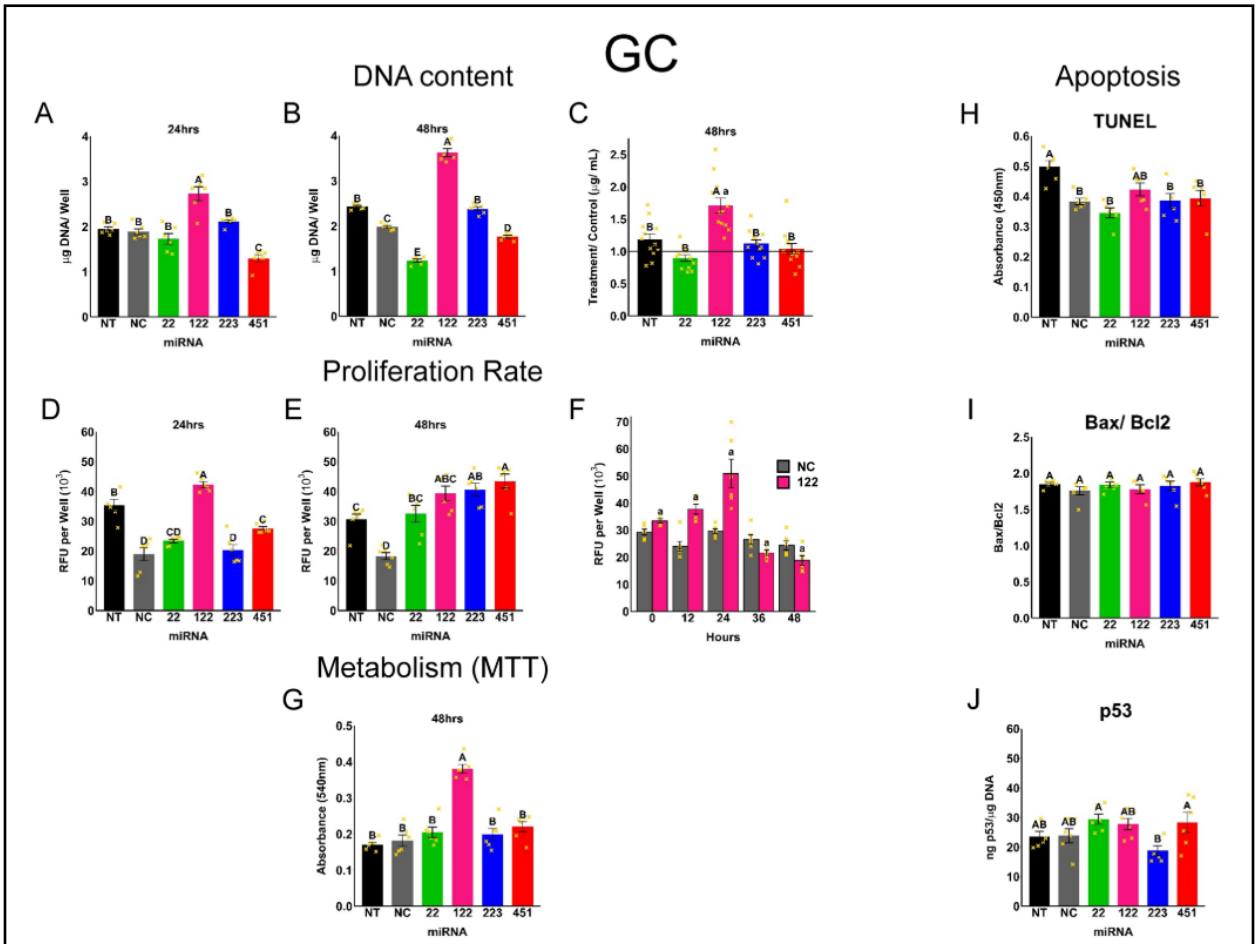

Figure 2.2 Proliferation and apoptosis of GC cells. (**A, B**) Total DNA at 24 & 48 hrs. (**C**) Treatment over control of total DNA at 48 hrs for twelve experiments. (**D, E**) Proliferation rate at 24 & 48 hrs, (**F**) time course every 12 hrs for 48 hrs. (**G**) Metabolism of GC cells at 48 hrs. (**H–J**) Apoptosis indicators (Tunnel, Bax / Bcl2 ratio and p53) were assayed at 48 hrs. Mean ± SE, groups not sharing a letter are statistically different (α = 0.05), *NT*: no treatment, *NC*: negative control microRNA.

Alkaline Phosphatase Activity and ECM Composition

Chondrocytes demonstrated an increase in alkaline phosphatase activity in response to microRNA 223-3p with 122-5p and 451-5p having a significant reduction compared to NC (Fig. 2.3 A). Looking at 5 separate experiments confirmed these results with microRNA 223-3p increased compared to NC and microRNA 122-5p and 451-5p decreased (Fig. 2.3 B).

Production of two ECM components – sGAGs and collagen 2 – was sensitive to microRNA transfection. MicroRNA 122-5p increased sGAG levels compared to all other groups while decreasing levels of collagen 2 (Fig. 2.3 C,D). Collagen X was also examined and found to be below the standard for all samples (data not shown).

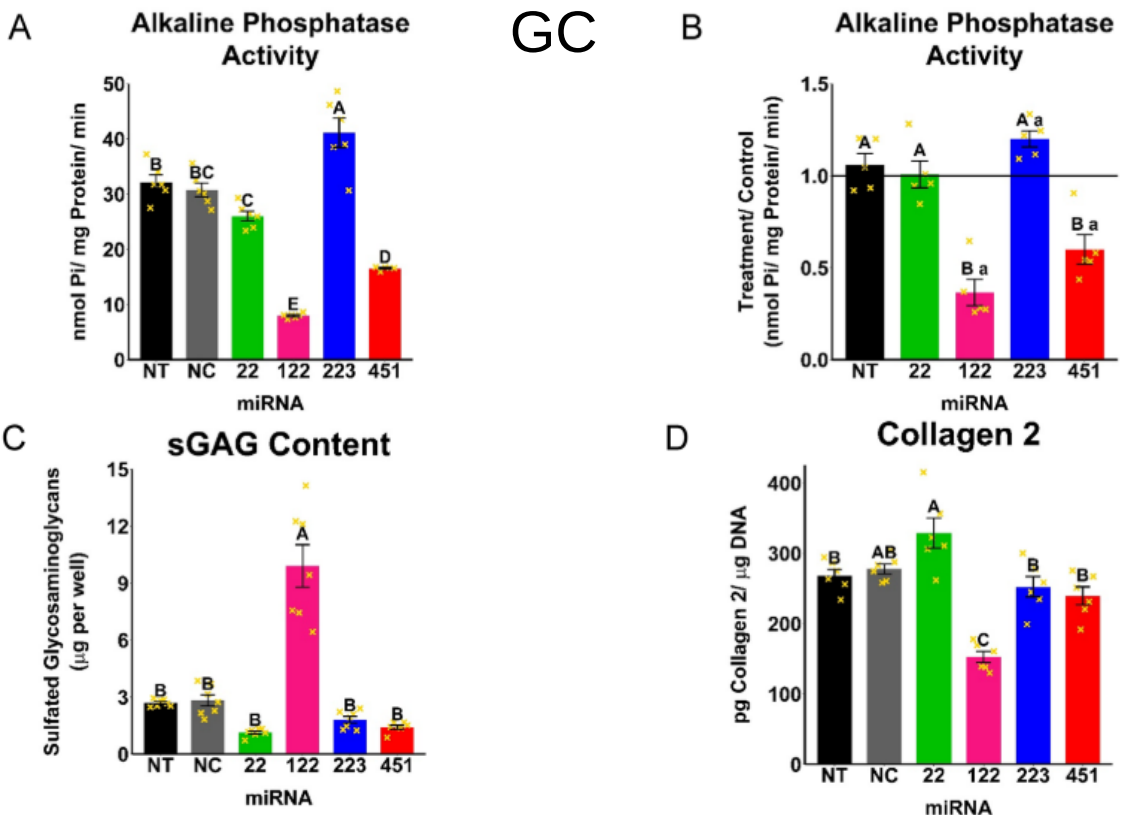

Figure 2.3 Alkaline phosphatase activity and ECM composition of GC cells. (**A, B**) Alkaline phosphatase activity of GC cells at 48 hrs & treatment over control of five experiments. (**C, D**) sGAG & collagen 2 production by GC cells. Mean ± SE, groups not sharing a letter are statistically different (α = 0.05), *NT*: no treatment, *NC*: negative control microRNA.

Growth Plate Factors

Seven different ELISAs were used to investigate the production of growth plate proteins (BMP-2, Ihh, OPG, PHTrP, RANKL, TGF-β1 and VEGF) with protein levels normalized to total DNA per well. BMP-2 was below the standard for all samples (data not shown). VEGF increased following microRNA 22-3p transfection and decreased in response to microRNAs 122-5p and 451-5p (Fig. 2.4 A). OPG production increased in response to microRNA 122-5p or 451-5p, while RANKL was not detected in any of the samples (Fig. 2.4 B,C). GC cells exhibited an increase in Ihh and PTHrP production following microRNA 22-3p and a decrease following microRNA 122-5p (Fig. 2.4 D,E). Transfected chondrocytes increased latent TGF-β1 as a response to microRNA 22-3p compared to the control cultures, but levels were not different than NT and no change in active TGF-β1 was observed (Fig. 2.4 F,G).

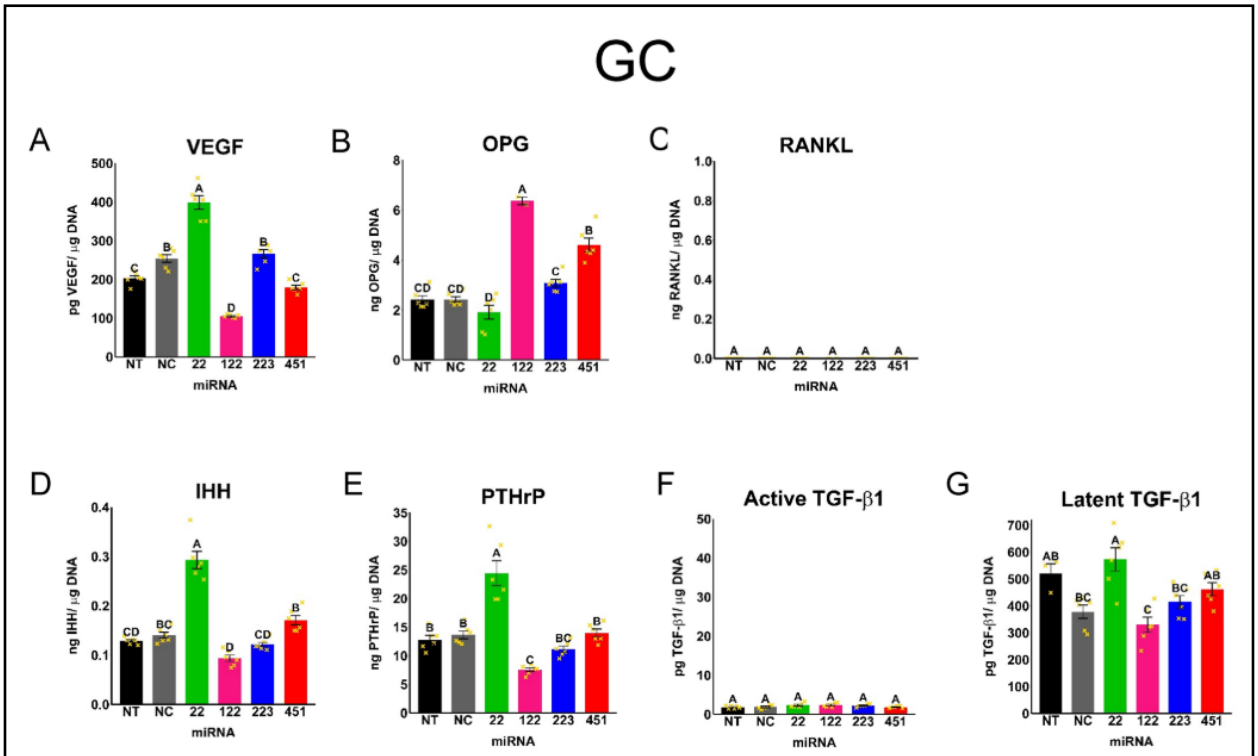

Figure 2.4 Growth plate factor production of GC cells at 48 hrs (**A**) VEGF, (**B**) OPG, (**C**) RANKL, (**D**) Ihh, (**E**) PTHrP, (**F**) Active TGF-β1 and (**G**) Latent TGF-β1. Mean ± SE, groups not sharing a letter are statistically different (α = 0.05), *NT*: no treatment, *NC*: negative control microRNA.

Response of RC Chondrocytes

Proliferation and Apoptosis

Total DNA, TUNEL and p53 of RC chondrocytes were assessed at 48 hours. Total DNA increased in cells following microRNA 122 transfection whereas it was decreased by microRNAs 22-3p, 223-3p and 451-5p (Fig. 2.5 A). Apoptosis as measured by TUNEL and p53 was unaffected by the four microRNAs (Fig. 2.5 B,C).

Alkaline Phosphatase Activity and ECM Composition

RC chondrocytes exhibited a reduction in alkaline phosphatase activity for all four microRNA when compared to control with microRNA 122 resulting in a significantly greater decrease (Fig. 2.5 D). We normalized the five microRNA treatments over control (NT) for three separate experiments at 48 hours and observed a similar response (Fig. 2.5 E). ECM composition was assessed by sGAG levels with microRNA 22-3p resulting in a decrease in sGAG levels and microRNA 122-5p an increase (Fig. 2.5 F).

Growth Plate Factors

Ihh and PTHrP were found to be increased as a result of microRNA 22-3p transfection and decreased following transfection with microRNA 122-5p (Fi g. 2.5 G,H).

Selective microRNA Inhibitors

In order to examine the sensitivity of the mimics used in the transfection experiments, RC and GC chondrocytes were transfected with a select microRNA inhibitor (22-3p or 122-5p) at

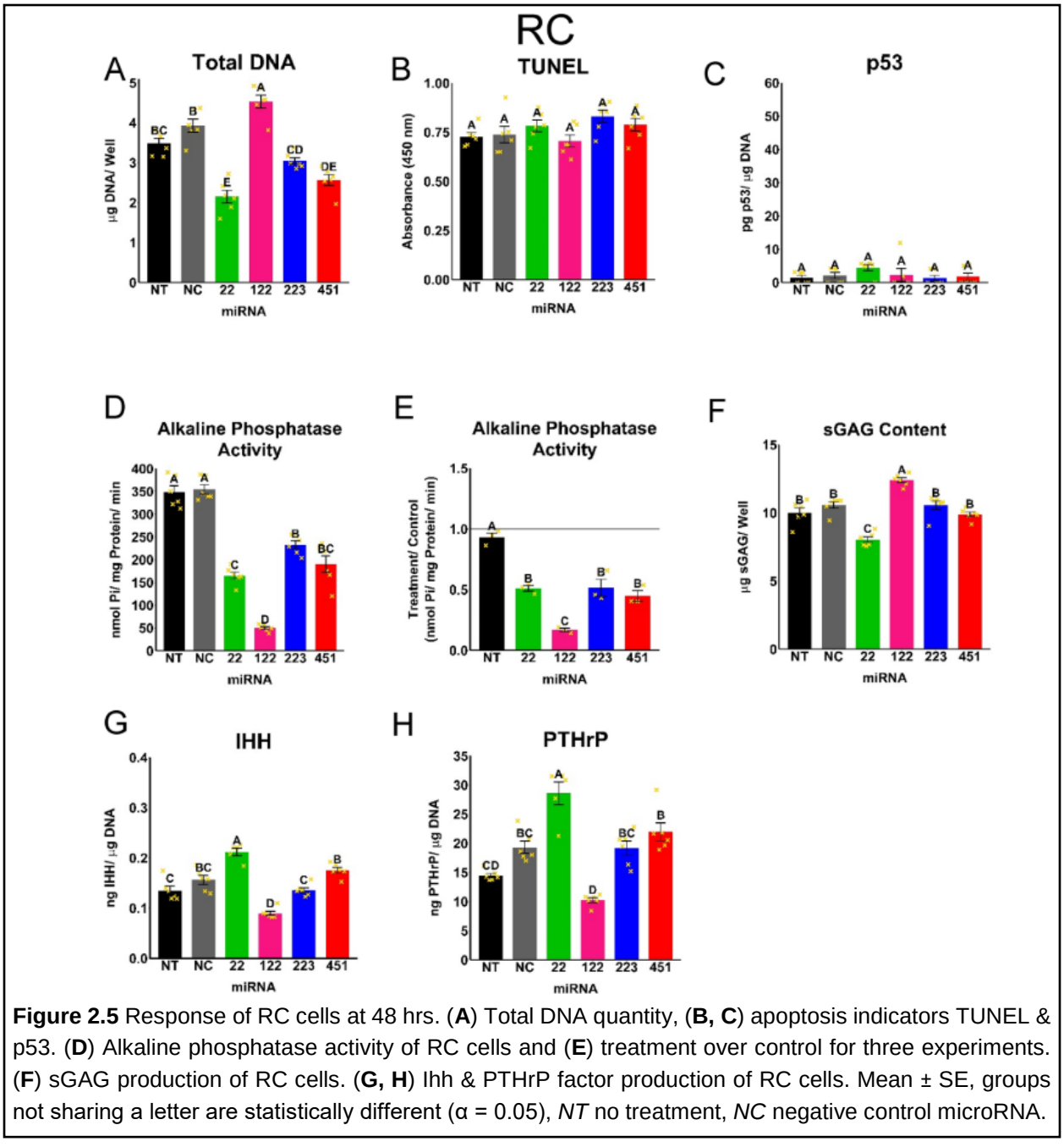

Figure 2.5 Response of RC cells at 48 hrs. (**A**) Total DNA quantity, (**B, C**) apoptosis indicators TUNEL & p53. (**D**) Alkaline phosphatase activity of RC cells and (**E**) treatment over control for three experiments. (**F**) sGAG production of RC cells. (**G, H**) Ihh & PTHrP factor production of RC cells. Mean ± SE, groups not sharing a letter are statistically different (α = 0.05), *NT* no treatment, *NC* negative control microRNA.

three different concentrations, with and without the corresponding mimic along with a NT group and a mimic only group. Alkaline phosphatase activity and total DNA production were assayed.

Response of GC Chondrocytes

MicroRNA 22-3p decreased DNA production and this effect was reversed by transfection alongside the inhibitor with inhibitor alone having a slight reduction in DNA production compared to NT (Fig. 2.6 A). Alkaline phosphatase activity was not significantly different for all but the mimic plus inhibitor (30 or 50 nM) groups where slight decreases were observed (Fig. 2.6 B).

MicroRNA 122-5p inhibitor alone had no effect on total DNA production, 122-5p mimic alone increased DNA production and mimic + inhibitor was able to reduce DNA production but not back to NT levels (Fig. 2.6 C). Alkaline phosphatase activity underwent no change with inhibitor alone but was significantly reduced when transfected with 122-5p mimic on its own. The addition of 122-5p inhibitor to the mimic increased the alkaline phosphatase activity but was unable to return it to the NT level (Fig. 2.6 D).

Response of RC Chondrocytes

MicroRNA 22-3p decreased total DNA production when compared to all other groups. The addition of inhibitor to the mimic was able to bring DNA production nearly back to the NT group. Transfection with inhibitor alone resulted in a slightly greater decrease of total DNA production compared to mimic combined with inhibitor (Fig. 2.6 E). Alkaline phosphatase activity was largely unaffected by the 22-3p inhibitor alone with the highest concentration (50 nM) resulting in a slight decrease. Mimic alone resulted in a significant decrease that was largely reversed by addition of inhibitor (Fig. 2.6 F).

MicroRNA 122-5p inhibitor alone had no significant effect on total DNA production, mimic alone produced a significant increase in DNA production that was partially reversed by addition of inhibitor (Fig. 2.6 G). Similarly, the addition of inhibitor on its own resulted in no significant difference in alkaline phosphatase activity, whereas the 122-5p mimic on its own significantly

reduced alkaline phosphatase activity, which was partially reversed by addition of inhibitor (Fig. 2.6 H).

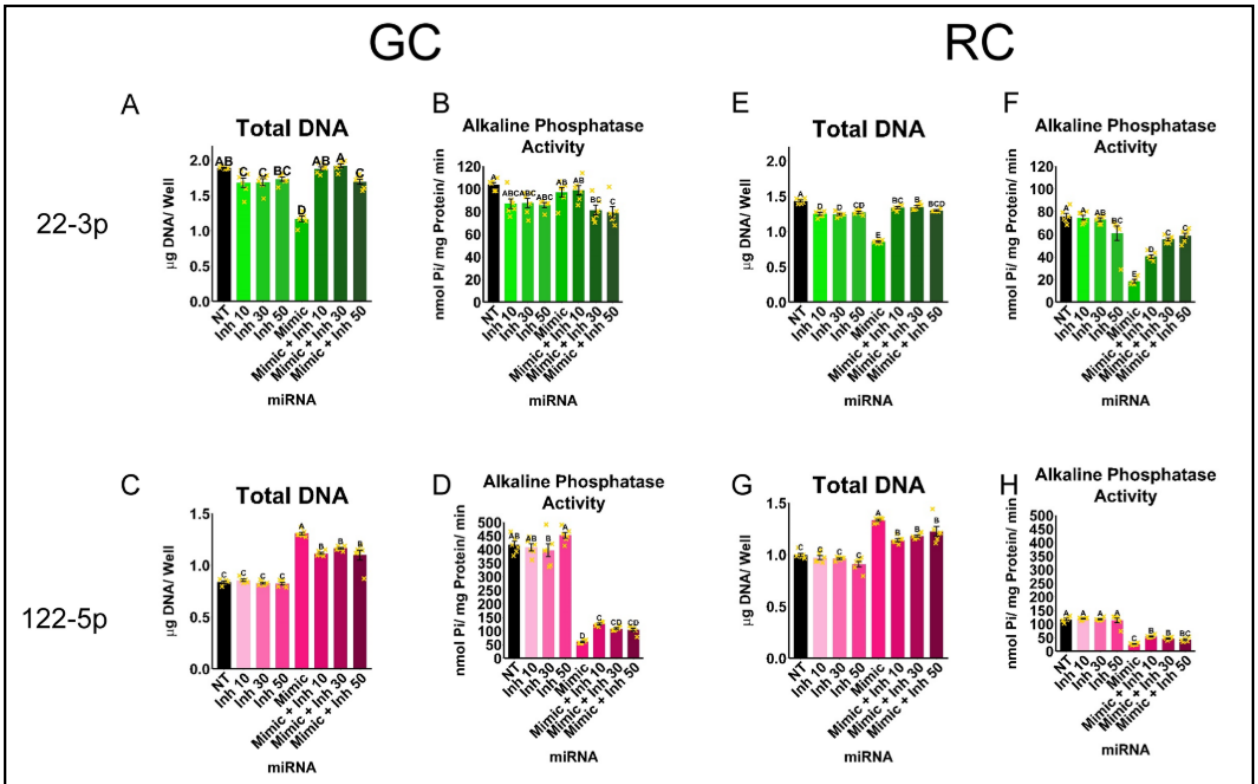

Figure 2.6 Selective microRNA inhibitors effect on GC and RC cells at 48 hrs. (**A–D**) Response of GC cells, (**A, B**) total DNA & alkaline phosphatase activity following transfection with 22-3p, (**C, D**) following transfection with 122-5p. (**E–F**) Response of RC cells, (**E, F**) total DNA and alkaline phosphatase activity following transfection with 22-3p, (**G, H**) following transfection with 122-5p. Mean ± SE, groups not sharing a letter are statistically different (α = 0.05), *NT*: no treatment.

Angiogenesis

MicroRNA 122-5p had a clear visual effect on HUVECs when compared to scrambled vector transfection (Fig. 2.7 A) and also resulted in a decrease in total DNA production when compared to NC (Fig. 2.7 B). MicroRNA 22-3p, 122-5p, 223-3p, and 451-5p all resulted in a decrease in the connection length at 20 hours with only microRNA 122-5p and 451-5p driving a reduction in connection number (Fig. 2.7 C).

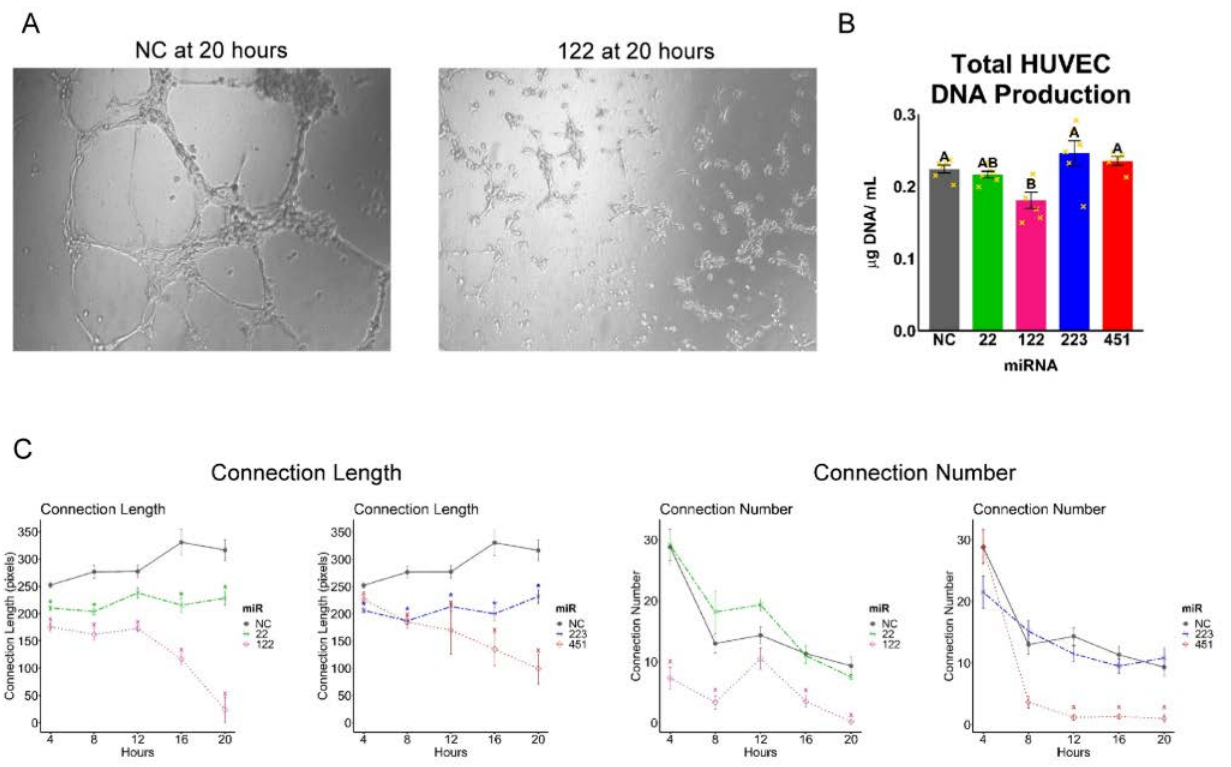

Figure 2.7 Angiogenesis of HUVEC cells following transfection. **(A)** Representative images of NC and 122 transfection at 20 hours. **(B)** Total DNA production by HUVEC cells at 48 hours. **(C)** Connection length and connection number counted every 4 hours over a 20 hour time period. Mean ± SE, groups not sharing a letter are statistically different (α = 0.05), * and x are statistically different from NC (α = 0.05), *NC:* negative control microRNA

Discussion

This study using rat costochondral cartilage cell cultures as a model system, demonstrates the potential of growth plate chondrocyte microRNA, packaged in MVs and exported into the ECM, to exert a regulatory influence back on the chondrocytes in a paracrine and potentially autocrine fashion. These selectively packaged microRNA produce clear and maturation zone dependent effects on growth plate chondrocytes.[2,55] Establishing regulatory capability for MV microRNAs lays out additional roles for MVs, providing protection against degradation for microRNA and directly modulating chondrocyte gene expression.[35,64] MicroRNA have robust potential as a regulatory molecule as a result of each microRNA's ability to impact the production of multiple proteins within a cell.

Our study examined the effects that MV microRNAs can exert on growth plate chondrocytes. Previous work examined the importance of microRNA for a functioning growth plate

and the role that microRNAs have in regulating factor production.[144,145] This study found two microRNA that exhibited significant maturation dependent regulatory effects on chondrocytes. MicroRNA 22-3p demonstrated an ability to modulate ECM and factor production by both RC and GC chondrocytes. MicroRNA 122-5p demonstrated a maintenance type of effect increasing production of components associated with healthy cartilage while delaying terminal differentiation and increasing proliferation.

MicroRNA 122-5p transfection resulted in consistent responses from both RC and GC cells that are characteristic of proliferating chondrocytes. Cell proliferation increased, alkaline phosphatase activity decreased and sGAG production increased (with GC cells approaching levels found in RC cells). To further study the maintenance aspect of microRNA 122-5p we used HUVEC cells to examine the potential angiogenic effect of microRNA 122-5p in the growth plate (an avascular tissue). When transfected into HUVEC cells, microRNA 122-5p drove a reduction in both connection number and length between the cells indicating a potential inhibitory effect on blood vessel formation useful for avascular tissue maintenance.

A stark response demonstrated by both RC and GC chondrocytes to microRNA 122-5p transfection was an increase in proliferation that may be connected to the reduction of both Ihh and PTHrP production that was also observed. Proliferating cells of the growth plate are located within the PTHrP and Ihh feedback loop sandwiched by resting cells producing PTHrP on one end and cells differentiating to a hypertrophic phenotype and producing Ihh on the other. Between these two regions chondrocytes are proliferating with expression of Ihh and PTHrP largely absent.[136] Whether the reduction in PTHrP and Ihh is driving the increase in proliferation or if other effectors are involved is unknown. What was made very clear is that microRNA 122-5p has numerous impactful effects on growth plate chondrocytes (increasing proliferation, stopping vascularization and maintaining production of ‘healthy’ ECM).

The response of both RC and GC cells to microRNA 22-3p was unexpected. Transfection with microRNA 22-3p was able to impact the ECM composition of both chondrocyte populations, as well as proliferation and differentiation markers of RC cells. Its strongest impact was on factors

produced by cells from both growth plate zones. Although microRNA 22-3p was active in both RC and GC chondrocytes, it did not appear to drive either population of cells toward a more proliferative or hypertrophic phenotype. Instead, it increased the production of proteins that are characteristic of both regions. MicroRNA 22-3p's relatively abundant presence in RC and GC cells and their corresponding MVs, the observed response of chondrocytes to microRNA 22-3p transfection not being characteristic of either zone indicate that it is potentially functioning as part of a larger microRNA regulatory network within growth plate chondrocytes.[146]

As a result of microRNA 22-3p and 122-5p exhibiting the majority of effects we decided to assess the specificity of these mimics by transfecting them along with their specific inhibitor. Both mimics and inhibitor are transfected as double stranded RNA molecules that require cellular processing in order to be activated. We observed partial or complete reversal of the effects of the mimic when transfected alongside specific inhibitors. It is likely that a portion of the mimics are loaded into the RNA induced silencing complex and able to regulate available mRNA before being sequestered by the co-transfected inhibitors even when the inhibitor is administered at three times the concentration of the mimic.

In addition to examining the specificity of the mimics, we wanted to verify the presence of these microRNA in tissue samples to ensure they are not an artifact of cell culture. Our first approach was using a NanoString microRNA panel to examine RNA isolated from GC and RC tissue samples. At first glance, the absence of microRNA 122-5p and 223-3p in any of the tissue samples and microRNA 451-5p in the RC tissue samples are concerning. However, in the RNAseq data these microRNA range from 0 to 4.9 x 10^{-4}% in the cell samples and 4.3 x 10^{-3} to 1.1% in the MV samples. The quantity of MV RNA that is isolated from cell culture preparations is very low compared to the corresponding cell pellet (average of 300 times less according to bioanalyzer analysis, data not shown). These three microRNA (122-5p, 223-3p & 451-5p) were found primarily if not exclusively in the MV isolation and so are likely to be present in extremely low numbers in actual tissue. Results from the NanoString are not conclusive that the microRNA are *not* present in native tissue given the low read numbers in the RNAseq data from tissue

culture. Colleagues in our lab have found microRNA 122-5p and 451-5p in articular cartilage using qPCR from *ex vivo* samples.[147] Additionally, a recent publication comparing four different microRNA quantification methods (small RNAseq, FirePlex, EdgeSeq and nCounter) found the nCounter system to be the least sensitive of the four with fewer microRNAs determined to be above background levels.[148] MicroRNA 22-3p was found by the NanoString panel in both RC and GC tissue samples (average of 11.19% and 5.15% respectively). These values are similar to the results from the small RNAseq data (cells: 2.2% RC and GC, MV: 20% RC and 17% GC). These data do confirm the presence of both microRNA 22-3p and 451-5p in *ex-vivo* GC tissue samples.

In order to further validate the presence of the microRNA in tissue we performed RT-qPCR on RNA isolated from RC and GC tissue. The standard curve generated produced an upward trend in CT values as the dilution increased for snRNA U6 (positive control) and microRNA 22-3p. There is no clearly discernable trend for microRNAs 122-5p and 451-5p however the ability to amplify a detectable product was lost as dilutions increased. In a similar fashion all snRNA U6 and microRNA 22-3p samples fell below 35 CT (a commonly used cut off point for mRNA RT-qPCR) along with all but one of the GC microRNA 122-5p and 451-5p groups. Both the increase in CT values from microRNA 22-3p to microRNAs 122-5p and 451-5p and the standard curve becoming undetectable for microRNAs 122-5p and 451-5p follows the trend that was observed in the small RNAseq data with microRNA 22-3p being more abundant than either microRNAs 122-5p or 451-5p. These RT-qPCR results provide compelling evidence of their presence at a low level in tissue (Supplemental Fig. 2.1).

Investigating the *in vivo* chondrocyte response to microRNA 22-3p and 122-5p is an intriguing next step. MicroRNA 122-5p transfection was able to generate a response from both RC and GC cells that was analogous to proliferating chondrocytes while the strong factor response to microRNA 22-3p makes both microRNAs interesting candidates for future animal studies. Delivery of targeted cocktails of microRNA packaged into vesicles look to be potential methods for treating cartilage disorders. A more detailed understanding of MV packaging and

release would be beneficial in designing treatment delivery mechanisms that closely mimic existing biological systems.

This study demonstrates that microRNA, first discovered in cell culture isolations, are likely involved in the complex regulation of growth plate chondrocytes as they proliferate and mature. These microRNA that are exported into the ECM within MVs are able to produce phenotypic effects on growth plate chondrocytes that fall within understood zonal behaviors for these cells. Gaining a better understanding of the regulation that microRNA production and export falls under as well as a more precise view into the regulatory effects that individual microRNA are able to elicit will be fundamental in selecting microRNA for potential treatment avenues.

Experimental Procedures

Chondrocyte Cultures

Costochondral cartilage was removed from 100 to 125 g male Sprague Dawley rats, isolated by enzymatic digestion and cultured as previously described by Boyan *et al.*[8,91] All animal procedures followed a protocol approved by the Institutional Animal Care and Use Committee at Virginia Commonwealth University. Animals were killed by CO_2 asphyxiation followed by cervical dislocation. Rib cages were removed by sharp dissection and placed in Dulbecco's modified Eagle's medium (DMEM; Life Technologies, Carlsbad, CA) containing 1 g/L glucose with 150 U penicillin/mL and 150 µg streptomycin/mL (Lonza, Basel, Switzerland). Tissue was removed from around the ribs and RC and GC cartilage sections were dissected out. A small region of GC tissue was between the bone and RC tissue and the three different regions were clearly visible under a dissection scope. One or two transition slices between the RC and GC regions were discarded and the dissected tissue incubated overnight in DMEM. RC and GC slices were incubated in 0.25% trypsin-EDTA (Gibco, Gaithersburg, MD) for 1 hour, washed and incubated in 0.2% collagenase type II (Worthington Biochemical, Lakewood, NJ) for 3 hours on a shaker. Cells were filtered through a 40 µm nylon mesh strainer, collected by centrifugation (751 g for 10 minutes) and re-suspended in DMEM FM (1 g/L glucose DMEM with 10% FBS, 50 U/mL penicillin, 50 µg/mL streptomycin and 50 µg/mL ascorbic acid). Cells were plated at a density of

20,000 GC cells/cm^2 or 10,000 RC cells/cm^2 and incubated at 37˚C and 5% CO_2. The culture media were changed 24 hours after plating and then every 48 hours thereafter. Confluent cells were passaged using 0.25% trypsin and plated as above. Fourth passage cells were used for all experiments.

Bioinformatic Analysis

Small RNA-seq data from chondrocytes and MVs that were isolated in a previous study (Lin *et al.* 2016) were used for this study.[2] Reads were aligned against the rat genome and analyzed using the miARma-Seq tool.[149] In brief the read quality was assessed using FASTQC; reads were aligned to the NCBI *Rattus norvegicus* annotation release 105 (Rnor_6.0) using Bowtie2. Resulting bam files were processed by miARma-Seq to quantify microRNAs and differential expression calculated using edgeR.[150] Normalized read counts from edgeR were used to determine the percent of each microRNA in the sample $percent\ X\ microRNA = \left(\frac{specific\ microRNA}{total\ microRNA} * 100\right)$. Log 2 fold change of GC microRNA in cell vs. MV was visualized against –log 10 false discovery rate in a volcano plot and the three microRNA with a log 2 fold change less than -10 highlighted. Differentially expressed microRNA with a false discovery rate (FDR) less than 0.05 were loaded into a stacked bar chart with $\%\ GC\ MV = \frac{percent\ MV\ microRNA}{percent\ total\ (MV+\ Cell)\ microRNA}$ over $\%\ GC\ Cell = \frac{percent\ Cell\ microRNA}{percent\ total\ (MV+\ Cell)\ microRNA}$ for each of the 111 DE microRNA.

Nanostring

We used NanoString's nCounter system to quantify the presence of microRNA in costochondral tissue. Tissue slices were harvested, cleaned and directly transferred to Qiazol lysis reagent (Qiagen, Hilden, Germany) for homogenization with no intermediate. In brief, the RC and GC zones were carefully cut into thin slices taking extra care to remove surrounding tissue from the ribs and discarding one or two slices separating the zones. The tissue was not exposed to media or FBS. Cartilage slices (avg ~15 mg per sample) were transferred to BeadBug homgenizer tubes (Benchmark Scientific, Sayreville, NJ) with 6.0mm zirconium bead (previously treated to degrade any contaminating RNA: 2 hours under UV light and 2 hours in 75˚C). 700 µL

Qiazol was added to the tube and slices were homogenized on a BeadBug (cycle settings: speed = 400, time = 40 sec) with GC slices requiring 19 cycles for homogenization and 8 cycles for RC samples. RNA was extracted using Qiagen's miRNeasy micro kit and resuspended in nuclease free water. Samples were submitted for analysis at the Biobehavioral Research Lab at VCU using Nanostring's Rat v1.5 miRNA panel.

Ex-Vivo RT-qPCR

Tissue was removed in identical manner to 'chondrocyte cultures' above. Following trypsin digestion, tissue slices were washed with Hank's Balanced Salt Solution (HBSS) and deposited into a BeadBug homogenizer tube (same tube and treatment as 'Nanostring'). 700 µL of Qiazol was added to the tube and allowed to sit at room temperature for 5 minutes. GC and RC tubes were then run on the BeadBug homogenizer (cycle settings: speed = 400, time = 60 sec) for four cycles. RNA was purified using Qiagen's miRNeasy micro kit and resuspended in nuclease free water. RT-PCR was performed on four GC and RC samples normalized to 1,250 ng of RNA per well using Qiagen's HiSpec Buffer and incubating in thermocylcer at 37˚C for 60 min followed by 95˚C for 5 min. qPCR was run on the resulting cDNA diluted to a final working concentration of 3.125 ng/µL using Qiagen's miScript II RT kit and primers for snRNA U6, microRNA 22-3p (Qiagen), 122-5p and 451-5p (Eurofins Scientific, Luxembourg). An eight-point standard curve was generated by mixing 4 µL from each of the eight samples together and performing a 1:3 serial dilution starting at 5 ng/µL and run in duplicate. 10 µL reactions were run in a 96 well plate using a QuantStudio 3 RT-PCR system (ThermoFisher): activation: 95˚C for 15 min, 60 cycles of (denaturation: 94˚C for 15 sec, annealing: 55˚C for 30 sec, extension: 70˚C for 30 sec) followed by melt curve. Data was collected on the extension and melt curve steps.

MicroRNA Transfection

Once fourth passage chondrocytes were 60 – 70% confluent they were transfected with microRNA mimics (*mir*Vana; Invitrogen, Carlsbad, CA) at final concentration of 14.5 nM using Lipofectamine RNAiMAX transfection reagent (Invitrogen) at a final dilution of 1:500. Four microRNA mimics were used for these experiments: (microRNA 22-3p, 122-5p, 223-3p and 451-

5p). Transfection was carried out in DMEM 1 g/L glucose with 10% FBS and incubated at 37 ˚C and 5% CO_2 for 24 hours. At transfection completion the media were changed to DMEM FM until harvest. Harvest was carried out according to the requirements of each specific assay with reported hours being hours *post* transfection completion. Two control groups were included in the experiments: a NT group that received neither lipofectamine nor microRNA mimics and a NC group that included lipofectamine along with a mimic designed not to interact with known mRNA.

Specific microRNA inhibitors (22-3p and 122-5p miRCURY LNA miRNA Inhibitors, Qiagen) were transfected following the same procedure as for the microRNA mimics. Final concentration of microRNA inhibitors was 10, 30 or 50 nM. When transfected along with microRNA mimics the inhibitors were prepared and administered together with the mimics in one treatment solution. Lipofectamine concentration and media formulations unchanged. MicroRNA inhibitors for 223-3p and 451-5p were not investigated.

Cell Response

DNA Content

Double stranded DNA was quantified after sonicating the cell monolayer (40 amps, 10 sec per well) and assaying bound fluorescent dye (QuantiFluor® dsDNA system; Promega, Madison, WI) using a plate reader (Synergy H1 Hybrid Reader; BioTek, Winooski VT) with excitation of 485 nm and emission of 538 nm.

Proliferation Rate

Four hours before indicated timepoint cells were pulsed with EdU at 10 μM concentration and incubated at 37 ˚C for four hours. Cells were then fixed, labeled and read (excitation 568 nm emission 585 nm) according to manufacturer's protocol (Click-iT® EdU Microplate Assay; Invitrogen) to quantify all EdU that was incorporated by the actively proliferating cells during the four hour pulse.

Metabolic Activity

100 µL of MTT solution (5 mg/mL in PBS) was added to the 500 µL of serum-free media per well and incubated at 37 ˚C for four hours. Media was aspirated and replaced with 500 µL of DMSO per well and placed on a shaker for 5 minutes. 200 µL of the DMSO per well was transferred to a 96 well plate and absorbance read at 570 nm.

Production of Proteins

Proteins were quantified by ELISA normalized to DNA content. Assays were carried out following accompanying protocols for: BMP-2 (PeproTech, Rocky Hill, NJ), type II collagen, type X collagen, Ihh, p53 and PTHrP (LS Bio, Seattle, WA), OPG, TGF-β1 and VEGF (R&D Systems, Minneapolis, MN). Media and cell monolayer were isolated at 48 hours.

In cell western analysis was used to quantify specific protein levels with results normalized to DNA content. At 48 hours cells were fixed using 3.7 % formaldehyde, with 0.1 % Triton X-100, blocked for 1.5 hours (Odyssey Blocking Buffer) and incubated overnight at 4 ˚C with primary antibody specific for Bax or Bcl at 1:100 and 1:20 dilution respectively. Wells were washed and incubated for 1 hour at room temperature with DRAQ5 (1:10,000 dilution) and corresponding secondary antibody (1:1,000 dilution). Wells were washed and imaged on the Li-Cor Odyssey CLx (LI-COR, Lincoln, NE).

TUNEL

Cells were fixed with 3.7 % buffered formaldehyde solution, permeabilized with proteinase K and labeled with TdT labeling buffer. Absorbance was measured at 450 nm on a plate reader.

Alkaline Phosphatase Activity

At 48 hours media were aspirated and cell monolayer washed twice with 1 X PBS. Monolayer was removed with 0.05% Triton X 100 and lysed by three cycles of freeze thawing. Alkaline phosphatase activity was quantified using a colorimetric assay that determines the amount of enzyme needed to hydrolyze 1 µmole of *p*-nitrophenyl phosphate to 1 µmole of *p*-

nitrophenol at 37 ˚C. Absorbance was read in plate reader at 405nm. Activity was normalized to protein content as determined by Pierce BCA assay (ThermoFisher, Waltham, MA).

Sulfated Glycosaminoglycan Production

At 48 hours media were aspirated and cell monolayer washed twice with 1 X PBS. Cell monolayer was removed from wells with papain digest solution (3.8 U/mL papain in 55 mM sodium citrate, 10 mM cysteine) and digested overnight at 60 ˚C. sGAG content was assessed using 1,9-dimethylmethylene blue dye with pH of 1.5 and absorbance measured at 525 nm on a plate reader.

Regulation of Vasculogenesis

HUVECs were grown on Geltrex and cultured using endothelial cell growth media from the Angiogenesis Starter Kit (ThermoFisher). The four select microRNA were transfected into HUVECs, as detailed above, and the connection length (measured in pixels) and the connection count taken every four hours over a 20 hour period.

Statistical Analysis

DNA content, proliferation rate, MTT, ELISA, in cell western, TUNEL, alkaline phosphatase activity and sGAG are presented as mean ± standard error for six independent cultures per variable. Differences between groups were examined by ANOVA with post-hoc Tukey HSD. A p-value less than 0.05 was considered significant. Experimental observations validated with at least one repeat experiment. Connection length and number examined by ANOVA with post-hoc Tukey HSD. Significance discussed is between treatment and NC group based on a p-value less than 0.05. Statistical analysis and presentation for all examinations were carried out using R 3.6.0.[151] Following R packages were used: egg, grid, gridExtra, ggplot2, ggsignif, magrittr, multcompview, outliers, plyr and sfsmisc.[151–160]

Supplementary materials

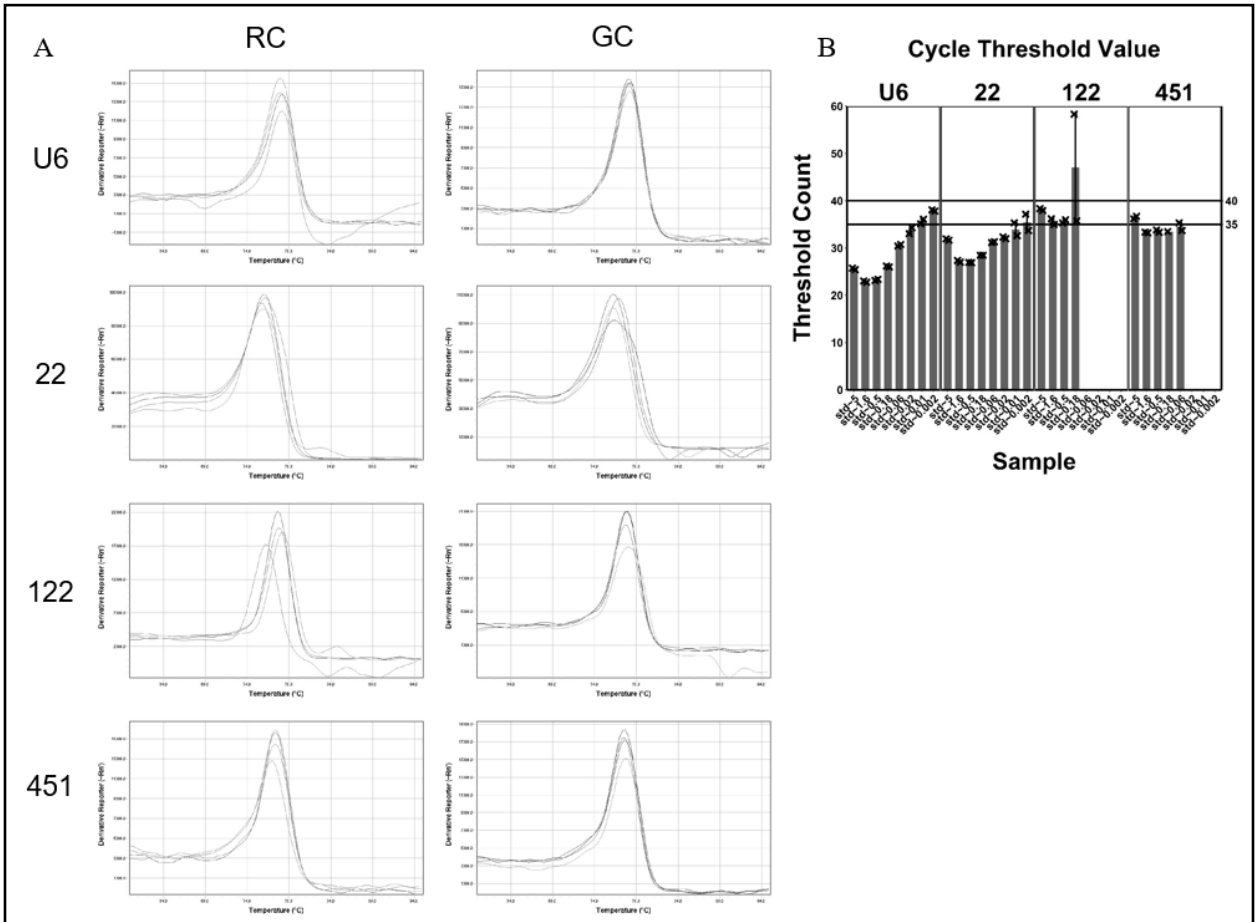

Supplemental Figure 2.1 RT-qPCR melt curve and standards. (**A**) Melt curves for RC and GC for all four primers. (**B**) Cycle threshold values for standards diluted from 5 to 0.002 ng / µL. Mean ± SE.

1α,25-Dihydroxyvitamin D3 Regulates Packaging of microRNAs within Extracellular Matrix Vesicles and Their Release in the Matrix

Under Review

Abstract

Chondrocytes in the growth plate are regulated by numerous factors and hormones as they mature during endochondral bone formation. Chondrocytes in the growth zone (GC) of the growth plate produce and export matrix vesicles (MVs) into the extracellular matrix under the regulation of 1α,25-dihydroxyvitamin D3 [1α,25$(OH)_2D_3$]. In addition, 1α,25$(OH)_2D_3$ secreted by the cells acts directly on the MV membrane, releasing its contents into the matrix. This study examined the regulatory role that 1α,25$(OH)_2D_3$ has over the production and packaging of microRNA into MVs by GC chondrocytes along with the ability to release microRNA from MVs once they are in the extracellular matrix in order to regulate cartilage maturation. We treated GC chondrocytes with 1α,25$(OH)_2D_3$ for 24 hours and then sequenced the microRNA in the cells and MVs. We also treated MVs with 1α,25$(OH)_2D_3$ and determined if the microRNA was released into solution. Finally, to assess whether MVs can act directly with cartilage cells and if this is regulated by 1α,25$(OH)_2D_3$, we stained isolated MVs with a membrane dye and used them to treat GC chondrocytes. 1α,25$(OH)_2D_3$ regulated the production and packaging of microRNA into matrix vesicles but did not affect the cell population of microRNA. MicroRNA were not released when MVs were treated with 1α,25$(OH)_2D_3$, indicating a heterogeneous MV population or retention within the MV via a protective factor. Stained MVs were endocytosed by GC cells in vitro and this was increased with 1α,25$(OH)_2D_3$ treatment. This study adds a new regulatory role for 1α,25$(OH)_2D_3$ with respect to packaging and transport of microRNA in MVs and their interaction with GC chondrocytes.

Introduction

Chondrocytes are the drivers of elongation within mammalian growth plates and are responsible for endochondral ossification.[161] During this process chondrocytes are arranged in well-organized columns as the cells move from the reserve zone (resting zone cartilage, RC) where the cells maintain a hyaline-like extracellular matrix (ECM) consisting of large proteoglycan aggregate and type II collagen. Cells in the lower reserve zone are actively proliferating, transitioning into the growth zone (GC), which includes the prehypertrophic zone and the upper

hypertrophic zone, where the cells increase in size and remodel their ECM, in preparation for mineralization.[12] Key players in the mineralization process are matrix vesicles (MVs).[29,34,131] They are small (50 to 150 nm in diameter) lipid bound vesicles produced by the chondrocytes and secreted by lateral budding off into the ECM.[19] MVs produced by GC cells contain enzymes needed for ECM mineralization, including matrix processing enzymes such as the matrix metalloproteinases (MMPs) and enzymes involved in calcium phosphate deposition such as alkaline phosphatase, along with factors and microRNA for chondrocyte regulation.[9,36,37]

Vitamin D metabolites are involved in both rapid acting and genomic regulation of this entire process and the specific metabolite involved is zone dependent. RC cells respond primarily to 24R,25-dihydroxyvitamin D3 [24R,25$(OH)_2D_3$] with an increase in alkaline phosphatase activity and the stimulation of cell proliferation while GC cells primarily respond to 1α,25-dihydroxyvitamin D3 [1α,25$(OH)_2D_3$] by decreasing cell proliferation and increasing alkaline phosphatase activity.[6,121,133] This zonal specificity holds true for MVs produced by these cells. 24R,25$(OH)_2D_3$ regulates the production of RC MVs, which exhibit increased alkaline phosphatase activity and a reduction in phospholipase A_2 (PLA_2) activity. In contrast, 1α,25$(OH)_2D_3$ regulates the production of GC MVs, with an increase in both alkaline phosphatase and PLA_2 activity.[3,57]

Vitamin D3 is taken up in the body through one's diet or by being synthesized from 7-dehydrocholesterol in the skin in the presence of ultraviolet irradiation.[162] Vitamin D3 is then transported to the liver bound to the vitamin D binding protein and hydroxylated at carbon 25 to become 25-hydroxyvitamin D3 [25$(OH)D_3$] the primary circulating form of vitamin D.[162] Cartilage is not vascularized, however, making local production of many regulatory factors important for controlling chondrocyte proliferation, differentiation, and maturation. RC and GC cells, in addition to the kidney, are able to use the circulating 25$(OH)D_3$ to produce metabolically active 24R,25$(OH)_2D_3$ and 1α,25$(OH)_2D_3$.[162,163] These metabolites are secreted by the chondrocytes into the ECM under cell-specific regulation, where they interact directly with the MV

membrane. Whereas 24R,25$(OH)_2D_3$ stabilizes the MV membrane, 1α,25$(OH)_2D_3$ destabilizes it through the activation of PLA_2, releasing the MV contents into the ECM.[7]

In addition to its direct action on MVs in the ECM, 1α,25$(OH)_2D_3$ is able to regulate GC cells through both genomic and rapid acting pathways. The genomic effect of 1α,25$(OH)_2D_3$ is realized through binding of 1α,25$(OH)_2D_3$ with the nuclear vitamin D receptor (nVDR), which forms a heterodimer within the nucleus and is able to bind to vitamin D response elements (VDRE) located in the promoter regions of target genes.[164] nVDR has over 1,000 target genes in human tissues and in chondrocytes has been shown to upregulate receptor activator of NF-κB ligand (RANKL) and vascular endothelial growth factor (VEGF) production.[165,166] Rapid acting effects of 1α,25$(OH)_2D_3$ in GC chondrocytes take place through the membrane associated vitamin D receptor protein disulfide isomerase, family A, type 3 (PDIA3) (also known as 1,25 membrane-associated rapid response steroid-binding proteins [1,25-MARRS]), as well as the classical VDR. Membrane-associated VDRs are able to regulate chondrocytes through various signal transduction systems (e.g. PLA_2, phosphatidyl inositol 3-kinase [PI3K], protein kinase A and C [PKA and PKC] pathways that increase cytosolic calcium levels and activate transcription factors nuclear factor kappa B [NF-κB] and extracellular-signal regulated kinase [ERK] 1/2) that elicit both a rapid response and activation of transcription factors.[121,164,167–169] In addition to the documented effects of 1α,25$(OH)_2D_3$ on chondrocytes and the pathways involved, 1α,25$(OH)_2D_3$ has been demonstrated to regulate microRNA production in other cell types including cancer cells and peripheral blood mononuclear cells.[170]

As noted above, 1α,25$(OH)_2D_3$ is involved in regulating the activity of MVs produced by growth plate chondrocytes. MVs lack a nucleus and the requisite machinery for genomic transcription and translation leaving rapid acting pathways as the method of action for MVs. During the production of MVs the PDIA3 receptor is associated with the lipid membrane.[96] In the ECM, 1α,25$(OH)_2D_3$ binds to PDIA3 on GC MVs and activates PLA_2, hydrolyzes membrane phospholipids to produce lysophospholipids, destabilizing the MV membrane.[43] One

consequence is the release, among other things, of stromelysin 1 (MMP-3), which activates latent TGF-β1 that has been secreted by chondrocytes into the ECM.[64,65,171]

We have recently demonstrated that growth plate chondrocytes produce MVs with a population of microRNA that is distinct from the parent cell, the MV RNA is safe from RNase activity, and that some of these microRNA are able to regulate the activity of both RC and GC cells.[2,9,55] 1α,25$(OH)_2D_3$ regulates numerous aspects of GC MV production including enzyme packaging and has been found to regulate microRNA production in other cell types. This leads to a clear question of whether 1α,25$(OH)_2D_3$ is regulating the production and/or packaging of microRNA into GC MVs as part of its regulatory role in the growth plate. In addition to the export of microRNA, we examined the ability of 1α,25$(OH)_2D_3$ to release microRNA from GC MVs and the impact that 1α,25$(OH)_2D_3$ has on the binding/endocytosis of GC MVs by GC cells.

Methods

Chondrocyte Cultures

Costochondral cartilage was removed from 100 to 125 g male Sprague Dawley rats. RC and GC chondrocytes were isolated by enzymatic digestion and cultured as previously described by Boyan *et al.*[8,91] All animal procedures conducted during the course of this work followed a protocol approved by the Institutional Animal Care and Use Committee (IACUC) at Virginia Commonwealth University. Experiments were carried out in accordance with all relevant guidelines and regulations. In brief, animals were killed by CO_2 asphyxiation followed by cervical dislocation. Rib cages were removed by sharp dissection and placed in Dulbecco's modified Eagle's medium (DMEM, Life Technologies, Carlsbad, CA) 1 g/L glucose with 150 U/mL penicillin and 150 µg/mL streptomycin. All tissue was removed from around the ribs and the RC and GC cartilage sections were dissected out discarding one or two transition slices. The cartilage slices were incubated in 0.25% trypsin-EDTA (Gibco, Gaithersburg, MD) for 1 hour, washed and incubated in 0.2% collagenase type II (Worthington Biochemical, Lakewood, NJ) for 3 hours on a shaker. Cells were filtered through a 40 µm nylon mesh strainer, collected by centrifugation (500 g for 10 minutes) and re-suspended in DMEM FM (1 g/L glucose DMEM with 10% FBS, 50 U/mL

penicillin, 50 µg/mL streptomycin, and 50 µg/mL ascorbic acid). Cells were plated at a density of 20,000 GC cells/cm^2. Cells were incubated at 37˚C and 5% CO_2 and the culture media were changed 24 hours after plating and then every 48 hours thereafter. Confluent cells were passaged using 0.25% trypsin and plated as above. Fourth passage cells were used for all experiments.

1α,25(OH)$_2$D$_3$ Treatment

Fourth passage GC cells were grown out to 100% confluency. 24 hours later the media were aspirated and replaced with fresh media containing 10^{-8} M 1α,25(OH)$_2$D$_3$ for 24 hours at which time the matrix vesicles were isolated, as described below.

Materials

Unless otherwise indicated: 0.9% NaCl was 0.2 µm filtered, ultracentrifugation was performed in 32.5 mL straight wall tubes (Beranek Laborgeräte, Nuβloch, Germany) using a 50.2 Ti fixed-angle rotor (Beckman Coulter, Indianapolis, IN), and exosome depleted FBS was derived from heat inactivated FBS (Life Technologies) that was centrifuged to remove exosomes (30 mL of FBS was spun [238,668 *g* for 4 hours at 4 ˚C] after which the top 10 mL of supernatant was carefully pipetted off and 0.2 µm filtered for use in MV isolation and the remaining 20 mL was discarded).

MV Isolation

Media were aspirated from the culture flask and discarded. The cell layer was washed with 1X DPBS and the MVs were separated from the ECM by digesting the cell layer with 0.25% trypsin and following that with differential centrifugation as has been described previously.[90] In brief: fourth passage GC cells in T-175 flasks were incubated in 10 mL 0.25% trypsin for a total of 10 min at 37˚C. At minute 4, the bottom of each flask was gently scrapped to ensure detachment of the cell monolayer and aid in initial breakdown of the ECM. After being scrapped the flasks were returned to 37˚C for the remainder of the 10 min. 10mL 1X DPBS with 10% exosome depleted FBS was used to quench the trypsin. The MVs were isolated from the digested ECM/cell suspension by differential ultracentrifugation. The suspension was spun (500*g* for 10 min at 4˚C) in a benchtop centrifuge to pellet the cells leaving MVs in the supernatant. The MV

supernatant was poured off and stored in -80 ˚C and the cell pellet resuspended in 10 mL 0.9% NaCl. Two 1 mL aliquots were made from the resuspended cell pellet and spun (500*g* at 4˚C for 10 min) in a benchtop centrifuge. The supernatant was discarded and one pellet resuspended in 700 µL of Qiazol lysis reagent (Qiagen, Hilden, Germany) for RNA extraction as described below, and the other in 200 µL of NP-40 lysis buffer (Boston BioProducts, Ashland, MA) with 1% protease inhibitor cocktail (Sigma, St. Louis, Missouri) for alkaline phosphatase activity. The remaining 8 mL of cell pellet resuspension was spun down (500*g* at 4˚C for 10 min) in a benchtop centrifuge and resuspended in 5 mL 0.25 M sucrose solution (0.25 M sucrose, 1 mM EDTA tetrasodium salt, 100 mM Tris) for plasma membrane isolation. All suspensions were stored at -80˚C.

To obtain the MVs, the MV supernatant was thawed on ice and processed in an ultracentrifuge. Any cell debris was spun down (24,000*g* for 20 min at 4˚C) and the resulting supernatant was transferred to new tubes and spun (100,000*g* for 70 min at 4˚C) to pellet the MVs. The supernatant was discarded and the vesicle pellet was washed with 20 mL 0.9% NaCl at 4˚C and centrifuged again (100,000*g* for 70min at 4˚C). This final supernatant was discarded and the MV pellet was resuspended in fresh 0.9% NaCl (100 µL for RNA, 200 µL for MV microRNA release and MV endocytosis, and 500 µL for alkaline phosphatase activity).

Validation of MV Isolation

Plasma membrane suspension was thawed on ice, poured into a glass homogenizer, 1 mL 0.25 M sucrose was added to sample tube, vortexed and added to homogenizer, tube was then rinsed with an additional 2 mL 0.25 M sucrose that was poured into homogenizer. The pestle was inserted into homogenizer, rotated 360˚ and lifted up. This was repeated a total of five times. The sample was poured out of homogenizer into ultracentrifuge tube, pestle and homogenizer were each rinsed with 2 mL 0.25 M sucrose solution that was poured into same ultracentrifuge tube. The tube was spun (1,480*g* at 4˚C for 20 min) and supernatant was discarded. The pellet was resuspended with 2 M sucrose solution and spun (20,000*g* at 4˚C for 20 min) and supernatant was poured off into a new ultracentrifuge tube. The tube was filled with ice cold ultrapure water

and spun (40,000*g* at 4˚C for 30 min). The supernatant was carefully poured off and the plasma membrane (PM) pellet resuspended in 1 mL of 0.9% NaCl.

MV, plasma membrane, and cell pellet (in NP-40) isolates had alkaline phosphatase activity quantified with a colorimetric assay that specifies the amount of phosphatase used at 37˚C to hydrolyze 1 μmole of *p*-nitrophenyl phosphate to 1 μmole of *p*-nitrophenol. Sample absorbance was quantified using a plate reader at 405 nm. Enzyme activity was normalized to sample protein content as determined by the Pierce BCA assay for cell pellet and plasma membrane and the micro BCA assay for MV samples (ThermoFisher, Waltham, MA).

RNA Analysis

Immediately after isolation, the MV pellets were resuspended in the 100 μL volume remaining in the centrifuge tube after decanting the supernatant and mixed with 700 μL Qiazol lysis reagent. Exosome depleted FBS was processed as above and resuspended in 100 μL 0.9% NaCl for RNA extraction. All samples were stored at -80˚C. After thawing, samples in Qiazol were processed using Qiagen's miRNeasy mini kit following the standard protocol for purification of total RNA from animal cells. In brief, chloroform was added, aqueous phase was removed and combined with ethanol, RNA was bound to a spin filter and washed with RWT and RPE buffers. MV and exosome depleted FBS samples were eluted in 30 μL of nuclease free water per sample and cell pellet samples in 50 μL.

RNA isolations were quantified with a RNA 6000 pico chip on a BioAnalyzer (Agilent, Santa Clara, CA). Samples were then pooled to maximize RNA distribution between the MV groups and submitted for smallRNAseq (ArrayStar, Rockville, MD) that included quality control, library construction, and sequencing on an Illumina instrument (Illumina, San Diego, CA).

MicroRNA Bioinformatic Analysis

Bioinformatic Analysis of smallRNAseq

Raw read files were processed with the miARma-Seq tool that evaluated read quality with FASTQC, aligned the reads using Bowtie2 against the *Rattus norvegicus* (Rnor_6.0) genome, and generated a count of the microRNA from the bam files. Bioinformatic analysis was carried

out using R version 4.0.3, normalization and differential expression were calculated with DESeq2, Venn diagrams built using VennDiagram, heatmaps with pheatmap and the static parallel coordinate plots with bigPint.[150,151,172]

miEAA Analysis

MicroRNA from four different comparisons (cell vehicle – cell 1α,25$(OH)_2D_3$, MV vehicle – MV 1α,25$(OH)_2D_3$, cell vehicle – MV vehicle, and cell 1α,25$(OH)_2D_3$ – MV 1α,25$(OH)_2D_3$) with absolute log 2 fold change > 1 and a p-value < 0.05 were uploaded to the miRNA enrichment analysis and annotation 2.0 tool (miEAA 2.0) and run through the over-representation analysis (ORA) pipeline.[83] Resulting annotations were searched for musculoskeletal associated terms (Table 1). Results from the full ORA as well as the musculoskeletal focus was loaded into Cytoscape 3.8.2 to visualize the microRNA interactions.

MV microRNA Release

We previously showed that MV metalloproteinases are released when MVs are treated with either detergent or 1α,25$(OH)_2D_3$ and small RNAs are released when MVs are treated with detergent, making them susceptible to degradation by RNAse.[55,64] In order to determine if microRNAs are released following loss of MV membrane integrity due to 1α,25$(OH)_2D_3$ action, we treated MVs with detergent or 1α,25$(OH)_2D_3$, followed by treatment with RNAase. MVs isolated in 0.9% NaCl were pooled together, the protein content, as determined by micro BCA assay, normalized to 45 μg/mL, and samples then aliquoted out into micro centrifuge tubes (six samples per group). The treatment was added to each tube (0.9% NaCl, Tween 20 + RNase, 1α,25$(OH)_2D_3$, or 1α,25$(OH)_2D_3$ + RNase) bringing the total sample volume to 100 μL and the tubes were incubated in a 37˚C water bath for three hours. 700 μL of Qiazol lysis reagent was added to each sample and processed with Qiagen's miRNeasy micro kit. RNA was eluted in 30 μL of nuclease free water per sample.

RNA was quantified with a RNA 6000 pico chip on a BioAnalyzer. The generated pseudo gel images were analyzed for specific band region using Licor's Image Studio Lite software (LICOR, Lincoln, NE).

MV Endocytosis

MVs and 0.9% NaCl were stained with PKH26 (Sigma) as follows. MVs were normalized to 75 µg/mL of protein and 120 µL of MV solution or 0.9% NaCl was added to 400 µL of diluent C (Sigma) in each ultracentrifuge tube. 2 µL of PKH26 dye mixed with 500 µL of diluent C was added to each ultracentrifuge tube and the mixture was allowed to sit at room temperature for 4 min (pipetting every 90 sec to mix). 1 mL of sterile filtered 1% BSA in PBS was added to quench the remaining PKH26 and then 8 mL of DMEM FM (without ascorbic acid) was added. The solution was ultracentrifuged (100,000*g* for 70min at 4˚C), the supernatant was discarded and the remaining red pellet resuspended in 100 µL sterile DPBS.

GC cells were grown to third passage and then passed onto 8 well glass chamber slides for the fourth passage. At 100% confluency the media were replaced and the stained MV and NaCl solutions were combined with either 1α,25$(OH)_2D_3$ or vehicle and used to treat the cells for 24 hours. All media were removed, wells were washed twice with 1X PBS, fixed with 300 µL 10% neutral buffered formalin for 30 min at room temperature, and counterstained with 100 µL 5 µM DRAQ-5 in 1X PBS for 27 min at 37˚C. The chamber and gasket were removed from each slide, Fluoro Gel with DABCO (EMS, Hatfield, PA) mounting media were added and then a coverslip attached. One image per well was taken on a LSM 880 confocal microscope (Zeiss, Jena, Germany) using a 20x objective for quantification and a 63x objective coupled with an airyscan detector for high resolution imaging.

Quantification was performed by two independent and blinded observers. The images were overlaid with a 3x3 grid and each observer counted the number of DRAQ5 stained nuclei and the number of cells with six or greater distinct PKH26 spots. The percent stained cells was calculated for each image and the average of both observers used for quantification. Additionally, CellProfiler 3.0 was used for automated quantification of the images.[173]

Statistical Analysis

MV microRNA release and alkaline phosphatase activity are presented as mean ± standard error of the mean for six samples for each group. An ANOVA with Tukey HSD post-hoc

test was used to examine differences between the groups. Significance was determined by a $p \leq 0.05$.

Results

1α,25$(OH)_2D_3$ Regulates Chondrocyte Cellular and MV microRNA

Enrichment of alkaline phosphatase specific activity in MVs compared to that of the plasma membrane was used to validate the MV preparation. MVs are isolated right-side out from the ECM whereas plasma membranes that are isolated both right-side and wrong-side out from cell lysates. Thus, specific activity of alkaline phosphatase, which is an exoenzyme, in MVs should be a minimum of twice that of the enzyme activity in plasma membranes (Supplemental Fig. 3.1).

A comparison of the 14 samples (3 cells+vehicle, 3 cells+1α,25$(OH)_2D_3$, 3 MVs+vehicle, 3 MVs+1α,25$(OH)_2D_3$, and 2 FBS exosomes) with principle component analysis (PCA) and a heatmap indicates that there are three distinct clusters, one for each sample type (cell, MV and exosome depleted FBS) (Fig. 3.1). There is visible difference between the main sample types (cell, MV & exosome depleted FBS) in the heatmap with the cell samples clustering in the first six columns, the MV samples in the following six and the exosome depleted FBS samples in the final two (Fig. 3.1 A). The microRNA can be divided into four distinct clusters as indicated on the y-axis. The sample grouping is also clearly visible in a principle component analysis with the sample types clustering on the x and y axes that together accounts for 90% of the variance between samples (Fig. 3.1 B). The exosome depleted FBS samples formed distinct clusters separate from both cell and MV groups and were not included in the differential expression analysis.

Examination of the differentially expressed (p-value ≤ 0.05 and absolute log 2 fold change ≥ 1) microRNA between parent cells and MVs indicated a selectively exported population of microRNA in the MVs with 211 differentially expressed in the vehicle group and 198 in the 1α,25$(OH)_2D_3$ group (Fig. 3.2 A,B,C). Of these microRNA, 44 were uniquely differentially expressed in the vehicle group and 31 in the 1α,25$(OH)_2D_3$ group (Fig. 3.2 D,E). The 167 shared MV microRNA were found to be selectively exported in identical fashion between vehicle and

1α,25$(OH)_2D_3$ groups (same set of microRNA enriched in the MV as compared to cell samples between vehicle and 1α,25$(OH)_2D_3$ groups) (Fig. 3.2 F).

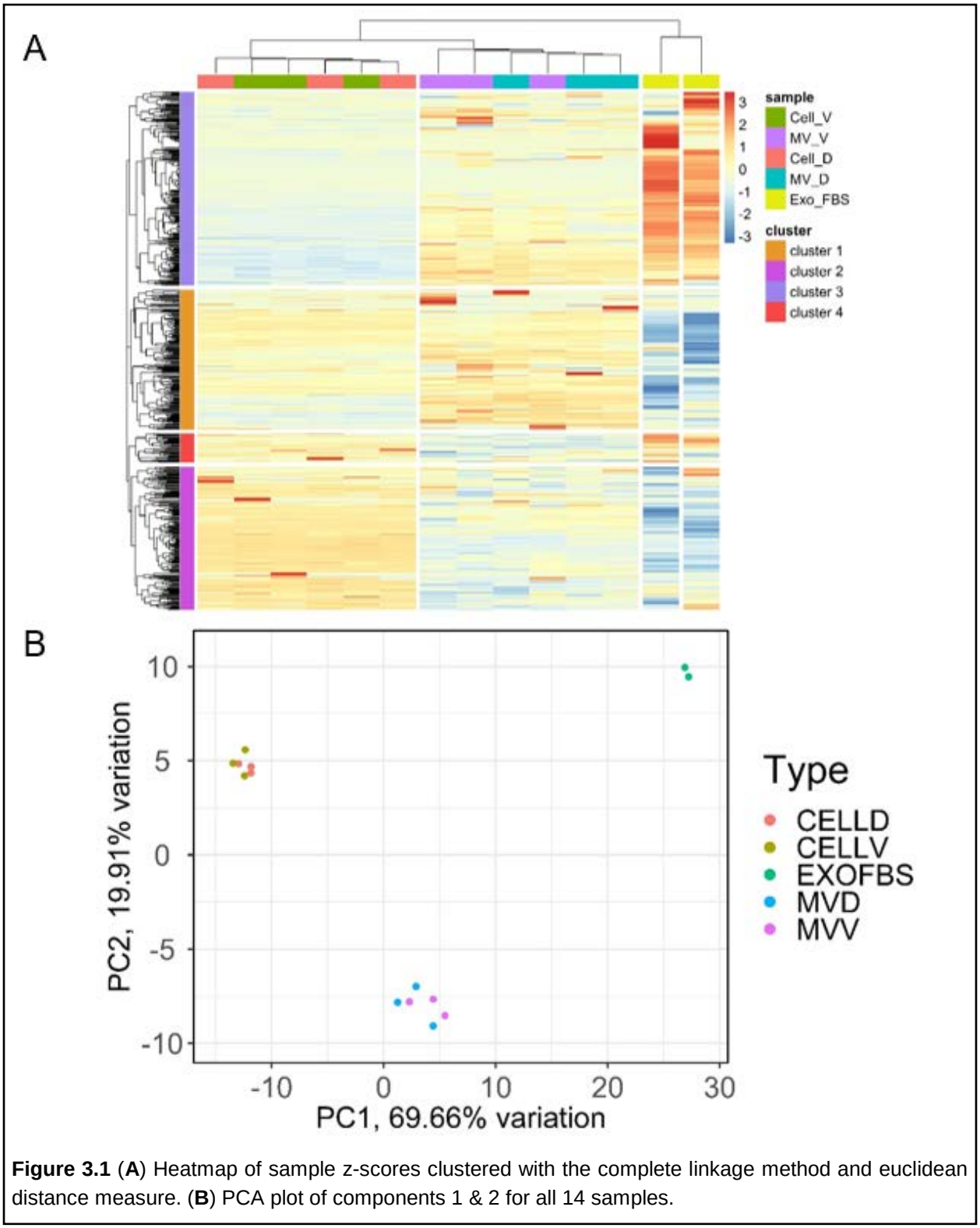

Figure 3.1 (**A**) Heatmap of sample z-scores clustered with the complete linkage method and euclidean distance measure. (**B**) PCA plot of components 1 & 2 for all 14 samples.

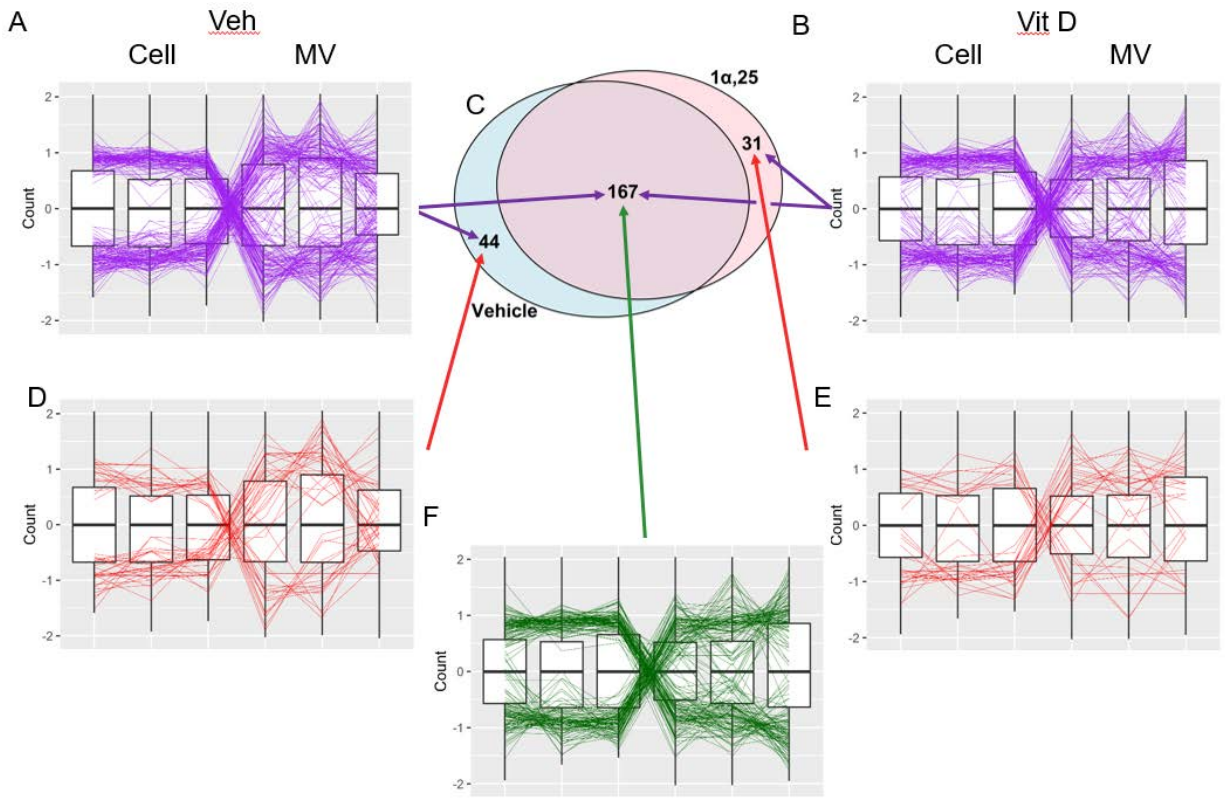

Figure 3.2 Differentially expressed microRNA (p-value ≤ 0.05 & absolute log 2 fold change ≥ 1). (**A**) Comparison between cell & MV with vehicle treatment, complete results. (**B**) Comparison between cell & MV with 1α,25 treatment, complete results. (**C**) Venn diagram displaying overlap of differentially expressed microRNA. (**D**) MicroRNA between cell & MV with vehicle treatment that are not differentially expressed when treating with 1α,25. (**E**) MicroRNA between cell & MV with 1α,25 that are not differentially expressed when treating with vehicle. (**F**) Differentially expressed microRNA that are shared in common between vehicle and 1α,25 treatments.

The microRNA populations within the cell samples had only one differentially expressed microRNA between the vehicle and 1α,25$(OH)_2D_3$ groups (Fig. 3.3 A). The MV samples however had 18 differentially expressed microRNA between the vehicle and 1α,25$(OH)_2D_3$ groups (Fig. 3.3 B). Table of differentially expressed microRNA that were discovered between the four comparisons (only the unique microRNA exported from the cell to MVs with and without treatment and the entire set of differentially expressed microRNA between cells and MVs with and without 1α,25$(OH)_2D_3$) (Table 3.1).

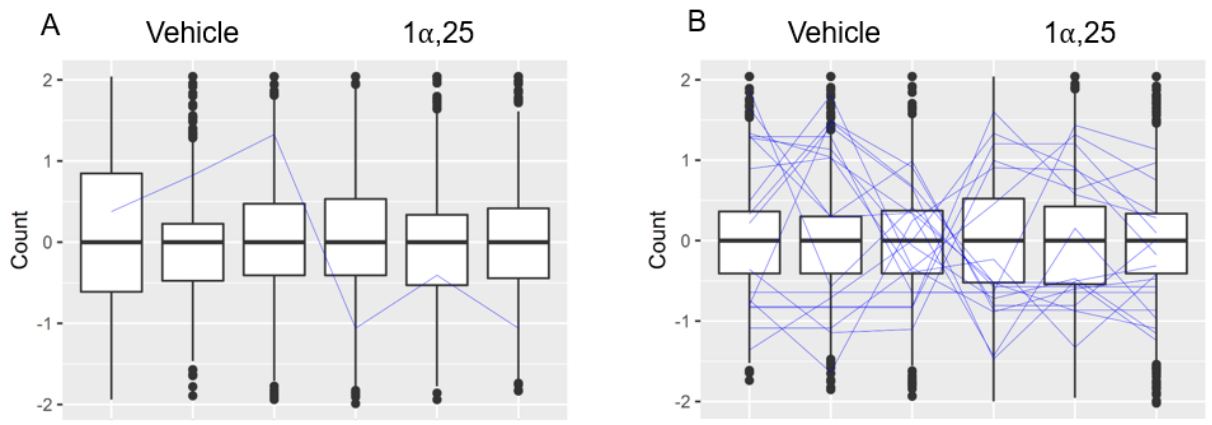

Figure 3.3 Differentially expressed microRNA (p-value ≤ 0.05 & absolute log 2 fold change ≥ 1). (**A**) Differentially expressed microRNA when comparing cell populations with vehicle or 1α,25 treatments. (**B**) Differentially expressed microRNA when comparing MV populations with vehicle or 1α,25 treatments.

Cell Veh to MV Veh Unique	Cell 1α,25 to MV 1α,25 Unique	Cell Veh to Cell 1α,25	MV Veh to MV 1α,25
rno-let-7e-3p	rno-let-7a-1-3p	rno-miR-301b-3p	rno-miR-124-3p
rno-let-7g-5p	rno-let-7c-2-3p		rno-miR-130b-3p
rno-miR-1247-3p	rno-miR-10b-5p		rno-miR-138-5p
rno-miR-127-3p	rno-miR-1224		rno-miR-188-5p
rno-miR-130b-3p	rno-miR-129-1-3p		rno-miR-190
rno-miR-135a-5p	rno-miR-135b-5p		rno-miR-19b-1-5p
rno-miR-138-2-3p	rno-miR-138-5p		rno-miR-19b-3p
rno-miR-140-5p	rno-miR-142-3p		rno-miR-206-3p
rno-miR-148a-3p	rno-miR-154-5p		rno-miR-219a-2-3p
rno-miR-150-3p	rno-miR-181b-1-3p		rno-miR-296-3p
rno-miR-16-5p	rno-miR-181c-3p		rno-miR-374-3p
rno-miR-17-1-3p	rno-miR-1843a-3p		rno-miR-377-5p
rno-miR-181a-2-3p	rno-miR-191a-5p		rno-miR-410-5p
rno-miR-193b-5p	rno-miR-196a-5p		rno-miR-488-3p
rno-miR-210-3p	rno-miR-212-3p		rno-miR-497-5p
rno-miR-219a-1-3p	rno-miR-218a-1-3p		rno-miR-592
rno-miR-223-3p	rno-miR-28-5p		rno-miR-9a-3p
rno-miR-223-5p	rno-miR-299b-3p		rno-miR-9a-5p
rno-miR-27b-5p	rno-miR-29b-1-5p		
rno-miR-29a-5p	rno-miR-300-3p		
rno-miR-324-5p	rno-miR-30c-5p		
rno-miR-331-5p	rno-miR-325-5p		
rno-miR-338-5p	rno-miR-326-3p		
rno-miR-3558-3p	rno-miR-369-3p		
rno-miR-3559-3p	rno-miR-369-5p		
rno-miR-361-3p	rno-miR-377-5p		
rno-miR-374-3p	rno-miR-384-3p		
rno-miR-376a-5p	rno-miR-412-3p		
rno-miR-377-3p	rno-miR-455-3p		
rno-miR-380-3p	rno-miR-503*		
rno-miR-409a-5p	rno-miR-770-5p		
rno-miR-410-3p			
rno-miR-412-5p			
rno-miR-429			
rno-miR-488-3p			
rno-miR-582-3p			
rno-miR-582-5p			
rno-miR-592			
rno-miR-615			
rno-miR-6331			
rno-miR-666-5p			
rno-miR-673-5p			
rno-miR-7b			
rno-miR-99b-3p			

Table 3.1 Differentially expressed microRNA (p-value ≤ 0.05 & absolute log 2 fold change ≥ 1). Columns 1 & 2: Unique microRNA exported in MVs with vehicle or 1α,25 treatment. Columns 3 & 4: differentially expressed when directly comparing cell or MVs.

miEAA analysis of the differentially expressed microRNA (between cell vehicle and cell 1α,25$(OH)_2D_3$, MV vehicle and MV 1α,25$(OH)_2D_3$, microRNA uniquely packaged following 1α,25$(OH)_2D_3$ treatment, and microRNA uniquely packaged following vehicle treatment) resulted in large numbers of potentially impacted pathways, targeted mRNA, related diseases and tissue locations for three of the four comparisons (no results were returned for the first comparison) (Fig. 3.4 A-C). Searching the initial results that covered the entire organism for musculoskeletal specific terms (Supplemental Table 3.1 A) significantly reduced the pathways and mRNA involved (Fig. 3.4 D-F).

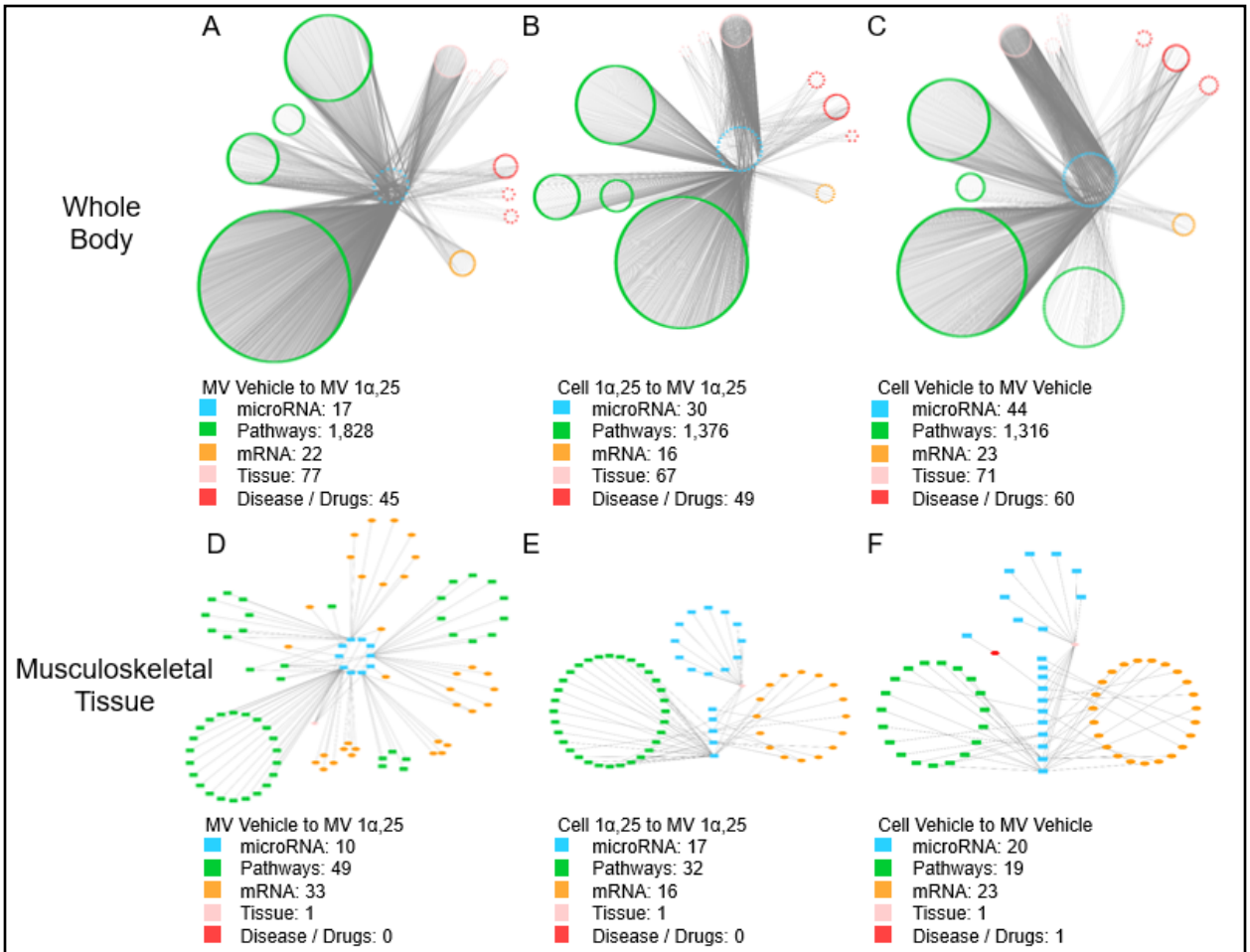

Figure 3.4 Visualization of miEAA search results of differentially expressed microRNA. (**A, B & C**) Unfiltered results. (**A**) Between MV with vehicle or 1α,25 treatment. (**B**) Uniquely exported from cell to MV with 1α,25 treatment. (**C**) Uniquely exported from cell to MV with vehicle treatment. (**D, E & F**) Results filtered for musculoskeletal search terms. (**D**) Between MV with vehicle or 1α,25. (**E**) Exported from cell to MV with 1α,25 treatment. (**F**) Exported from cell to MV with vehicle treatment.

Loading the microRNA expression tables into ingenuity pathway analysis (IPA) indicated that three chondrocyte pathways were being regulated by the microRNA populations: the proliferation of epiphyseal chondrocytes, the maturation of chondrocytes, and development of osteoarthritis (Fig. 3.5 A). Addition of vehicle to the cells promoted proliferation whereas addition of vehicle + 1α,25$(OH)_2D_3$ to the cultures promoted cell and MV microRNA associated with maturation and osteoarthritis (Fig. 3.5 B). A comparison of the cell miRNA with the miRNA in the MVs they produce showed that cell miRNA drive proliferation whereas MV miRNA promote maturation and osteoarthritis pathways.

A

Proliferation of Epiphyseal Chondrocytes

miR Family	Effect
miR-369-3p	↑
miR-374b-5p	↑
miR-379-5p	↑
miR-503-5p	↑

Osteoarthritis Pathway

miR Family	Effect
miR-142-3p	↑

Maturation of Chondrocytes

miR Family	Effect
miR-23a-3p	↓
miR-30c-5p	↓
miR-34a-5p	↓
miR-135a-5p	↓
miR-204-5p	↓
miR-205-5p	↓
miR-217-5p	↓

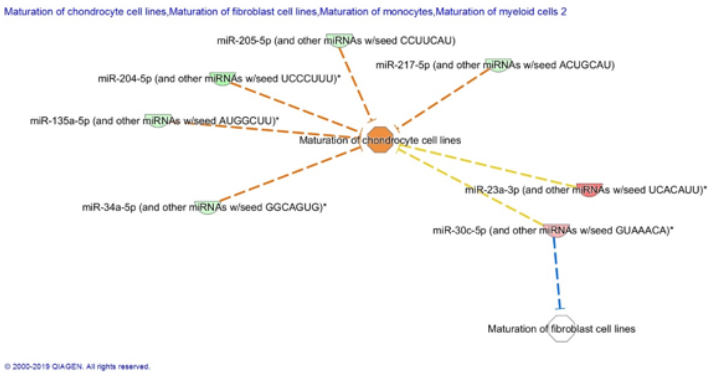

B

	MV Vehicle – MV 1α,25	Cell Vehicle – Cell 1α,25	Cell 1α,25 – MV 1α,25	Cell Vehicle – MV Vehicle
Proliferation	MV Vehicle	Cell Vehicle	Cell 1α,25	Cell Vehicle
Maturation	MV 1α,25	Cell 1α,25	MV 1α,25	MV Vehicle
Osteoarthritis	MV 1α,25	Cell 1α,25	MV 1α,25	MV Vehicle

Figure 3.5 Ingenuity pathway analysis results from differentially expressed microRNA. (**A**) Three chondrocyte effected pathways listing the impacted microRNA families and a sample interaction network for maturation of chondrocytes. (**B**) Table indicating which group is driving the pathway upregulation between the four differential expression comparisons.

1α,25(OH)$_2$D$_3$ Does Not Cause microRNA Release from MVs

Treatment of MVs with Tween 20 followed by RNase demonstrated that loss of membrane integrity and protein denaturing exposed smallRNA to enzymatic degradation, as demonstrated in RNA pseudo gels from a BioAnalyzer. Examination of the smallRNA region of the pseudo gel showed that the RNA bands for the tween 20 + RNase group had clear degradation when compared to negative control (0.9% NaCl), 1α,25(OH)$_2$D$_3$, and 1α,25(OH)$_2$D$_3$ + RNase groups (Fig. 3.6 A). Quantifying the smallRNA region of the gels using Licor's Image Studio Lite confirmed that there was a significant reduction in RNA for the tween 20 + RNase group when compared to all other groups (Fig. 3.6 B & Supplemental Fig. 3.2).

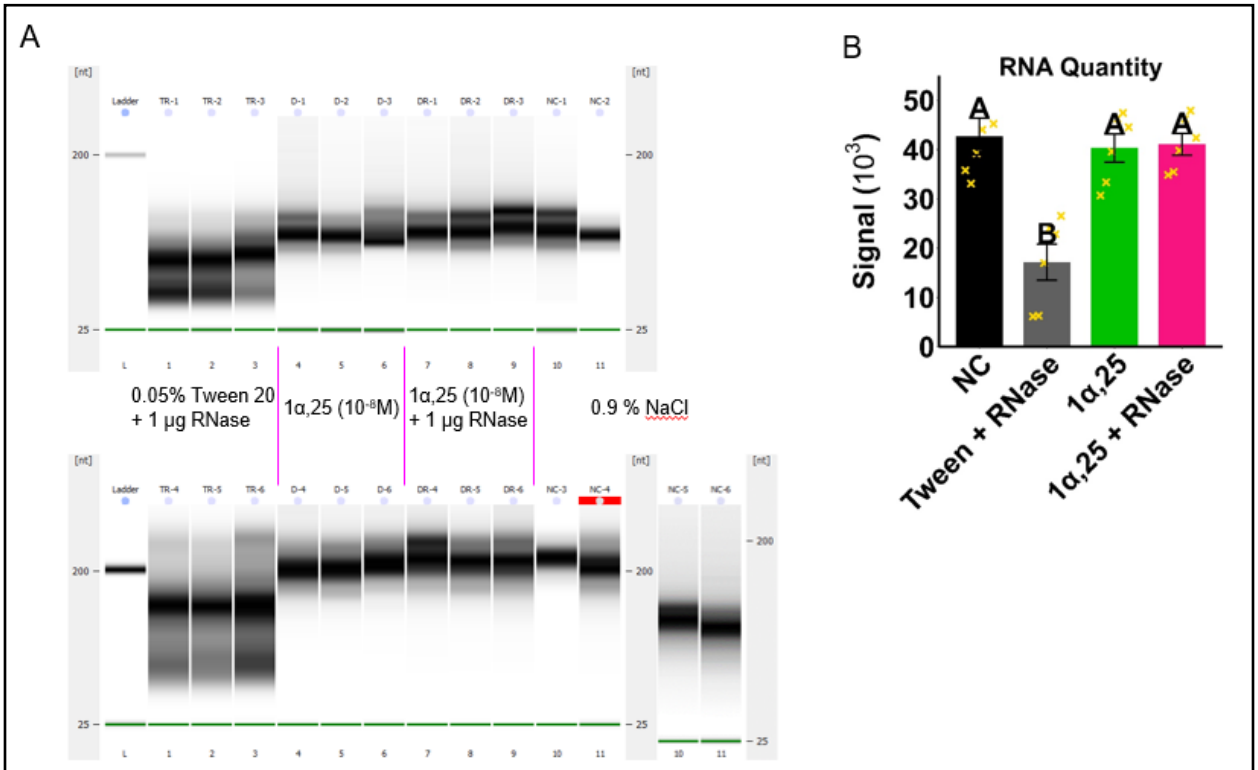

Figure 3.6 MicroRNA release from MVs with 1α,25 treatment. (**A**) Bioanalyzer gel results from MV samples. (**B**) Quantification of small RNA signal region. Mean ± SE, groups not sharing a letter are statistically different (α=0.05). *NC*: negative control, no treatment.

1α,25(OH)$_2$D$_3$ Promotes MV Endocytosis

The PKH26 dye was able to successfully stain GC cells in all treatment groups, visible at 20X (Fig. 3.7 A). Manual and automated quantification produced results with the same statistical trends with MV + 1α,25(OH)$_2$D$_3$ staining more cells than NC + 1α,25(OH)$_2$D$_3$ (Fig. 3.7 B, C). When

increasing the threshold for a stained cell up to 30 distinct spots on the automated quantification data, MV with 1α,25$(OH)_2D_3$ was greater than both MV + vehicle and NC + 1α,25$(OH)_2D_3$ (Fig. 3.7 D). High resolution view of stained MV + 1α,25$(OH)_2D_3$ cell with a cloud of distinct green spots (Fig. 3.7 E).

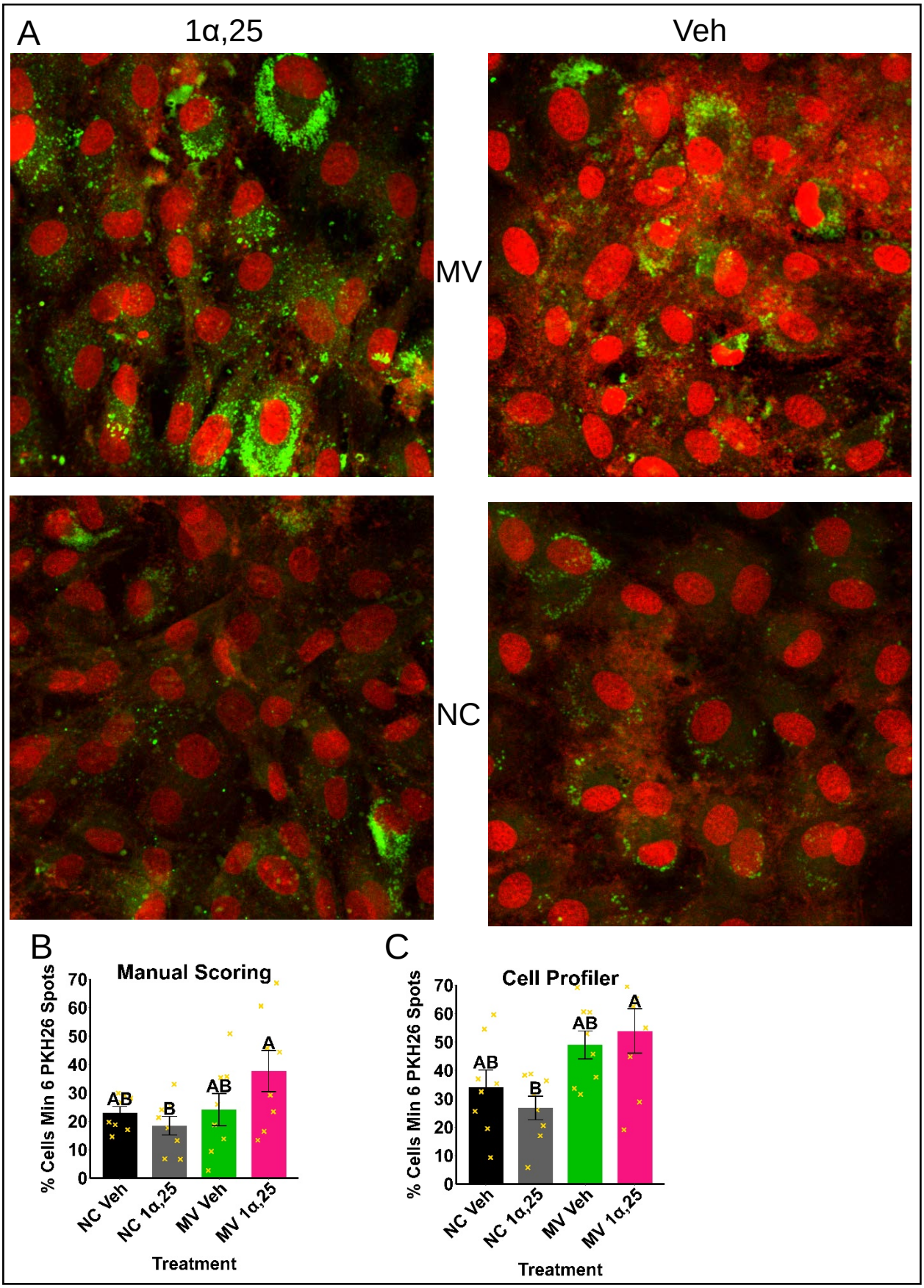
A
1α,25
Veh
MV
NC
B
Manual Scoring
% Cells Min 6 PKH26 Spots
70
60
50
40
30
20
10
0
AB
B
AB
A
NC Veh
NC 1α,25
MV Veh
MV 1α,25
Treatment
C
Cell Profiler
% Cells Min 6 PKH26 Spots
AB
B
AB
A
NC Veh
NC 1α,25
MV Veh
MV 1α,25
Treatment

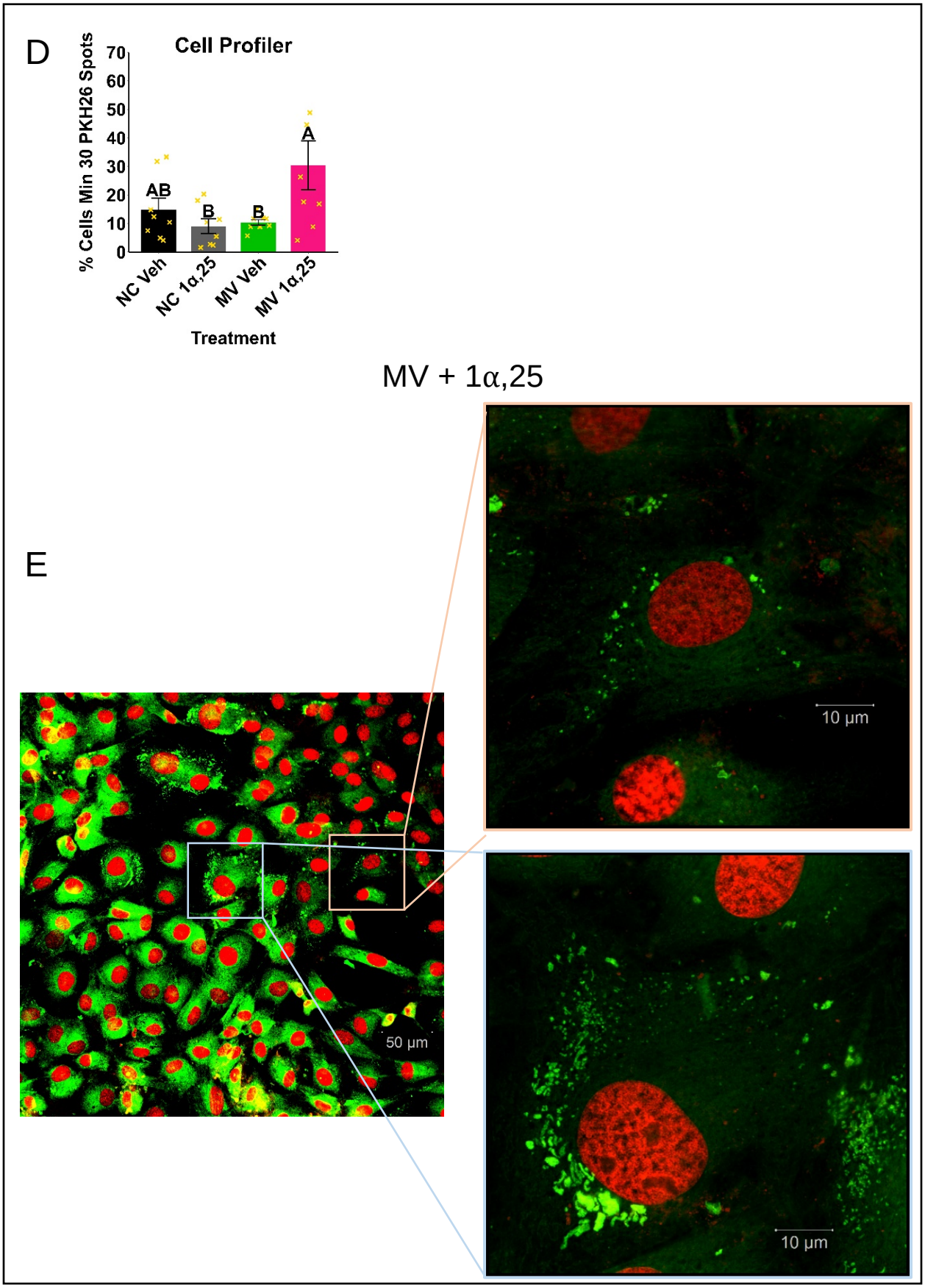
D
Cell Profiler
% Cells Min 30 PKH26 Spots
70
60
50
40
30
20
10
0
AB
B
B
A
NC Veh
NC 1α,25
MV Veh
MV 1α,25
Treatment
MV + 1α,25
E
50 µm
10 µm
10 µm

Figure 3.7 MV Endocytosis. (**A**) Representative images from each of the four groups: PKH26 stained MVs with 1α,25, PKH26 stained MVs with vehicle, PKH26 stained saline with 1α,25 & PKH26 stained saline with vehicle. (**B**) Percent of cells stained with 6+ PKH26 spots from human counting. (**C**) Percent of cells stained with 6+ PKH26 spots using cell profiler pathway. (**D**) Percent of cells stained with 30+ PKH26 spots using cell profiler pathway. (**E**) High magnification images of chondrocytes stained treated with PKH26 stained MVs with 1α,25. Mean ± SE, groups not sharing a letter are statistically different (α=0.05). *NC*: NaCl treated with PKH26. *MV*: MVs treated with PKH26.

Discussion

$1\alpha,25(OH)_2D_3$ has been known to have a strong regulatory impact on the growth plate and this study further expands on its regulatory capabilities with respect to GC cells and MVs. MicroRNA packaged into MVs was demonstrated to be under the regulatory influence of $1\alpha,25(OH)_2D_3$. In contrast, $1\alpha,25(OH)_2D_3$ had little effect on microRNA within the cells. This was demonstrated by the one differentially expressed microRNA when comparing the cell population treated with vehicle or $1\alpha,25(OH)_2D_3$. 18 microRNA were found to be differentially expressed between the two MV populations and around 200 when comparing the cells and the MVs they produced. We used these groups of differentially expressed microRNA to explore what known pathways are potentially being regulated. These were trimmed down to musculoskeletal related pathways and we found that just over half the microRNA have previous connection to musculoskeletal tissues (47 of 91) and of the 37 microRNA selectively exported in MVs known to be found in musculoskeletal tissues only 16 have known mRNA or pathways. There was a limited set of chondrocyte related pathways found to be connected to the exported microRNA using the IPA software with proliferation, osteoarthritis and maturation being the only previously established connections.

MicroRNA were found to be protected from RNAase activity within MVs with or without $1\alpha,25(OH)_2D_3$. Adding tween 20 detergent to the solution rendered the microRNA vulnerable to degradation while adding $1\alpha,25(OH)_2D_3$ to the solution resulted in no discernable degradation.

MVs stained with PKH26 were visible bound to GC cells under confocal imaging and the addition of $1\alpha,25(OH)_2D_3$ to cell culture during treatment increased the number of MVs binding to and being endocytosed by GC cells. Distinct green dots, likely clusters of MVs, were visible in the MV + PKH26 samples under high magnification and appeared to surround the cell's nucleus.

The role of 1α,25$(OH)_2D_3$ in modulating microRNA within the growth plate appears to be primarily through the coordinated production of microRNA by GC cells followed by the selective packaging of microRNA into MVs. 1α,25$(OH)_2D_3$ is potentially acting through both genomic and nongenomic avenues within GC chondrocytes to achieve this regulatory effect. In altering the MV microRNA population, 1α,25$(OH)_2D_3$ has the means to modulate a wide array of pathways well downstream of MV packaging and export. Depending on growth plate stage, this regulation may well be exerted on bone forming cells during vascular invasion and matrix turnover.

We examined the microRNA being exported into MVs in order to assess the likelihood of them regulating cartilage or bone. It has been well established that each microRNA is able to impact numerous pathways depending on their binding complementarity and what pathways are currently active within the cell. The differentially expressed microRNA in the GC MVs are no exception and this was validated by miEAA bioinformatic analysis, which returned numerous cartilage and bone associated pathways that are likely impacted by these microRNA. Interestingly the majority of selectively exported microRNA that are associated with musculoskeletal terms do not have any pathways or mRNA linked to them (12 of 17 for 1α,25$(OH)_2D_3$ export and 9 of 20 for vehicle export) and for exported microRNA only half have any known musculoskeletal connections (17 of 30 for 1α,25$(OH)_2D_3$ export and 20 of 44 for vehicle export).

1α,25$(OH)_2D_3$ has a quantifiable impact on the microRNA population found in MVs. The impact is most pronounced when looking at the microRNA that are being exported by the cells as opposed to comparing within the cell and MV samples as indicated by the PCA plot. One cellular microRNA was differentially expressed in response to 1α,25$(OH)_2D_3$. This stands in stark contrast to the roughly 200 microRNA differentially expressed between MVs and their parent cells. When examining the pathways that are potentially impacted by the set of differentially expressed microRNA we found thousands of pathways that we were able to trim down to hundreds of pathways using a manually curated set of musculoskeletal specific search terms. This resulted in a set of microRNA with associated pathways and / or mRNA, another set of microRNA that were just associated on a tissue level and had no pathways or mRNA associated with them, and a final

set of microRNA that were differentially expressed in our study but have no known containing musculoskeletal terms. All three groups of microRNA are clear avenues of further investigation in order to understand what pathways they are in fact modulating in chondrocytes and potentially bone forming cells.

MV microRNA have been demonstrated to be distinct populations when compared to the cells that produced the MVs and are able to impact the phenotype of chondrocytes *in vitro*. How these microRNA are making their way back to the chondrocytes to exert a regulatory influence remains unclear. 1α,25$(OH)_2D_3$ has been demonstrated to release the content of MVs by destabilizing the membrane and MVs are able to safeguard the microRNA cargo from RNase digestion. In beginning to examine the route that microRNA may take from MV to cell we treated harvested MVs with 1α,25$(OH)_2D_3$ in the presence of RNase to see if the microRNA is being released into solution. Surprisingly the 1α,25$(OH)_2D_3$ + RNase treatment did not result in increased RNA degradation indicating that the microRNA may be bound to protective carrier proteins within the MVs, bound to the inner leaflet of the MVs, or the MV population may be heterogeneous with some MVs reacting to 1α,25$(OH)_2D_3$ and releasing their contents into the matrix and others remaining intact with their cargo that includes microRNA.

Examining MV endocytosis by chondrocytes following fluorescent staining we observed an apparent increase in cells with distinct spots of PKH26 staining in the MV group as compared to the negative control. This was not statistically significant in the quantification of the images as there was a high degree of variability in the results and some background PKH26 staining in all groups. The background staining did not show up in any control images taken without PKH26 stain and so is not likely to be autofluorescence. Both the NC and MV groups had a visible red pellet that was resuspended for the cell treatment likely exposing all cells to a mix of bound and unbound PKH26. With the automated quantification results we were able to adjust the threshold for what is counted as a stained cell from 6 to 30 spots and this resulted in greater reductions for the NC vehicle, NC 1α,25$(OH)_2D_3$ and MV vehicle groups compared to MV 1α,25$(OH)_2D_3$. Treatment with 1α,25$(OH)_2D_3$ may be making the cells and/or the MVs more available for

endocytosis and as a result increasing the percent of cells with high concentrations of stained vesicles. Alternatively, the MVs may be rupturing as a result of 1α,25$(OH)_2D_3$ treatment increasing the number of distinct spots observed on the cells. A high resolution view of the cells demonstrates the distinct spots of PKH26 staining visible in the area around the counterstained nuclei.

Our results were not able to resolve the question of how the microRNA are gaining access to the chondrocytes to perform their regulatory role though we were able to demonstrate that the microRNA packaged within MVs is provided with protection from RNase. With the microRNA remaining protected from degradation we have additional emphasis to the intentional packaging of microRNA in MVs and additional questions as to the route taken by the microRNA on their way into the chondrocytes. With the high resolution images that involved stained MVs we were able to see what appears to be vesicles or vesicle fragments (the microRNA may be bound to the interior of the lipid bilayer) adhering to the cell membrane. The stained MVs are found a distance away from the stained nucleus and appear to be bound to or passing through the cell membrane.

1α,25$(OH)_2D_3$'s role continues to become more complex and integral to the overall functioning of the growth plate. As the cellular population of microRNAs are experiencing virtually no observable impact as a result of 1α,25$(OH)_2D_3$ treatment this regulation is likely happening through a coordinated combination of genomic and non-genomic pathways that regulate both the production and packaging of microRNA into MVs. How these exported microRNA are able to regulate not only growth plate chondrocytes but osteoblasts and other cells integral to bone growth could have numerous clinical applications. Gaining a more complete understanding of the role, if any, that 1α,25$(OH)_2D_3$ plays in MV microRNA release would be useful in any therapeutic application involving vesicles. Specifically understanding if the microRNA are contained / bound to a carrier protein, attached to the interior leaflet of the MV membrane or simply within a population of vesicles that don't respond to 1α,25$(OH)_2D_3$ will be essential to developing any microRNA based treatments. However, the increase of MV staining on chondrocytes following 1α,25$(OH)_2D_3$ treatment does indicate that 1α,25$(OH)_2D_3$ may be a key component of any vesicle based microRNA treatments to aid in endocytosis and increase delivery to the cells.

Supplementary materials

Search Terms
chondro
ossif
endochon
bone
cartilage
blast
clast
osteo
mesenchym
vitamin d
collag
growth zone
growth plate

Supplementary Table 3.1 Search terms used on miEAA results.

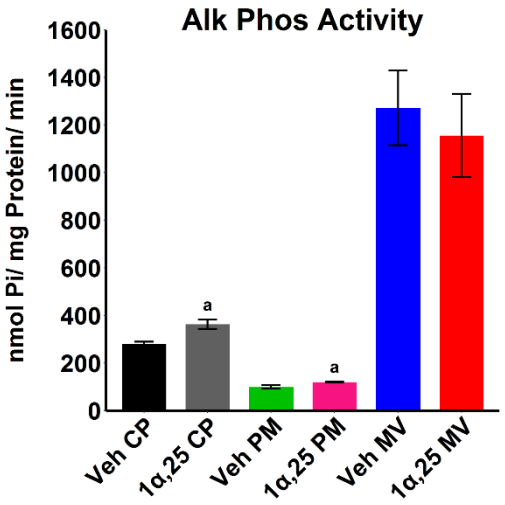

Supplementary Figure 3.1 Alkaline phosphatase activity in cell pellet (CP), plasma membrane (PM) and matrix vesicle (MV) samples with either vehicle or 1α,25 treatment. Mean ± SE, groups not sharing a letter are statistically different (α=0.05).

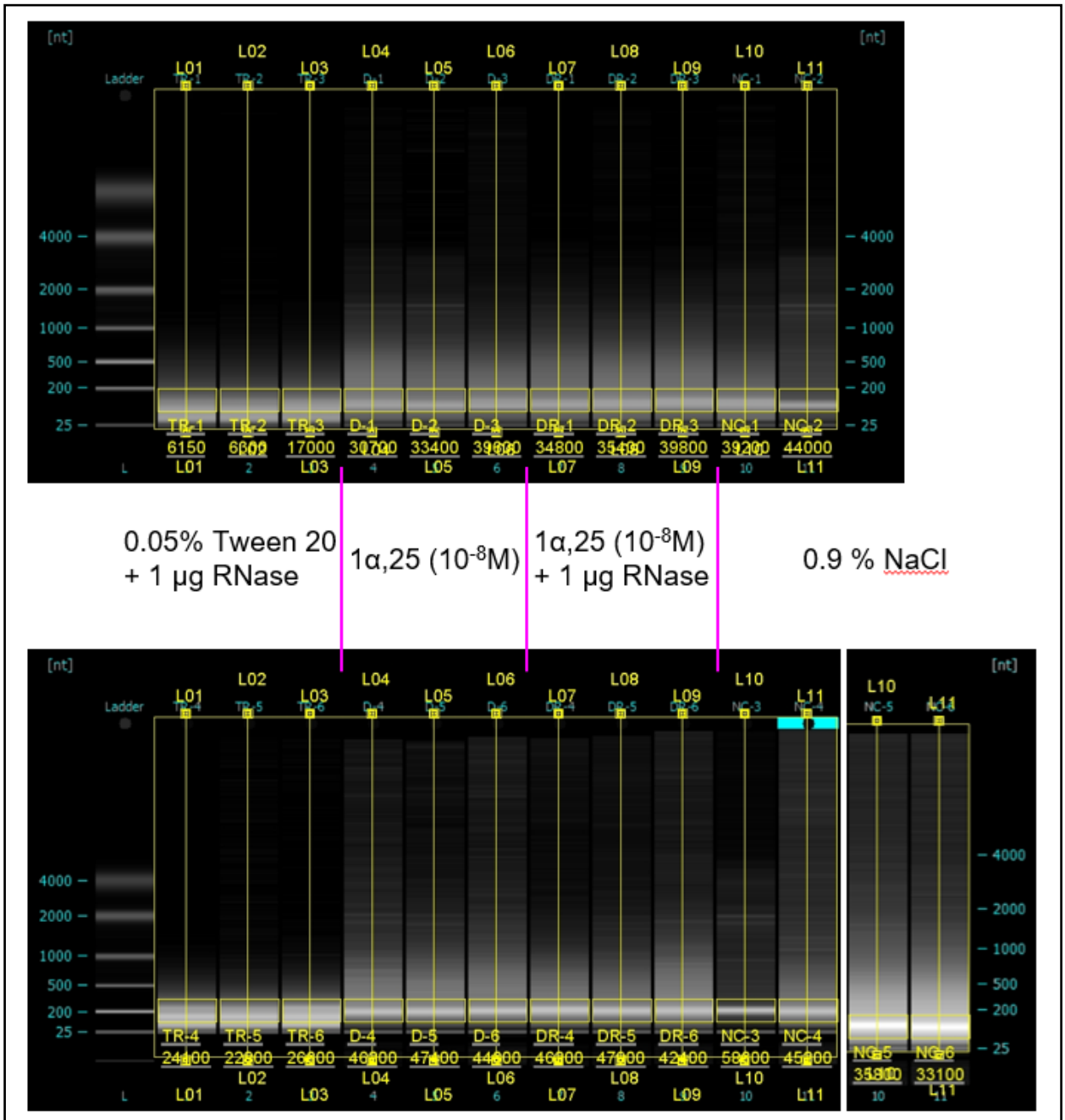

Supplementary Figure 3.2 Bioanalyzer gel quantified with Licor's Image Studio Lite software.

Specific microRNA–mRNA Complex Pulldown from Growth Zone Chondrocytes

In process

Abstract

MicroRNA are able to regulate mRNA through the RISC and typically bind to the target mRNA's 3` UTR. The binding is occurring through the microRNA's ~8 base long seed region which prohibits translation of the sequestered mRNA and with sufficient complementarity the mRNA ends up degraded by the RISC. Determining the phenotypic effects of a microRNA on a cell population depend on the cell's active transcriptome and the competing microRNA that are active in the cell. Going from microRNA prediction databases to accurate phenotypic responses remains a challenge. This study selected microRNA that have been found to be exported within MVs in the growth plate and construct a protocol to accurately determine the mRNA under their regulation. Biotin tagged microRNA LNA triple stranded mimics were transfected into GC cells and then pulled down with streptavidin coated magnetic beads 48 hours later. The RNA was isolated and sequenced on a desktop sequencer producing long read data that was aligned to the transcriptome. The resulting genes were analyzed for differential expression against the negative control group and the microRNA to mRNA 3` UTR binding energies estimated. The differentially expressed up-regulated mRNA was used for pathway analysis. Genes were found to be significantly differentially expressed between the five microRNA groups and the negative control with minimal overlap between them. The microRNA to mRNA minimum binding energies were found to be within range of what is considered possible mRNA targeting. This study provides a fairly direct method of assessing some of the mRNA that are being regulated by a specific microRNA within a certain cell type. Doing this *in vitro* allows the active transcriptome to accurately regulate what mRNA are available for regulation and provides a good starting point for investigating the potential phenotypic effects of a specific microRNA.

Introduction

The majority of mammalian skeletal growth occurs through the process of endochondral ossification where mesenchymal stromal cells condense and form a cartilage template populated by chondrocytes that mature, differentiate, and trigger mineralization of the ECM that is subsequently turned over into bone.[12,161] This process contains distinct phases where cells

and the matrix undergo measurable changes. Chondrocytes form into columns as they transition through the growth plate from proliferating cells in the RC to hypertrophic cells within the GC.[91] The composition of the matrix changes from one rich in collagen type II and sGAGs in the RC to one dominated by collagen type X and ALP in the GC.[24,131,174] Throughout this process chondrocytes are producing matrix vesicles (MV) and releasing them into the growth plate.[19,43,57]

MVs were initially discovered as focal points of tissue mineralization with hydroxyapatite crystals growing through the lipid membrane.[90] Subsequent research has discovered that MVs have a unique composition and cargo dependent on the parent cell's stage of maturation. MVs appear to bud of laterally from chondrocytes though the composition of their lipid membrane is distinct from that of the parent cell.[175] The cargo carried by MVs includes minerals and enzymes vital to the mineralization process but also contains factors for chondrocyte regulation, enzymes that facilitate in ECM turnover and factor activation, and microRNA for chondrocyte regulation.[9,36,37]

MicroRNA are short strands of RNA that are involved in the regulation of protein production within cells. Once in the cytoplasm they are loaded into the RISC as ~22 base long single strands of RNA.[66] Depending on the binding complementarity of a ~8 base long seed region within the microRNA to cytoplasmic mRNA the mRNA is either sequestered or degraded by the RISC.[67,68] MicroRNA are typically not limited to one specific mRNA and as a result can have a wide array of effects depending on the cell's current transcriptome.[68] This enables microRNA to have varying regulatory effects based on cell type and stage of maturation while also making a purely bioinformatic approach to target prediction and phenotypic effect increasingly difficult. Additionally, microRNAs are able to target multiple distinct pathways within one cell.

MV microRNA has been demonstrated to be a population distinct from the parent cell and to not only vary based on chondrocyte maturation level but fall under the regulatory control of 1alpha,25 dihydroxyvitamin D3 [$1\alpha,25,(OH)_2D_3$].[2,55](Asmussen *et al.* Under Review) These microRNA are capable of regulating the phenotype of both RC and GC chondrocytes indicating

that target pathways for the microRNA are active within the chondrocytes. It remains unclear how these microRNA find their way into chondrocytes (or possibly cells of the bone forming complex) though their selective export from chondrocytes into MVs with some microRNA being found almost exclusively in the cell or MV populations, their protection from RNase in MVs even following 1α,25,$(OH)_2D_3$ treatment, and the increase in MVs adhering to chondrocytes when treated alongside 1α,25,$(OH)_2D_3$ all point to intentional export of the microRNAs for the purpose of downstream regulation. (Asmussen *et al.* Under Review)

Some of the selectively exported microRNA have known or predicted target mRNAs and pathways within chondrocytes and other cells of the musculoskeletal tissues. However comprehensive targets for the microRNA remain incomplete and a large portion of the microRNA have no known or predicted targets within musculoskeletal tissues.

With the high likelihood of these microRNA performing regulatory functions on the growth plate chondrocytes and the potential for engaging these as treatments for growth plate disorders and possibly for use with articular cartilage it is important to gain a more complete understanding as to their direct regulatory role. What chondrocyte mRNA are being impacted by select microRNA? This study aims to provide a *in vitro* approach to answering this question using microRNA mimic transfection, RISC pulldown, and a tabletop long read sequencer.

Methods

Chondrocyte Cultures

Chondrocyte cells were isolated from male 100 to 125 g Sprague Dawley rats as has been previously detailed by Boyan *et.al.*[8,91] Animal procedures connected with this work were approved by the Institutional Animal Care and Use Committee at Virginia Commonwealth University. In brief, rats were killed by CO_2 asphyxiation followed with cervical dislocation. Sharp dissection was used to remove the rib cages and trim excess tissue. Ribs were placed in Dulbecco's modified Eagle's medium (DMEM, Life Technologies, Carlsbad, CA) 1 g/L glucose, 150 U/mL penicillin and 150 µg/mL streptomycin and kept on ice. Under a dissection microscope all tissue was cut from around the ribs and the cartilage adjacent to the bone cut into slices

separating out GC and RC sections discarding one or two transition slices. Slices were incubated (37 ˚C and 5% CO_2) overnight in 1 g/L glucose DMEM with 10% FBS, 50 U/mL penicillin, 50 µg/mL streptomycin. The following day the slices were washed twice with Hank's Balanced Salt Solution containing 50 U/mL penicillin and 50 µg/mL streptomycin then incubated in 0.25 % trypsin-EDTA (Gibco, Gaithersburg, MD) for 1 hour, washed once as before and incubated (37 ˚C and 5% CO_2) in 0.2% collagenase type II (Worthington Biochemical, Lakewood, NJ) on a shaker for 3 hours. Cell solution was passed through a 40 µm nylon mesh strainer, FBS added to 10% and cells pelleted by centrifugation (500 x *g*, for 10 minutes) followed by resuspension with DMEM FM (1 g/L glucose DMEM with 10% FBS, 50 U/mL penicillin, 50 µg/mL streptomycin, and 50 µg/mL ascorbic acid). Cells were counted and then plated with a density of 20,000 cells/cm^2 for GC and 10,000 cells/cm^2 for RC. Cells were incubated (37 ˚C and 5% CO_2) and media changed 24 hours after plating and then every 48 hours. Fourth passage cells were used for all experiments.

LNA Transfection

Fourth passage GC chondrocytes were grown to 70% confluency, media were aspirated and replaced with DMEM 1X with 10% FBS. Triple stranded LNA mimics biotinylated at the 3` end (Qiagen, Hilden, Germany) were diluted 100 fold to 666.7 nM in DMEM and combined 1:1 with a solution of lipofectamine RNAiMAX transfection reagent (Invitrogen, Carlsbad, CA) that had been diluted 26 fold in DMEM. This solution of mimics and lipofectamine sat at room temperature for 20 minutes. Cells were treated with transfection solution for a further 1:10 dilution bringing final LNA concentration to 32.6 nM. For concentration trial the LNA mimic solution was diluted 1.5X four times before combining with lipofectamine solution for final concentrations of 32.6, 21.8, 14.5, 9.7, and 6.5 nM. For DNA isolation cells were incubated in transfection media for 24 hours before changing media to DMEM FM for another 48 hours of incubation. For RISC pulldown the cells were incubated in transfection media for 48 hours before the cells were lysed and the LNA pulled down.

DNA Quantification

Media were aspirated and cell layer washed twice with 1X PBS. 100 µL of 0.05% triton-x 100 in H_2O was added per well and the plate moved to -80 ˚C for storage. Samples were thawed on ice and sonicated (40 amps, 10 sec per well). QuantiFluor dsDNA system (Promega, Madison, WI) was used for quantification following standard protocol with samples run diluted 1:10 and read on a plate reader (Synergy H1 Hybrid Reader, BioTek, Winooski, VT) with excitation of 485 nm and emission of 538 nm.

RISC PullDown and RNA Isolation

Protocol based on Dash et. al., in brief.[176] 30 µL per sample of streptavidin coated magnetic beads (Pierce, Waltham, MA) were washed the day before cell harvest (3 washes with 100 µL of 10 mM Tris-Cl pH 7.5, 0.5 mM EDTA, 1 M NaCl solution and 3 washes with 100 µL solution of 0.1 M NaOH, 0.05 M NaCl), resuspended (100 µL solution of 0.5 M NaCl), and blocked (200 µL of 1 µg/µL BSA, 2 µg/µL Yeast tRNA solution) overnight in 4 ˚C. Cells were removed from flasks with trypsin, pelleted (1,500 x *g* for 5 min at 4 ˚C), washed with sterile 1X DPBS, pelleted again as before, and resuspended in 600 µL lysis buffer (150 mM NaCl, 25 mM Tris-Cl pH 7.5, 5 mM DTT, 0.5% IGEPAL, 60 U/mL Superase, 1x Protease Inhibitor Cocktail) before being rapidly frozen in -80 ˚C and then thawed on ice. Cellular debris was pelleted (16,000 x g for 5 min at 4 ˚C) and supernatant combined with ¼ volume of 5 M NaCl to generate cell lysate solution. Beads from previous day were washed three times with 150 µL of pulldown wash buffer (10 mM KCl, 1.5 mM MgCl2, 10 mM Tris-Cl pH 7.5, 5 mM DTT, 1M NaCl, 0.5% IGEPAL, 60 U/mL Superase, 1x Protease Inhibitor Cocktail) and then resuspended in 300 µL of pulldown wash buffer. 300 µL of cell lysate solution was incubated with 300 µL streptavidin coated beads for one hour at room temperature. Beads were washed three times with 300 µL pulldown wash buffer and finally resuspended in 100 µL of nuclease free water on ice. 700 µL qiazol (Qiagen) was added to each tube before transferring to -80 ˚C. RNA was precipitated following miRNeasy micro kit (Qiagen) protocol for animal cell samples. RNA was eluted in 30 µL of nuclease free water per sample.

Library Preparation and RNAseq

RNA isolations were quantified with a RNA 6000 pico chip on a BioAnalyzer (Agilent, Santa Clara, CA) and library prepared according to specifications of the PCR-cDNA Barcoding kit (SQK-PCB109, Oxford Nanopore, Oxford, UK) for 12 samples and run on a Spot On Flow Cell Mk 1 R9 (Oxford Nanopore) for 72 hours. High precision basecalling was carried out on Nanopore's MinIT running MinKNOW (21.05.24) and guppy (5.0.16).

Bioinformatic Analysis

Fastq files that were considered to have passed basecalling were transferred to VCU's high performance research computing core facility where reads were aligned using minimap2 (2.21-r1071) to Ensemble's *Rattus norvegicus* transcriptome (Rnor_6.0) and quantified with salmon (v1.5.2).[177,178] The count data was then analyzed in R (4.1.0), differential expression determined using DESeq2 (1.32.0), PCA plots built with pca3d (0.10.2) and PCAtools (2.4.0), Venn diagrams made with VennDiagram (1.6.20), stacked bar figures with bigPint (1.8.0), and volcano plots with ggplot2 (3.3.5).[151,154,172,179–182] UTRdb was used to download the 3` UTRs of the differentially expressed genes.[85] Specific microRNA sequences were downloaded from mirBase.org.[80] RNAhybrid tool was used to determine the microRNA to mRNA 3`UTR minimum binding energies.[84] Pathway analysis was carried out using the PANTHER classification system (16.0) webtool.[183]

Statistical Analysis

DNA quantity is presented as mean ± standard error of the mean for six samples for each group. An ANOVA with Tukey HSD post-hoc test was used to examine differences between the groups. Significance was determined by a $p \leq 0.05$.

Results

microRNA 22-3p & 122-5p Concentration Trials

In determining optimal transfection concentration we transfected with different amounts (6.5, 9.7, 14.5, 21.8, and 32.6 nM) of scrambled negative control (NC), 22-3p, and 122-5p LNA mimics along with a no treatment control (NT) and the corresponding MirVana mimic (Thermo

Fisher, Waltham, MA) at 14.5 nM whose concentration had been determined in a previous study.[9] At 32.6 nM of LNA 122-5p we see an increase in DNA production nearly identical to what is observed for transfection with MirVana mimic 122-5p, 32.6 nM of LNA NC is nearly identical to NT group, and 32.6 nM of LNA 22-3p is slightly increased when compared to the MirVana mimic 22-3p (Fig. 4.1 A).

microRNA Mimic Selection

We selected five microRNA mimics that were highly exported into MVs from chondrocytes

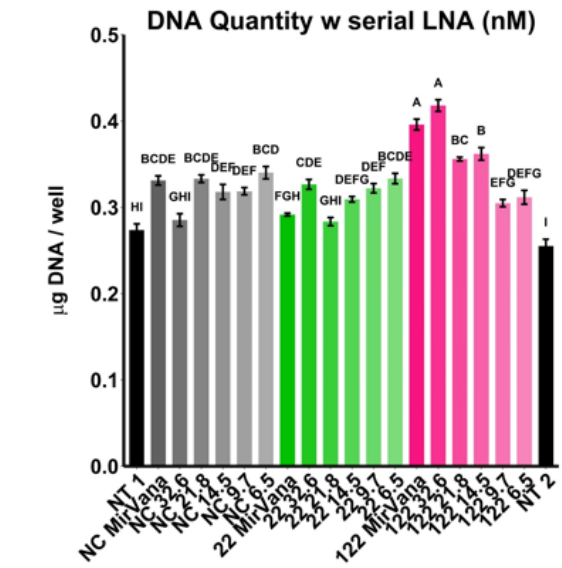

B

	Fold Change	
rno-miR-1-3p	29.24	Cell to MV with 1α,25
rno-miR-22-3p	7.46	Cell to MV
rno-miR-30c-5p	2.19	Cell to MV with 1α,25
rno-miR-122-5p	2,352.53	Cell to MV
rno-miR-133a-3p	60.97	Cell to MV with 1α,25

Figure 4.1 LNA transfection and microRNA selection. (**A**) Transfecting NC, microRNA 22-3p, and microRNA 122-5p LNA at concentrations of 6.5, 9.7, 14.5, 21.8, and 32.6 nM, and MirVana mimics of each at 14.5 nM with two NT groups. (**B**) Table of fold change values from Cell to MV in two separate experiments (one with 1α,25 treatment and one without). Mean ± SE, groups not sharing a letter are statistically different (α=0.05). *NC*: negative control, *NT*: no treatment.

based on previous experiments[9,55] (Asmussen *et al.* Under Review) These microRNA exhibited fold changes ranging from 2.19 to 2,352.53 when comparing the GC microRNA population with the MVs that they produced (Fig. 4.1 B).

Sample Clustering

13,664 genes were returned from the alignment of the sequencing reads between all 24 samples. A PCA plot of these reads resulted in minimal clustering with just over 20% of variation represented between PC 1 & 2 (Fig. 4.2 A). Examining the 502 differentially expressed genes between each targeted microRNA and NC resulted in three distinct clusters with NC alone in one

cluster, microRNAs 22-3p and 122-5p having minimal overlap in a second cluster and microRNAs 1-3p, 30c-5p, and 133a-3p grouping together in a third cluster (Fig. 4.2 B). A scree plot of the differentially expressed genes shows that roughly 35% of variation is explained by PCs 1-3 (Fig. 4.2 C). This can be visualized in a 3d PCA plot which shows distinct clusters forming when viewed with PCs 1-3 (Fig. 4.2 D).

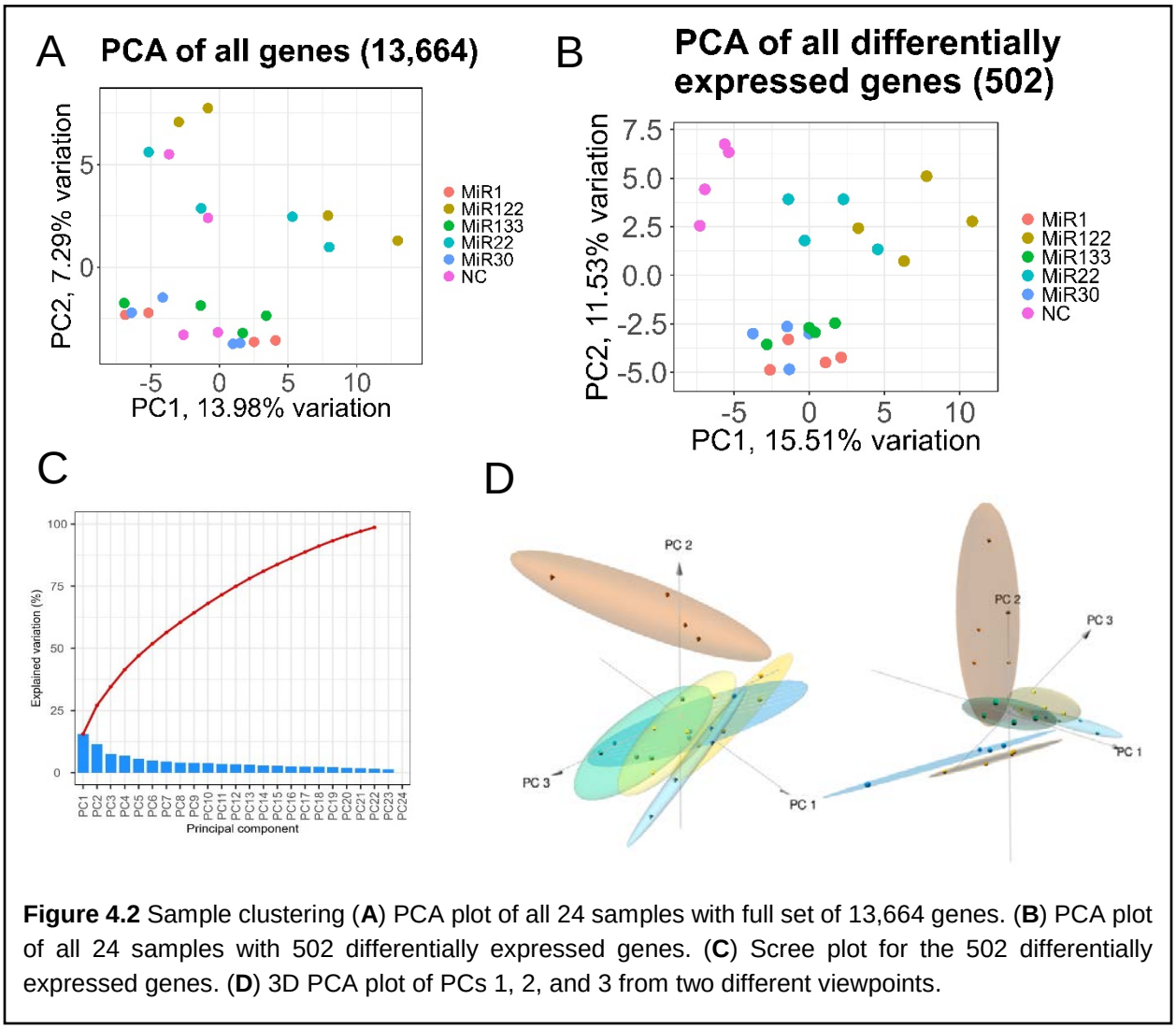

Figure 4.2 Sample clustering (**A**) PCA plot of all 24 samples with full set of 13,664 genes. (**B**) PCA plot of all 24 samples with 502 differentially expressed genes. (**C**) Scree plot for the 502 differentially expressed genes. (**D**) 3D PCA plot of PCs 1, 2, and 3 from two different viewpoints.

Differential Expression

MicroRNA groups (1-3p, 22-3p, 30c-5p, 122-5p, and 133-3p) are compared against NC using DESeq2 with a cut off for differential expression of absolute log 2 fold change ≥ 1 and a p-value ≤ 0.05. Results of all five comparisons are visualized in volcano plots with a horizontal line at $-\log_{10}(0.05)$ and vertical lines at $\log_2(0.5)$ and $\log_2(2)$ (Fig. 4.3 A-E). All five comparisons have differentially up and down-regulated genes compared to NC. The differentially expressed up-

regulated genes when viewed across the eight samples in the two groups in question have minimal fluctuation within each group (Supplemental Fig. 4.1).

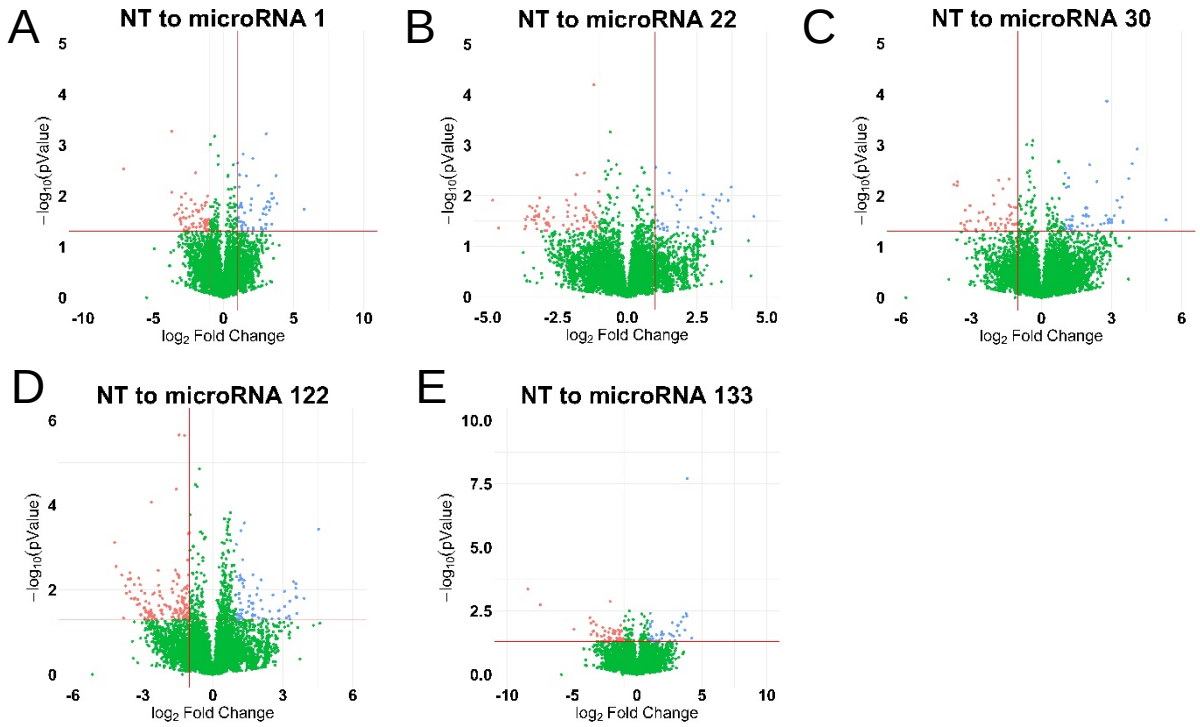

Figure 4.3 Volcano plots of differentially expressed genes between each of the five microRNA groups and NC. (**A**) NC and microRNA 1-3p. (**B**) NC and microRNA 22-3p. (**C**) NC and microRNA 30c-5p. (**D**) NC and microRNA 122-5p. (**E**) NC and microRNA 133a-3p. Horizontal red line at $\log_{10}(0.05)$, vertical red lines at $\log_2(0.5)$ and $\log_2(2)$ with the differentially expressed genes indicated by red for down-regulated and blue for up-regulated.

Examining the 502 differentially expressed genes between all five comparisons for overlap 415 of the genes are only differentially expressed within one comparison and 62 are shared by two comparisons (82.7%) (Fig. 4.4 A). Of the 502 differentially expressed genes 165 of them are increased in the microRNA sample compared to NC with 112 (67.9%) of these uniquely increased within one microRNA and 33 (20.0%) shared between two (Fig. 4.4 B and Table 4.1). An increased proportion of genes are uniquely decreased in one sample (307 out of 339 or 90.6%) with 27 genes (8.0%) decreased in two microRNA groups (Fig. 4.4 C).

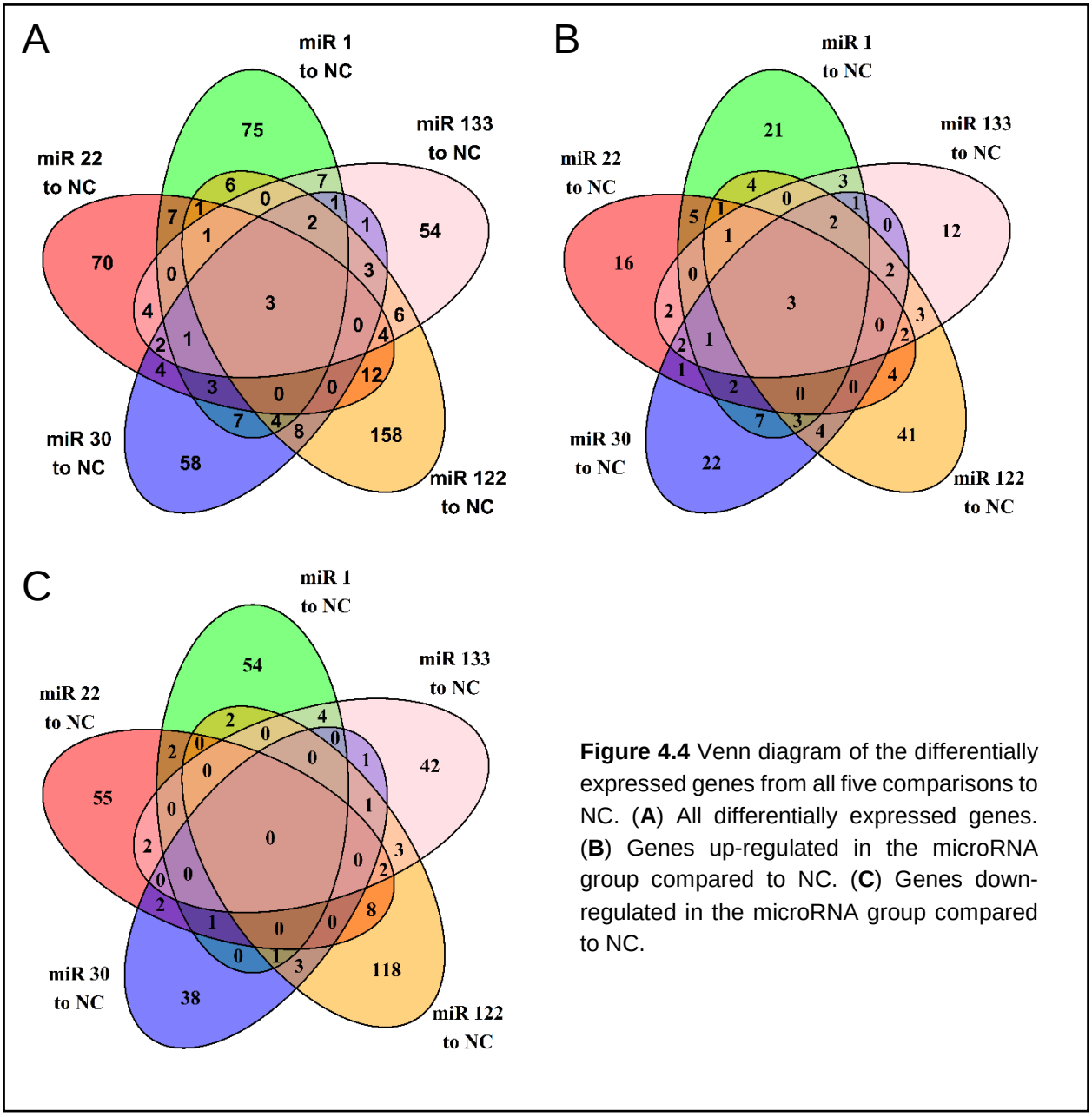

Figure 4.4 Venn diagram of the differentially expressed genes from all five comparisons to NC. (**A**) All differentially expressed genes. (**B**) Genes up-regulated in the microRNA group compared to NC. (**C**) Genes down-regulated in the microRNA group compared to NC.

NC to microRNA-1-3p		NC to microRNA-22-3p		NC to microRNA-30c-5p		NC to microRNA-122-5p		NC to microRNA-133a-3p	
Gene	log 2 FC	Gene	log 2 FC	Gene	log 2 FC	Gene	log 2 FC	Gene	log 2 FC
APOOL	1.334	ARF1	1.005	ARSA	1.328	AAGAB	2.576	CNGB1	3.282
ARF6	3.046	CEP162	2.754	CARF	3.01	AARD	2.84	Cplane2	1.925
ATP6AP2	2.111	CZIB	1.089	CBR3	2.014	ADPRM	1.906	CYB561A3	1.917
BAMBI	1.587	DARS2	2.18	CDR2L	2.058	ALKBH3	1.118	DDX42	1.028
Bmyc	1.519	DR1	4.543	CEBPA	2.923	Akbh6	1.647	DEGS1	1.03
C15orf62	2.684	FBXO34	3.25	CPXM2	1.333	ARF1	1.116	DR1	4.227
CARF	3.019	H1f2	1.426	CUEDC1	1.755	ATRAID	1.188	EIF4G1	1.176
CFAP45	1.738	HPF1	1.258	DDX42	1.17	CDCA3	1.715	G6PD	1.001
CPNE8	3.273	Hrct1	3.078	EIF2AK4	1.943	CDK4	1.292	Gpbp1l2	1.88
CSF2RA	1.447	ID4	1.803	ELOVL5	3.48	CIBAR1	1.186	Hrct1	3.082
CUEDC1	1.96	INSIG2	3.189	ENKD1	1.782	CNN2	1.137	INSIG2	3.16
DDX42	1.142	KCTD19	3.349	ENO2	5.327	CRELD2	1.333	Timm17b	1.234
ECH1	1.127	LRRC17	3.041	FGF7	1.432	DEGS1	1.178	LRRC17	2.823
EIF4G1	1.41	MIOS	2.636	H2AC12	3.502	ELOVL5	3.917	LYAR	1.132
ENKD1	2.01	MND1	3.612	HARBI1	1.215	ELOVL6	1.166	MND1	2.926
ENO2	5.763	MTM1	3.072	HEXIM2	2.858	ENKD1	1.701	MRPS6	1.016
F830045P16Rik	2.118	NGF	1.303	Hrct1	4.104	FZR1	2.832	MTM1	2.542
FBXO34	3.085	OAZ2	1.782	ID4	2.376	GALNT11	2.842	NAT2	2.548
HAX1	1.324	PEX11B	1.021	IDUA	2.76	Hist_H4-K20_MeTrfase	2.816	NELFA	3.885
Hrct1	3.738	PLAAT1	1.921	IGF1R	1.335	Hrct1	3.08	PGM1	1.335
ID4	1.742	PLPP5	1.104	KLHL29	3.45	INSIG2	3.46	PLIN3	2.502
INSIG2	3.153	POMT2	2.49	KLHL7	1.963	JAGN1	1.054	PSMD10	3.824
JAGN1	1.263	PPIL3	1.175	Timm17b	1.237	KRAB	3.607	RDH10	3.696
KLHL29	3.466	PRELID3B	1.305	LPCAT3	1.542	LIMS2	1.082	RNF103	1.493
KYAT1	3.447	PSMD10	3.73	LRP5	2.418	Timm17b	1.717	Rsl1d1l1	2.722
LATS2	1.28	Pwwp2a	3.008	LRRC17	3.246	LPCAT3	1.894	SEC24D	1.897
ME2	1.343	Rsl1d1l1	2.731	MDK	1.077	LRBA	1.812	SEPTIN2	2.026
MIOS	2.597	RSPH9	2.492	ME2	1.215	MND1	3.572	SLC25A38	3.571
MTM1	3.049	RTCA	1.51	MIOX	1.17	mt-Atp8	1.009	SRP68	1.085
NSMCE1	1.098	SEC24D	1.826	MTM1	2.692	MYCBP	1.127	TAP2	3.781
PDGFD	3.027	SLC25A10	3.15	PSMD10	3.119	NME4	1.198	Transmembrane protein 258	1.476
PEX11B	1.037	SLC25A38	3.311	REXO1	3.363	NSMCE1	1.041	VPS37A	1.712
PSMD10	3.334	SPC24	1.611	RPRD1B	2.539	OAZ2	1.726	WDR44	3.415
RARRES2	1.271	SPR	1.445	SEC24D	1.906	PCLAF	1.54	ZNHIT3	2.64
RDH10	3.836	SSBP2	1.885	SLC25A38	2.903	PDGFD	3.592		
REXO1	3.585	SYPL1	2.116	Srsf5	1.019	PEX11B	1.21		
RHOBTB3	1.649	Tipin/Tipinl1	1.262	SSBP2	1.877	PFN2	1.167		
RHOT1	1.234	TOP2A	1.489	TAP2	3.735	PGM1	1.487		
RNF114	1.35	TYW5	3.376	TBC1D9B	1.023	PIAS2	1.715		
RNF214	1.338	ZNHIT3	2.453	TENT5A	1.183	PLIN3	2.448		
RSPH9	2.908			TGIF1	1.073	PPAN	1.97		
RTCA	1.269			TLL1	2.799	PRAF2	1.243		
SEPTIN2	2.488			TMC5	1.288	PRELID3B	1.532		
SLC25A38	3.285			Tmem234	1.301	PSMD10	3.309		
SLC7A7	3.04			TRIM47	2.999	RNF214	1.425		
SYPL1	1.954			TYW5	2.846	ROGDI	1.701		
TAP2	2.797			UFD1	1.055	SFT2D1	1.347		
TAPT1	2.819			VPS37A	1.9	SLC25A38	4.528		
TENT5A	1.067			WDR44	3.885	SMIM10L1	2.081		
TGIF1	1.164			WDR54	2.189	STEAP1	2.186		
TYW5	2.718					TAP2	3.556		
UBE2D1	1.181					TBC1D13	3.275		
WDR44	3.436					Tgds	2.127		
WDR54	2.14					TGIF1	1.134		
						Tipin/Tipinl1	1.346		
						TMED1	1.056		
						Tmem234	1.575		
						TRAFPC1	1.019		
						TTC37	2.535		
						TXNDC12	1.282		
						UBALD2	3.148		
						UBE2C	1.221		
						UFD1	1.075		
						VAMP7	1.246		
						VPS37A	2.056		
						WDR44	3.569		
						WDR54	2.145		
						ZDHHC4	1.271		
						ZNF606	3.297		
						ZNHIT3	3.089		

Table 4.1 All of the differentially expressed up-regulated genes in the five comparisons to NC.

GO Pathway Analysis

All of the differentially expressed up-regulated mRNA were submitted to the PANTHER online gene ontology tool to begin to examine the pathways they are connected to. The results were searched for musculoskeletal related terms in order to filter down the 5,725 total pathways that were returned. This left 25 pathways for microRNA 1-3p, 15 for microRNA 22-3p, 39 for microRNA 30c-5p, 19 for microRNA 122-5p, and 21 for microRNA 133a-3p (Table 4.2).

microRNA 1-3p		microRNA 22-3p		microRNA 30c-5p		microRNA 122-5p		microRNA 133a-3p	
label	# of genes	label	# of genes	label	# of genes	label	# of genes	label	# of genes
bone development	1	bone development	2	bone development	3	bone development	1	bone development	2
bone morphogenesis	1	bone marrow development	1	bone marrow development	2	bone morphogenesis	1	bone marrow development	1
cartilage development	1	bone morphogenesis	1	bone morphogenesis	1	cellular response to transforming growth factor beta stimulus	1	bone morphogenesis	1
cellular response to transforming growth factor beta stimulus	2	cranial skeletal system development	1	bone remodeling	1	negative regulation of osteoblast proliferation	1	mesenchymal cell development	1
embryonic skeletal system development	2	negative regulation of osteoclast differentiation	1	cartilage homeostasis	1	positive regulation of biomineralization	1	mesenchymal cell differentiation	1
embryonic skeletal system morphogenesis	1	ossification	1	extracellular matrix organization	1	positive regulation of bone mineralization	1	mesenchyme development	1
mesenchymal cell development	1	osteoblast differentiation	1	negative regulation of cartilage development	1	positive regulation of ossification	1	negative regulation of osteoclast differentiation	1
mesenchymal cell differentiation	1	regulation of osteoclast differentiation	1	negative regulation of ossification	1	positive regulation of osteoblast differentiation	1	positive regulation of calcium ion transmembrane transport	1
mesenchyme development	1	skeletal system development	2	negative regulation of osteoblast differentiation	1	regulation of biomineralization	1	positive regulation of calcium ion transmembrane transport via high voltage-gated calcium channel	1
negative regulation of osteoblast differentiation	1	skeletal system morphogenesis	1	negative regulation of osteoclast differentiation	1	regulation of bone mineralization	1	positive regulation of calcium ion transport	1
ossification	2	vesicle budding from membrane	2	ossification	2	regulation of ossification	1	regulation of calcium ion transmembrane transport	1
osteoblast differentiation	1	vesicle cargo loading	1	osteoblast development	1	regulation of osteoblast differentiation	1	regulation of calcium ion transmembrane transport via high voltage-gated calcium channel	1
positive regulation of epithelial to mesenchymal transition	1	vesicle localization	1	osteoblast differentiation	2	regulation of osteoblast proliferation	1	regulation of calcium ion transport	1
positive regulation of transforming growth factor beta production	1	vesicle organization	2	positive regulation of angiogenesis	1	vesicle fusion	1	regulation of osteoclast differentiation	1
positive regulation of transforming growth factor beta1 production	1	vesicle-mediated transport	2	positive regulation of bone resorption	1	vesicle localization	2	regulation of vesicle-mediated transport	2
regulation of cellular response to transforming growth factor beta stimulus	2			positive regulation of cartilage development	1	vesicle organization	2	skeletal system development	3
regulation of epithelial to mesenchymal transition	1			positive regulation of collagen catabolic process	1	vesicle transport along microtubule	1	skeletal system morphogenesis	2
regulation of osteoblast differentiation	1			positive regulation of collagen metabolic process	1	vesicle-mediated transport	6	vesicle budding from membrane	1
regulation of transforming growth factor beta production	1			positive regulation of epithelial to mesenchymal transition	1	vesicle-mediated transport to the plasma membrane	1	vesicle cargo loading	1
regulation of transforming growth factor beta receptor signaling pathway	2			positive regulation of mesenchymal cell proliferation	1			vesicle organization	1
regulation of transforming growth factor beta1 production	1			positive regulation of osteoblast differentiation	1			vesicle-mediated transport	2
regulation of vesicle-mediated transport	1			positive regulation of osteoblast proliferation	1				
response to transforming growth factor beta	2			regulation of angiogenesis	1				
transforming growth factor beta receptor signaling pathway	1			regulation of bone remodeling	2				
vesicle-mediated transport	3			regulation of bone resorption	1				
				regulation of cartilage development	2				
				regulation of chondrocyte differentiation	1				
				regulation of collagen catabolic process	1				
				regulation of collagen metabolic process	1				
				regulation of epithelial to mesenchymal transition	1				
				regulation of mesenchymal cell proliferation	1				
				regulation of ossification	1				
				regulation of osteoblast differentiation	1				
				regulation of osteoblast proliferation	1				
				regulation of osteoclast differentiation	1				
				vesicle budding from membrane	1				
				vesicle cargo loading	1				
				vesicle organization	1				
				vesicle-mediated transport	2				

Table 4.2 Musculoskeletal related pathways connected to differentially expressed up-regulated mRNA in the 'label' column and the number of genes associated with the particular pathway found in the microRNA differential expression list in the '# of genes' column.

microRNA to mRNA Binding Energy

The RNAhybrid command line tool was used to predict the MFE of the specific microRNA with the differentially expressed upregulated mRNA's 3` UTR when comparing the microRNA in question with NC. The average MFE for all of the microRNA to target mRNA combinations is -20.8 kcal / mol (Fig. 4.5 A). The MFE prediction is based on the most advantageous binding location estimated within the provided 3` UTR target sequence. A sample of the results is provided with a corresponding range of MFE and p-value estimations (Fig. 4.5 B).

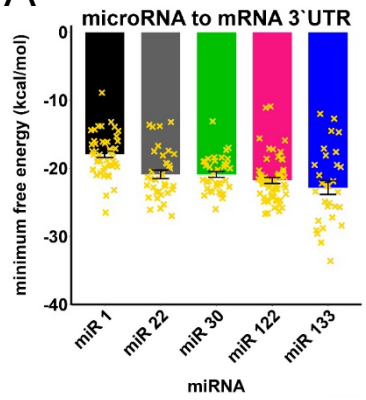

B

```
target: utr|3RNOR024718
length: 396
miRNA : rno-miR-133a-3p
length: 22

mfe: -29.6 kcal/mol
p-value: 0.025440

position  297
target 5'   U       GG       C   3'
             CUGGUUG  GGGG CU
             GACCAAC  CCCC GG
miRNA  3' GUC       UU    U  UUU 5'
```

```
target: utr|3RNOR030577
length: 218
miRNA : rno-miR-30c-5p
length: 23

mfe: -23.5 kcal/mol
p-value: 0.201401

position  122
target 5'  G    C    AA      G     G 3'
            UGAG GGUG  GGGGUG   GCA
            ACUC UCAC  UCCUAC   UGU
miRNA  3' CG         A       AAA     5'
```

```
target: utr|3RNOR013988
length: 204
miRNA : rno-miR-1-3p-mB
length: 22

mfe: -18.9 kcal/mol
p-value: 0.843001

position  122
target 5'    A       GUA     A   G 3'
              GCACUUC     GUU CCA
              UGUGAAG     UAA GGU
miRNA  3' UAUG       AAAUG         5'
```

Figure 4.5 MicroRNA to mRNA 3` UTR binding energies. (**A**) Histogram of the binding energies of all up-regulated genes matched to their corresponding microRNA. (**B**) Representative samples of the range of binding energies found between microRNA and mRNA 3` UTR.

Discussion

This study aims to establish an approach to gain a more complete understanding of what impact specific microRNA may be having within certain tissues. The specific microRNA in question are well studied and have long lists of predicted targets within the rat genome. We began by analyzing the response of the GC cells to the biotin tagged LNA mimics of two previously well studied microRNA. The higher concentration of LNA mimic was selected as it produced the most consistent phenotypic response with our previous research and since the objective is to pulldown active RISC the potential side effects of disproportionally occupying the RISC with the mimic was not a large concern in this study.

Initial examination of the sequencing results produced 13,664 genes between the six groups. Many of these genes had very low copy counts in the raw data and when selecting for the 502 genes found to be differentially expressed between NC and the select microRNA we were

able to get more distinct clustering of the six groups. The magnetic beads are blocked with yeast tRNA to reduce off target RNA binding and during the pulldown procedure the beads go through numerous wash steps as part of the RNA isolation procedure however this may only produce incomplete reduction of noise in the actual pulldown.

The differentially expressed genes had both up and down-regulated sub populations in comparison to NC and when all five comparisons were examined for overlap the majority of genes were found to be unique within their respective group. The differentially expressed mRNA in this study contain some predicted mRNA for the microRNA in question but are primarily genes not found in the microRNA-mRNA prediction databases. To try and further evaluate the likelihood of these being accurate mRNA targets we examined the MFE between each microRNA and the 3` UTR of their differentially expressed up-regulated mRNA targets. The average MFE for all of our microRNA to mRNA bindings was -20.8 kcal / mol which is slightly higher than the -25 to -30 kcal / mol that prediction algorithms often use.[86,87] Additionally a reference example of high-quality binding provided with the RNAhybrid tool is between let-7 microRNA and hbl-1 mRNA producing a MFE of -28.2 kcal / mol and a p-value of 0.064. While the average MFE of our microRNA is slightly higher than what is commonly used for computational predictions it is certainly not outside the bounds of possible microRNA to mRNA binding.

An initial pathway exploration found 5,725 different pathways associated with the differentially expressed up-regulated mRNAs. Of these, 119 pathways are directly associated with musculoskeletal tissues (e.g., “osteoblast differentiation” and “positive regulation of cartilage development”) and chondrocyte behaviors (e.g., “vesicle cargo loading”). The total list of 5,725 pathways is tissue independent and requires filtering to obtain relevant information. Most of the existing pathway analysis tools are designed around analyzing transcriptomic data that generally has a complete, or nearly so, representation of the active transcriptome under study. Since we are working with microRNA based pull down genes, we have a very incomplete representation of the transcriptome and are instead examining a regulatory mechanism. This invalidates most of the pathway tools designed to estimate likelihood of activity based on the genes in the sequencing

results. We are essentially looking at the inverse – what could the effect of down-regulating these specific genes have on the pathways that may otherwise be active within the cell.

The differentially expressed and up-regulated mRNA in this study provide a likely target list for each of the specific microRNA used in the pulldown experiment. Additional pathway analysis and interpretation is warranted to further understand what role the microRNA may be playing within the chondrocytes followed by wet lab confirmation. This is also necessary to better understand how transfecting specific microRNA will interact with the endogenous population of microRNA within the cells. This work provides a solid basis of likely mRNA targeting by specific microRNA that have been found to be selectively exported into MVs. The results, if confirmed, also call further into question relying entirely on bioinformatic prediction tools for microRNA targeting. We can see in the results from RNAhybrid that while the binding energies may not be optimal for the microRNA to mRNA there are viable binding sites for all of the microRNA within the 3` UTR of the differentially expressed mRNAs. Given that the mimics used were LNA based which have a near irreversible binding chemistry it is possible that some off target binding took place in the cytoplasm however the LNA is delivered in a 'triple' stranded configuration (where the mimic's passenger strand is composed of two separate and very short RNA strands that are designed to produce minimal interference when the mimic is processed and loaded into the RISC) and should remain triple stranded and unavailable to random mRNA binding until being processed and loaded by the RISC. This study provides a valuable resource for better understanding the direct role that microRNA will have in certain cells by making the targeted mRNA within this cell population known allowing researchers to better predict and understand what pathways are likely to be affected by a given microRNA.

Supplementary materials

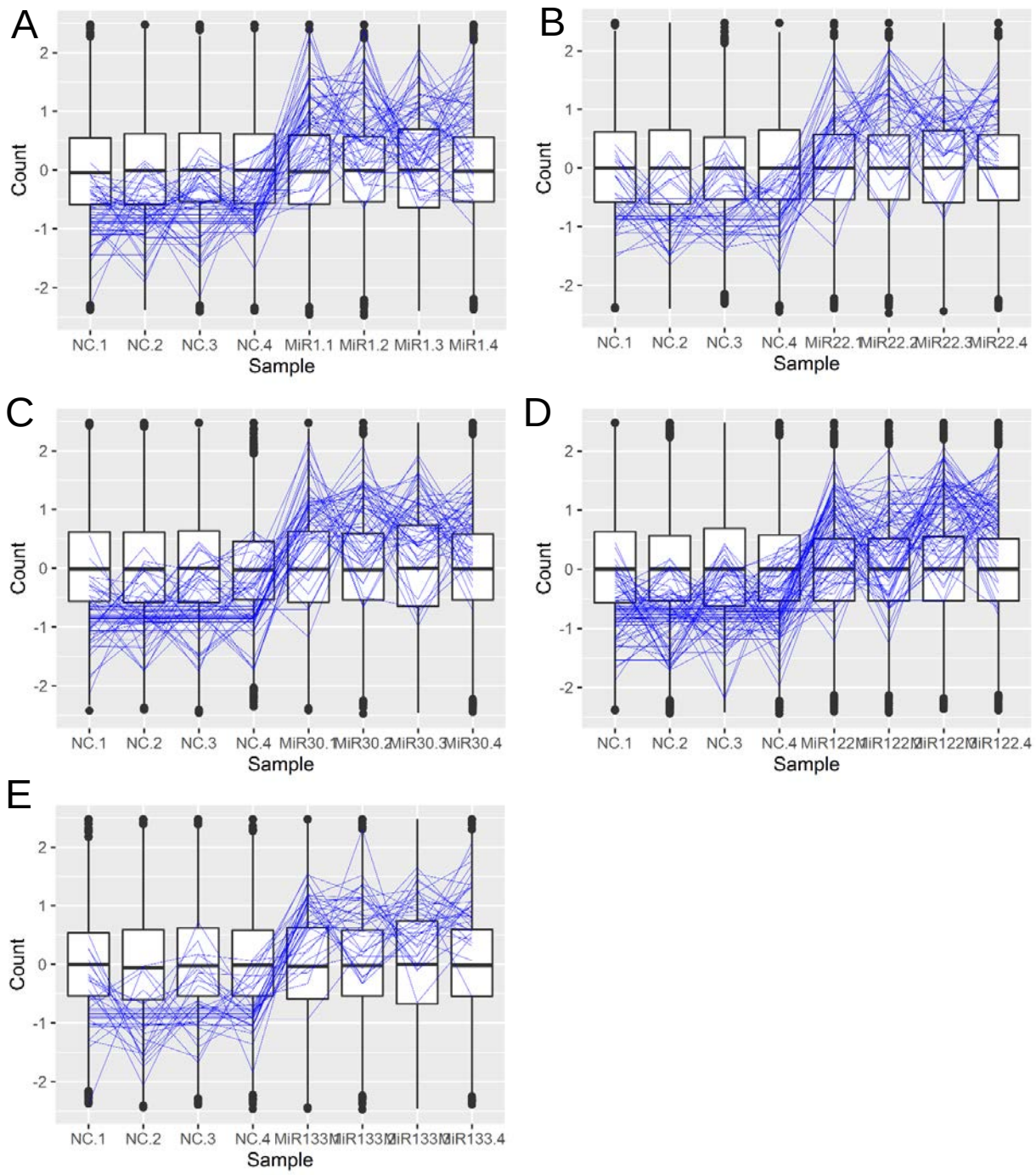

Supplemental Figure 4.1 Stacked bar plots of the differentially expressed up-regulated genes. (**A**) NC and microRNA 1-3p. (**B**) NC and microRNA 22-3p. (**C**) NC and microRNA 30c-5p. (**D**) NC and microRNA 122-5p. (**E**) NC and microRNA 133a-3p. Differentially expressed up-regulated genes have a p-value ≤ 0.05 and log 2 fold change ≥ 1.

Discussion

Studies contained in this thesis examine the role of MV microRNA in the growth plate from different angles and support the likelihood of microRNA exported in MVs to be selectively packaged, exported, and protected for the purpose of downstream cell regulation. Not all aspects of the MV microRNA lifecycle were examined in this work, though the facets that we did examine reinforced the selective export of microRNA as a regulatory factor within the growth plate while also opening numerous potential avenues of further investigation. Additionally, we adapted approaches that enabled us to investigate the *in vitro* interaction between individual microRNA and the population of mRNA it targets.

Expanding on previous work in this lab we demonstrated zonal regulation of microRNA expression and packaging. MicroRNA populations differ between the chondrocytes and MVs found in the RC and GC zones. With microRNA being selectively exported by both RC and GC chondrocytes the questions of what might be regulating the zonal production and packaging and how these microRNA might be affecting chondrocytes in the growth plate arose. We hypothesized that the microRNA with some of the highest fold change values for export into the ECM and lowest p-values would be a good place to start looking for phenotypic changes. Additionally, the question of what regulatory molecule might be regulating MV export was raised. Given what is already known about $1\alpha,25(OH)_2D_3$ and MVs, it was decided to be a good starting point.

We began by transfecting chondrocytes (both RC and GC) with individual microRNA to assess the potential for phenotypic changes. Starting with broad assays measuring total DNA content, metabolism, and alkaline phosphate activity we noticed effects following transfection with specific microRNA. The observed phenotypic effects were not something that could be correlated to bioinformatic prediction lists with any degree of confidence as we didn't observe a direct connection between something like TNAP mRNA and microRNA 122-5p. We continued to assay a wide range of proteins, factors, and responses following microRNA transfection and found numerous surprising results including the regulation of Ihh, PTHrP, VEGF and TGF- β1 following

transfection with microRNA 22-3p. microRNA 22-3p was also able to decrease total DNA production and sGAG production in RC chondrocytes.

MicroRNA 122-5p had robust phenotypic effects on the chondrocytes with what became a defining characteristic: the ability to increase various measures of chondrocyte proliferative activity (as measured by total DNA production, EdU incorporation and MTT metabolism) were all significantly increased following microRNA 122-5p transfection. Additionally, microRNA 122-5p was able to decrease collagen II production and alkaline phosphatase activity in GC chondrocytes as well as increase sGAG content to quantities similar to what is found in RC based chondrocytes grown under the same conditions. Cumulatively, microRNA 122-5p appeared to be producing a RC like phenotype in GC chondrocytes. The microRNA being examined were exported with greater fold changes in GC as opposed to RC chondrocytes; however, with the exception of microRNA 22-3p, they all appeared to be primarily exported into MVs and not kept within the cell.

How exactly exported microRNA find their way back into cells remains an open question, in addition to what type of cell is it exported for? Could a portion or all of the GC MVs be exported specifically for the zone of vascular invasion where bone forming cells are transported in by the expanding vasculature and turn over the ECM where MVs may be residing? What responses these different cell types might have to the exported microRNA may be worthy of future research especially if any MV uptake by the bone forming cells can be documented.

The confirmation of phenotypic effects in growth plate cells in addition to the selective export of microRNA made the question about a regulatory molecule for the production and packaging of microRNA by chondrocytes more intriguing. We decided to start by examining the response to $1\alpha,25(OH)_2D_3$ treatment of GC chondrocytes since $1\alpha,25(OH)_2D_3$ already has well established roles with regards to GC MV production. The selective export of microRNA that was observed in the initial study was repeated in this round of RNAseq and the suspected involvement of $1\alpha,25(OH)_2D_3$ confirmed. While the bulk of exported microRNA was unchanged, a subset of microRNA was robustly regulated by the hormone. Additionally, almost no impact was observed on the cell population indicating that the production and packaging of the microRNA was being

carried out in coordinated fashion leaving the chondrocyte microRNA population virtually unaffected. This indicates that few if any immediate phenotypic effects from $1\alpha,25(OH)_2D_3$ treatment are likely attributable to an altered microRNA population. Examining RC cells for similar response to $24R,25(OH)_2D_3$ treatment would be an interesting follow up.

$1\alpha,25(OH)_2D_3$ treatment of isolated MVs produced a somewhat surprising though confirming result when the small RNA population remained protected from RNase activity. It was expected that $1\alpha,25(OH)_2D_3$ treatment would cause MVs to become leaky and release their contents making the once protected RNA molecules vulnerable to the RNase in solution. However, the RNA remained protected and no degradation was observed. This provides additional reinforcement to microRNA being a regulatory factor that is exported by chondrocytes for downstream regulatory action. It would be interesting to discover how the microRNA remain protected – if they are in a MV population that remains intact following $1\alpha,25(OH)_2D_3$ exposure or if they have been released into the ECM in some form yet remain shielded from RNase. It could also be useful in understanding the observed increase in stained MVs binding to chondrocytes following $1\alpha,25(OH)_2D_3$ treatment. Does $1\alpha,25(OH)_2D_3$ trigger a response in the cells or MVs that results in greater binding affinity of the MVs in solution and/or are the MVs beginning to break apart and more fragments are able to bind cells as distinct points? Either option, or a combination of the two, may well be aiding in the delivery of microRNA, as regulatory factors, to the GC chondrocytes. Resolving some of these unknowns will be key for developing any potential clinical application of vesicle bound microRNA.

Biotin tagged microRNA mimics were able to be transfected into cells, the microRNA-mRNA complexes pulled down and the mRNA sequenced. The resulting gene lists, after being filtered for differentially expressed up-regulated genes in the individual microRNA when compared to NC, provided over five thousand potentially impacted pathways. These pathways are a great starting point for additional wet lab testing to see if the microRNAs are able to impact the pathways and produce a quantifiable phenotypic response. Following this it would be necessary to begin examining the network effect that transfecting a group of heterogeneous microRNA has on

chondrocytes as this is both how they are packaged within a MV population and would likely make for the most impactful treatment option. However, the ability to determine what microRNA are being exported by the cells and the genes and subsequent pathways that these microRNAs target is all vital information to have when assessing microRNA for any therapeutic roles.

Demonstrating that exported microRNA have phenotypic effects on growth plate cells (both RC and GC) and that their packaging into MVs by GC cells is being regulated by $1\alpha,25(OH)_2D_3$ provides further insight into the role of microRNA in the mammalian growth plate. The regulation that $1\alpha,25(OH)_2D_3$ provides to MV release and subsequent endocytosis by GC cells adds to the roles and complexity of $1\alpha,25(OH)_2D_3$ and MVs in the growth plate. Finally having a more direct approach to determining the targets of individual microRNA within chondrocytes aids in evaluating the potential effects of candidate microRNAs. All together the work presented here provides a solid foundation to the role of MV microRNA within the growth plate, a regulatory factor of MV microRNA, and an *in vitro* approach to evaluating the microRNA's impact.

There are many further avenues of investigation that are opened by this work. There is no existing bioinformatic approach to take investigators from differential microRNA expression to phenotypic effect. Without more in-depth data on a given cell's active transcriptome, beginning to predict the impact of specific microRNAs will remain a challenge. As was demonstrated in this work, this would only be the first step as the compounding downstream effects of microRNA regulation would have to be accurately predicted as well. Targeted RISC pulldown allowed us to partially bypass this issue and build a profile of regulated mRNAs. More extensive information is available on mRNA expression results though even when following searches for related pathways a significant amount of manual searching and curation of the results is required. This is a clear next step for the differentially expressed mRNA from aim 3 of this work. Potentially impacted pathways will require *in-vitro* confirmation before examining multiple select microRNAs for complementarity effects. Of the five microRNAs examined in the RISC pulldown study the two microRNAs (22-3p and 122-5p) from untreated cells in the first small RNAseq study were clustered together while the three microRNAs (1-3p, 33c-5p, and 133a-3p) found to be

differentially exported into MVs following 1α,25$(OH)_2D_3$ treatment were clustered together. This treatment-based clustering of the differentially expressed mRNA could indicate an overall synergistic effect from the microRNA. Are microRNAs that are exported together by GC cells functioning in a cohesive manner? Additional RISC pulldown and transcriptomics studies of select exported microRNAs would potentially add vital data to further address this.

As researchers continue to consider microRNA for clinical treatments more thorough interrogation of their specific impact within cells and tissues is required. The ability to study the mRNA that are being regulated by specific microRNA is a clear first step in this process. Examining the impact of transfecting multiple microRNA simultaneously along with tissue specific delivery vehicles for *in vivo* studies are logical next steps.

Conclusions

This work confirms the hypothesis that the microRNA packaged in growth plate MVs have a regulatory effect on both RC and GC chondrocytes resulting in effects that are both quantifiable and relevant to the growth plate. Production of microRNA by GC chondrocytes and the packaging of these microRNA into MVs is being regulated by $1\alpha,25(OH)_2D_3$. In addition to the core aspects of the hypothesis we confirmed that MVs are able to protect RNA from degradation by RNase when in solution and that the MV RNA remains protected following $1\alpha,25(OH)_2D_3$ treatment. This provides added confidence that the microRNA exported in MVs are being released into the ECM for downstream regulation of chondrocytes or potentially bone forming cells. Additionally $1\alpha,25(OH)_2D_3$ appears able to increase endocytosis of MVs by growth zone cells when incubated together.

Given that there is a low number of known cartilage relevant pathways or mRNA associated with the microRNAs of interest we were able to successfully adapt a RISC pulldown approach to directly examine the binding between a specific microRNA and its mRNA targets. This approach holds great promise for the continued screening of microRNA providing cell type specific information on the mRNA that are being targeted.

References

1. Slavkin, H.C.; Bringas, P.; Bavetta, L.A. Ribonucleic Acid within the Extracellular Matrix during Embryonic Tooth Formation. *Journal of Cellular Physiology* **1969**, *73*, 179–190, doi:10.1002/jcp.1040730304.
2. Lin, Z.; Rodriguez, N.E.; Zhao, J.; Ramey, A.N.; Hyzy, S.L.; Boyan, B.D.; Schwartz, Z. Selective Enrichment of MicroRNAs in Extracellular Matrix Vesicles Produced by Growth Plate Chondrocytes. *Bone* **2016**, *88*, 47–55, doi:10.1016/j.bone.2016.03.018.
3. Boyan, B.D.; Doroudi, M.; Scott, K.; Schwartz, Z. Cartilage. In *Vitamin D*; Elsevier, 2018; Vol. 1, pp. 405–417 ISBN 9780128099650.
4. Doroudi, M.; Olivares-Navarrete, R.; Boyan, B.D.; Schwartz, Z. A Review of 1α,25(OH)2D3 Dependent Pdia3 Receptor Complex Components in Wnt5a Non-Canonical Pathway Signaling. *J Steroid Biochem Mol Biol* **2015**, *152*, 84–88, doi:10.1016/j.jsbmb.2015.04.002.
5. Boyan, B.D.; Dean, D.D.; Sylvia, V.L.; Schwartz, Z. Nongenomic Regulation of Extracellular Matrix Events by Vitamin D Metabolites. *J Cell Biochem* **1994**, *56*, 331–339, doi:10.1002/jcb.240560309.
6. Schwartz, Z.; Brooks, B.; Swain, L.; del Toro, F.; Norman, A.; Boyan, B. Production of 1,25-Dihydroxyvitamin D3 and 24,25-Dihydroxyvitamin D3 by Growth Zone and Resting Zone Chondrocytes Is Dependent on Cell Maturation and Is Regulated by Hormones and Growth Factors. *Endocrinology* **1992**, *130*, 2495–2504, doi:10.1210/endo.130.5.1572278.
7. Boyan, B.D.; Wong, K.L.; Fang, M.; Schwartz, Z. 1alpha,25(OH)2D3 Is an Autocrine Regulator of Extracellular Matrix Turnover and Growth Factor Release via ERp60 Activated Matrix Vesicle Metalloproteinases. *The Journal of Steroid Biochemistry and Molecular Biology* **2007**, *103*, 467–472, doi:10.1016/j.jsbmb.2006.11.003.
8. Boyan, B.D.; Schwartz, Z.; Park-Snyder, S.; Dean, D.D.; Yang, F.; Twardzik, D.; Bonewald, L.F. Latent Transforming Growth Factor-Beta Is Produced by Chondrocytes and Activated

by Extracellular Matrix Vesicles upon Exposure to 1,25-(OH)2D3. *The Journal of Biological Chemistry* **1994**, *269*, 28374–28381.

9. Asmussen, N.C.; Cohen, D.J.; Lin, Z.; McClure, M.J.; Boyan, B.D.; Schwartz, Z. Specific MicroRNAs Found in Extracellular Matrix Vesicles Regulate Proliferation and Differentiation in Growth Plate Chondrocytes. *Calcified Tissue International* **2021**, *109*, 455–468, doi:10.1007/s00223-021-00855-y.
10. Purcell, P.; Trainor, P.A. The Mighty Chondrocyte: No Bones about It. *Journal of Dental Research* **2015**, *94*, 1625–1627, doi:10.1177/0022034515605457.
11. Kronenberg, H.M. PTHrP and Skeletal Development. *Ann N Y Acad Sci* **2006**, *1068*, 1–13, doi:10.1196/annals.1346.002.
12. Emons, J.; Chagin, A.S.; Sävendahl, L.; Karperien, M.; Wit, J.M. Mechanisms of Growth Plate Maturation and Epiphyseal Fusion. *Hormone Research in Paediatrics* **2011**, *75*, 383–391, doi:10.1159/000327788.
13. de Frutos, C.A.; Vega, S.; Manzanares, M.; Flores, J.M.; Huertas, H.; Martínez-Frías, M.L.; Nieto, M.A. Snail1 Is a Transcriptional Effector of FGFR3 Signaling during Chondrogenesis and Achondroplasias. *Developmental Cell* **2007**, *13*, 872–883, doi:10.1016/j.devcel.2007.09.016.
14. Inada, M.; Yasui, T.; Nomura, S.; Miyake, S.; Deguchi, K.; Himeno, M.; Sato, M.; Yamagiwa, H.; Kimura, T.; Yasui, N.; et al. Maturational Disturbance of Chondrocytes in Cbfa1-Deficient Mice. *Developmental Dynamics* **1999**, *214*, 279–290, doi:10.1002/(SICI)1097-0177(199904)214:4<279::AID-AJA1>3.0.CO;2-W.
15. Kember, N.F. Cell Kinetics and the Control of Growth in Long Bones. *Cell Tissue Kinet* **1978**, *11*, 477–485.
16. Zelzer, E.; Glotzer, D.J.; Hartmann, C.; Thomas, D.; Fukai, N.; Soker, S.; Olsen, B.R. Tissue Specific Regulation of VEGF Expression during Bone Development Requires Cbfa1/Runx2. *Mech Dev* **2001**, *106*, 97–106, doi:10.1016/S0925-4773(01)00428-2.

17. Zhang, X.; Siclari, V.A.; Lan, S.; Zhu, J.; Koyama, E.; Dupuis, H.L.; Enomoto-Iwamoto, M.; Beier, F.; Qin, L. The Critical Role of the Epidermal Growth Factor Receptor in Endochondral Ossification. *J Bone Miner Res* **2011**, *26*, 2622–2633, doi:10.1002/jbmr.502.

18. Li, J.; Dong, S. The Signaling Pathways Involved in Chondrocyte Differentiation and Hypertrophic Differentiation. *Stem Cells Int* **2016**, *2016*, 2470351, doi:10.1155/2016/2470351.

19. Anderson, H.C. Matrix Vesicles and Calcification. *Current Rheumatology Reports Current* **2003**, *5*, 222–226.

20. Boyan, B.D.; Sylvia, V.L.; Dean, D.D.; Pedrozo, H.; del Toro, F.; Nemere, I.; Posner, G.H.; Schwartz, Z. 1,25-(OH)2D3 Modulates Growth Plate Chondrocytes via Membrane Receptor-Mediated Protein Kinase C by a Mechanism That Involves Changes in Phospholipid Metabolism and the Action of Arachidonic Acid and PGE2. *Steroids* **1999**, *64*, 129–136, doi:10.1016/S0039-128X(98)00099-3.

21. Boyan, B.D.; Sylvia, V.L.; Dean, D.D.; del Toro, F.; Schwartz, Z. Differential Regulation of Growth Plate Chondrocytes by 1,25-(OH)2D3 and 24R,25-(OH)2D3 Involves Cell-Maturation-Specific Membrane-Receptor-Activated Phospholipid Metabolism. *Critical Reviews in Oral Biology and Media* **2002**, *13*, 143–154.

22. Dean, D.D.; Boyan, B.D.; Schwart, Z.; Muniz, O.E.; Carreno, M.R.; Maeda, S.; Howell, D.S. Effect of 1alpha,25-Dihydroxyvitamin D3 and 24R,25-Dihydroxyvitamin D3 on Metalloproteinase Activity and Cell Maturation in Growth Plate Cartilage in Vivo. *Endocrine* **2001**, *14*, 311–323, doi:10.1385/endo:14:3:311.

23. White, A.; Wallis, G. Endochondral Ossification: A Delicate Balance between Growth and Mineralisation. *Current Biology* **2001**, *11*, 589–591, doi:10.1016/S0960-9822(01)00359-1.

24. Ağırdil, Y. The Growth Plate: A Physiologic Overview. *EFORT Open Rev* **2020**, *5*, 498–507, doi:10.1302/2058-5241.5.190088.

25. Mackie, E.J.; Ahmed, Y.A.; Tatarczuch, L.; Chen, K.S.; Mirams, M. Endochondral Ossification: How Cartilage Is Converted into Bone in the Developing Skeleton. *International Journal of Biochemistry and Cell Biology* **2008**, *40*, 46–62, doi:10.1016/j.biocel.2007.06.009.

26. Kozhemyakina, E.; Lassar, A.B.; Zelzer, E. A Pathway to Bone: Signaling Molecules and Transcription Factors Involved in Chondrocyte Development and Maturation. *Development* **2015**, *142*, 817–831, doi:10.1242/dev.105536.

27. Golub, E.E. Biomineralization and Matrix Vesicles in Biology and Pathology. *Semin Immunopathol* **2011**, *33*, 409–417, doi:10.1007/s00281-010-0230-z.

28. Orimo, H. The Mechanism of Mineralization and the Role of Alkaline Phosphatase in Health and Disease. *Journal of Nippon Medical School* **2010**, *77*, 4–12, doi:10.1272/jnms.77.4.

29. Anderson, H.C. Electron Microscopic Studies of Induced Cartilage Development and Calcification. *Journal of Cell Biology* **1967**, *35*, 81–101, doi:10.1083/jcb.35.1.81.

30. Anderson, H.C.; Garimella, R.; Tague, S.E. The Role of Matrix Vesicles in Growth Plate Development and Biomineralization. *Frontiers in Bioscience* **2005**, *10*, 822–837, doi:10.2741/1576.

31. Becker, A.; Thakur, B.K.; Weiss, J.M.; Kim, H.S.; Peinado, H.; Lyden, D. Extracellular Vesicles in Cancer: Cell-to-Cell Mediators of Metastasis. *Cancer Cell* **2016**, *30*, 836–848, doi:10.1016/j.ccell.2016.10.009.

32. Bommanavar, S.; Hosmani, J.; Togoo, R.A.; Baeshen, H.A.; Raj, A.T.; Patil, S.; Bhandi, S.; Birkhed, D. Role of Matrix Vesicles and Crystal Ghosts in Bio-Mineralization. *Journal of Bone and Mineral Metabolism* **2020**, doi:10.1007/s00774-020-01125-x.

33. Cecil, R.N.A.; Clarke Anderson, H. Freeze-Fracture Studies of Matrix Vesicle Calcification in Epiphyseal Growth Plate. *Metabolic Bone Disease and Related Research* **1978**, *1*, 89–95, doi:10.1016/0221-8747(78)90043-7.

34. Golub, E.E. Role of Matrix Vesicles in Biomineralization. *Biochim Biophys Acta* **2009**, *1790*, 1592–1598, doi:https://doi.org/10.1016/j.bbagen.2009.09.006.

35. Dean, D.D.; Schwartz, Z.; Muniz, O.E.; Gomez, R.; Swain, L.D.; Howell, D.S.; Boyan, B.D. Matrix Vesicles Are Enriched in Metalloproteinases That Degrade Proteoglycans. *Calcified Tissue International* **1992**, *50*, 342–349, doi:10.1007/BF00301632.

36. Dean, D.D.; Schwartz, Z. v; Muniz, O.E.; Gomez, R.; Swain, L.D.; Howell, D.S.; Boyan, B.D. Matrix Vesicles Contain Metalloproteinases That Degrade Proteoglycans. *Bone Miner* **1992**, *17*, 172–176, doi:10.1007/BF00301632.

37. Nishimura, R.; Wakabayashi, M.; Hata, K.; Matsubara, T.; Honma, S.; Wakisaka, S.; Kiyonari, H.; Shioi, G.; Yamaguchi, A.; Tsumaki, N.; et al. Osterix Regulates Calcification and Degradation of Chondrogenic Matrices through Matrix Metalloproteinase 13 (MMP13) Expression in Association with Transcription Factor Runx2 during Endochondral Ossification. *Journal of Biological Chemistry* **2012**, *287*, 33179–33190, doi:10.1074/jbc.M111.337063.

38. Golub, E.E.; Boesze-Battaglia, K. The Role of Alkaline Phosphatase in Mineralization. *Current Opinion in Orthopaedics* **2007**, *18*, 444–448, doi:10.1097/BCO.0b013e3282630851.

39. Majeska, R.J.; Holwerda, D.L.; Wuthier, R.E. Localization of Phosphatidylserine in Isolated Chick Epiphyseal Cartilage Matrix Vesicles with Trinitrobenzenesulfonate. *Calcified Tissue International* **1979**, *27*, 41–46, doi:10.1007/BF02441159.

40. Nahar, N.N.; Missana, L.R.; Garimella, R.; Tague, S.E.; Anderson, H.C. Matrix Vesicles Are Carriers of Bone Morphogenetic Proteins (BMPs), Vascular Endothelial Growth Factor (VEGF), and Noncollagenous Matrix Proteins. *Journal of Bone and Mineral Metabolism* **2008**, *26*, 514–519, doi:10.1007/s00774-008-0859-z.

41. Balcerzak, M.; Malinowska, A.; Thouverey, C.; Sekrecka, A.; Dadlez, M.; Buchet, R.; Pikula, S. Proteome Analysis of Matrix Vesicles Isolated from Femurs of Chicken Embryo. *Proteomics* **2008**, *8*, 192–205, doi:10.1002/pmic.200700612.

42. Yadav, M.C.; Bottini, M.; Cory, E.; Bhattacharya, K.; Kuss, P.; Narisawa, S.; Sah, R.L.; Beck, L.; Fadeel, B.; Farquharson, C.; et al. Skeletal Mineralization Deficits and Impaired Biogenesis and Function of Chondrocyte-Derived Matrix Vesicles in Phospho1(-/-) and Phospho1/Pi T1 Double-Knockout Mice. *J Bone Miner Res* **2016**, *31*, 1275–1286, doi:10.1002/jbmr.2790.

43. Wuthier, R.E.; Lipscomb, G.F. Matrix Vesicles: Structure, Composition, Formation and Function in Calcification. *Front Biosci (Landmark Ed)* **2011**, *16*, 2812–2902, doi:10.1095/biolreprod.107.067082.

44. D'Angelo, M.; Billings, P.C.; Pacifici, M.; Leboy, P.S.; Kirsch, T. Authentic Matrix Vesicles Contain Active Metalloproteases (MMP): A Role for Matrix Vesicle-Associated MMP-13 in Activation of Transforming Growth Factor-B. *Journal of Biological Chemistry* **2001**, *276*, 11347–11353, doi:10.1074/jbc.M009725200.

45. Miao, D.; Scutt, A. Histochemical Localization of Alkaline Phosphatase Activity in Decalcified Bone and Cartilage. *J Histochem Cytochem* **2002**, *50*, 333–340, doi:10.1177/002215540205000305.

46. Schwartz, Z.; Knight, G.; Swain, L.D.; Boyan, B.D. Localization of Vitamin D3-Responsive Alkaline Phosphatase in Cultured Chondrocytes. *J Biol Chem* **1988**, *263*, 6023–6026.

47. Anderson, H.C. The Role of Matrix Vesicles in Physiological and Pathological Calcification. *Current Opinion in Orthopaedics* **2007**, *18*, 428–433, doi:10.1097/BCO.0b013e3282e9ab49.

48. Amir, D.; Schwartz, Z.; Sela, J.; Weinberg, H. The Relationship Between Extracellular Matrix Vesicles and the Calcifying Front on the 21st Day after Injury to Rat Tibial Bone. *Clinical Orthopaedics and Related Research* **1988**, 142–148.

49. Boyan, B.D.; Wang, L.; Wong, K.L.; Jo, H.; Schwartz, Z. Plasma Membrane Requirements for 1alpha,25(OH)2D3 Dependent PKC Signaling in Chondrocytes and Osteoblasts. *Steroids* **2006**, *71*, 286–290, doi:10.1016/j.steroids.2005.09.018.

50. Boyan, B.D.; Schwartz, Z.; Swain, L.D.; Khare, A. Role of Lipids in Calcification of Cartilage. *The Anatomical Record* **1989**, *224*, 211–219, doi:10.1002/ar.1092240210.

51. Millán, J.L. The Role of Phosphatases in the Initiation of Skeletal Mineralization. *Calcif Tissue Int* **2013**, *93*, 299–306, doi:10.1007/s00223-012-9672-8.

52. Narisawa, S.; Fröhlander, N.; Millán, J.L. Inactivation of Two Mouse Alkaline Phosphatase Genes and Establishment of a Model of Infantile Hypophosphatasia. *Developmental Dynamics* **1997**, *208*, 432–446, doi:10.1002/(SICI)1097-0177(199703)208:3<432::AID-AJA13>3.0.CO;2-1.

53. Anderson, H.C.; Sipe, J.B.; Hessle, L.; Dhanyamraju, R.; Atti, E.; Camacho, N.P.; Millán, J.L.; Dhamyamraju, R. Impaired Calcification around Matrix Vesicles of Growth Plate and Bone in Alkaline Phosphatase-Deficient Mice. *Am J Pathol* **2004**, *164*, 841–847, doi:10.1016/S0002-9440(10)63172-0.

54. Russell, R.G.G.; Bisaz, S.; Donath, A.; Morgan, D.B.; Fleisch, H. Inorganic Pyrophosphate in Plasma in Normal Persons and in Patients with Hypophosphatasia, Osteogenesis Imperfecta, and Other Disorders of Bone. *The Journal of Clinical Investigation* **1971**, *50*, 961–969, doi:10.1172/JCI106589.

55. Lin, Z.; McClure, M.J.; Zhao, J.; Ramey, A.N.; Asmussen, N.; Hyzy, S.L.; Schwartz, Z.; Boyan, B.D. MicroRNA Contents in Matrix Vesicles Produced by Growth Plate Chondrocytes Are Cell Maturation Dependent. *Scientific Reports* **2018**, *8*, 3609, doi:10.1038/s41598-018-21517-4.

56. Sylvia, V.L.; Schwartz, Z.; Holmes, S.C.; Dean, D.D.; Boyan, B.D. 24,25-(OH)2D3 Regulation of Matrix Vesicle Protein Kinase C Occurs Both During Biosynthesis and in the Extracellular Matrix. *Calcified Tissue International* **1997**, *61*, 313–321.

57. Boyan, B.D.; Schwartz, Z.; Swain, L.D. Matrix Vesicles as a Marker of Endochondral Ossification. *Connect Tissue Res* **1990**, *24*, 67–75.

58. Boyan, B.D.; Chen, J.; Schwartz, Z. Mechanism of Pdia3-Dependent 1α,25-Dihydroxy Vitamin D3 Signaling in Musculoskeletal Cells. *Steroids* **2012**, *77*, 892–896, doi:10.1016/j.steroids.2012.04.018.

59. Schwartz, Z.; Sylvia, V.L.; Larsson, D.; Nemere, I.; Casasola, D.; Dean, D.D.; Boyan, B.D. 1alpha,25(OH)2D3 Regulates Chondrocyte Matrix Vesicle Protein Kinase C (PKC) Directly via G-Protein-Dependent Mechanisms and Indirectly via Incorporation of PKC during Matrix Vesicle Biogenesis. *Journal of Biological Chemistry* **2002**, *277*, 11828–11837, doi:10.1074/jbc.M110398200.

60. Sylvia, V.L.; Schwartz, Z.; Ellis, E.B.; Helm, S.H.; Gomez, R.; Dean, D.D.; Boyan, B.D. Nongenomic Regulation of Protein Kinase C Isoforms by the Vitamin D Metabolites 1 Alpha,25-(OH)2D3 and 24R,25-(OH)2D3. *J Cell Physiol* **1996**, *167*, 380–393, doi:10.1002/(SICI)1097-4652(199606)167:3<380::AID-JCP2>3.0.CO;2-L.

61. Kawakami, Y.; Rodriguez-León, J.; Belmonte, J.C.I. The Role of TGFBs and Sox9 during Limb Chondrogenesis. *Current Opinion in Cell Biology* **2006**, *18*, 723–729, doi:10.1016/j.ceb.2006.10.007.

62. Wang, W.; Rigueur, D.; Lyons, K.M. TGFB Signaling in Cartilage Development and Maintenance. *Birth Defects Research Part C* **2014**, *102*, 37–51, doi:10.1002/bdrc.21058.

63. Boyan, B.D.; Doroudi, M.; Schwartz, Z. Chapter 28 - Cartilage. In *Vitamin D (Third Edition)*; Feldman, D., Pike, J.W., Adams, J.S., Eds.; Academic Press: San Diego, 2011; pp. 507–519 ISBN 978-0-12-381978-9.

64. Maeda, S.; Dean, D.D.; Gay, I.; Schwartz, Z.; Boyan, B.D. Activation of Latent Transforming Growth Factor Beta1 by Stromelysin 1 in Extracts of Growth Plate Chondrocyte-Derived Matrix Vesicles. *J Bone Miner Res.* **2001**, *16*, 1281–1290, doi:10.1359/jbmr.2001.16.7.1281.

65. Gay, I.; Schwartz, Z.; Sylvia, V.L.; Boyan, B.D. Lysophospholipid Regulates Release and Activation of Latent TGF-Beta1 from Chondrocyte Extracellular Matrix. *Biochim Biophys Acta* **2004**, *1684*, 18–28, doi:10.1016/j.bbalip.2004.04.006.

66. Makarova, K.S.; Grishin, N. v; Shabalina, S. a; Wolf, Y.I.; Koonin, E. v A Putative RNA-Interference-Based Immune System in Prokaryotes: Computational Analysis of the Predicted Enzymatic Machinery, Functional Analogies with Eukaryotic RNAi, and Hypothetical Mechanisms of Action. *Biol Direct* **2006**, *1*, 7, doi:10.1186/1745-6150-1-7.

67. Bartel, D.P. MicroRNAs: Genomics, Biogenesis, Mechanism, and Function. *Cell* **2004**, *116*, 281–297, doi:10.1016/S0092-8674(04)00045-5.

68. Feig, J.L.; Giles, K.M.; Osman, I.; Franks, A.G. How MicroRNAs Modify Protein Production. *Journal of Investigative Dermatology* **2015**, *135*, e32, doi:10.1038/jid.2015.99.

69. Boon, R.A.; Vickers, K.C. Intercellular Transport of MicroRNAs. *Arteriosclerosis, Thrombosis, and Vascular Biology* **2013**, *33*, 186–192, doi:10.1161/ATVBAHA.112.300139.

70. Mirzamohammadi, F.; Papaioannou, G.; Kobayashi, T. MicroRNAs in Cartilage Development, Homeostasis, and Disease. *Curr Osteoporos Rep* **2014**, *12*, 410–419, doi:10.1007/s11914-014-0229-9.

71. Maeda, Y.; Farina, N.H.; Matzelle, M.M.; Fanning, P.J.; Lian, J.B.; Gravallese, E.M. Synovium-Derived MicroRNAs Regulate Bone Pathways in Rheumatoid Arthritis. *Journal of Bone and Mineral Research* **2016**, 1–37, doi:10.1002/jbmr.3005.

72. Lewis, B.P.; Burge, C.B.; Bartel, D.P. Conserved Seed Pairing, Often Flanked by Adenosines, Indicates That Thousands of Human Genes Are MicroRNA Targets. *Cell* **2005**, *120*, 15–20, doi:10.1016/j.cell.2004.12.035.

73. Barh, D.; Jain, N.; Tiwari, S.; Field, J.K.; Padin-Iruegas, E.; Ruibal, A.; López, R.; Herranz, M.; Bhattacharya, A.; Juneja, L.; et al. A Novel in Silico Reverse-Transcriptomics-Based Identification and Blood-Based Validation of a Panel of Sub-Type Specific Biomarkers in Lung Cancer. *BMC Genomics* **2013**, *14 Suppl 6*, S5, doi:10.1186/1471-2164-14-S6-S5.

74. Liu, W.; Liu, S.-Y.; He, Y.-B.; Huang, R.-L.; Deng, S.-Y.; Ni, G.-X.; Yu, B. MiR-451 Suppresses Proliferation, Migration and Promotes Apoptosis of the Human Osteosarcoma

by Targeting Macrophage Migration Inhibitory Factor. *Biomedicine & pharmacotherapy* **2017**, *87*, 621–627, doi:10.1016/j.biopha.2016.12.121.

75. Zhuang, G.; Meng, C.; Guo, X.; Cheruku, P.S.; Shi, L.; Xu, H.; Li, H.; Wang, G.; Evans, A.R.; Safe, S.; et al. A Novel Regulator of Macrophage Activation: MiR-223 in Obesity-Associated Adipose Tissue Inflammation. *Circulation* **2012**, *125*, 2892–2903, doi:10.1161/CIRCULATIONAHA.111.087817.

76. Tsai, W.C.; Hsu, S. Da; Hsu, C.S.; Lai, T.C.; Chen, S.J.; Shen, R.; Huang, Y.; Chen, H.C.; Lee, C.H.; Tsai, T.F.; et al. MicroRNA-122 Plays a Critical Role in Liver Homeostasis and Hepatocarcinogenesis. *Journal of Clinical Investigation* **2012**, *122*, 2884–2897, doi:10.1172/JCI63455.

77. Mateescu, B.; Kowal, E.J.K.; van Balkom, B.W.M.; Bartel, S.; Bhattacharyya, S.N.; Buzás, E.I.; Buck, A.H.; de Candia, P.; Chow, F.W.N.; Das, S.; et al. Obstacles and Opportunities in the Functional Analysis of Extracellular Vesicle RNA – an ISEV Position Paper. *Journal of Extracellular Vesicles* **2017**, *6*, 1286095, doi:10.1080/20013078.2017.1286095.

78. Damek-Poprawa, M.; Golub, E.; Otis, L.; Harrison, G.; Phillips, C.; Boesze-Battaglia, K. Chondrocytes Utilize a Cholesterol Dependent Lipid Translocator To Externalize Phospatidylserine. *Biochemistry* **2006**, *45*, 3325–3339, doi:10.1038/nbt.3121.ChIP-nexus.

79. Liu, W.; Wang, X. Prediction of Functional MicroRNA Targets by Integrative Modeling of MicroRNA Binding and Target Expression Data. *Genome Biol* **2019**, *20*, 18, doi:10.1186/s13059-019-1629-z.

80. Kozomara, A.; Griffiths-Jones, S. MiRBase: Integrating MicroRNA Annotation and Deep-Sequencing Data. *Nucleic Acids Research* **2011**, *39*, 152–157, doi:10.1093/nar/gkq1027.

81. Lu, Y.; Baras, A.S.; Halushka, M.K. MiRge 2.0 for Comprehensive Analysis of MicroRNA Sequencing Data. *BMC Bioinformatics* **2018**, *19*, 275, doi:10.1186/s12859-018-2287-y.

82. Wong, N.; Wang, X. MiRDB: An Online Resource for MicroRNA Target Prediction and Functional Annotations. *Nucleic Acids Res* **2015**, *43*, D146-52, doi:10.1093/nar/gku1104.

83. Kern, F.; Fehlmann, T.; Solomon, J.; Schwed, L.; Grammes, N.; Backes, C.; van Keuren-Jensen, K.; Craig, D.W.; Meese, E.; Keller, A. MiEAA 2.0: Integrating Multi-Species MicroRNA Enrichment Analysis and Workflow Management Systems. *Nucleic Acids Res* **2020**, *48*, W521–W528, doi:10.1093/nar/gkaa309.

84. Rehmsmeier, M.; Steffen, P.; Hochsmann, M.; Giegerich, R. Fast and Effective Prediction of MicroRNA/Target Duplexes. *RNA* **2004**, *10*, 1507–1517, doi:10.1261/rna.5248604.

85. Grillo, G.; Turi, A.; Licciulli, F.; Mignone, F.; Liuni, S.; Banfi, S.; Gennarino, V.A.; Horner, D.S.; Pavesi, G.; Picardi, E.; et al. UTRdb and UTRsite (RELEASE 2010): A Collection of Sequences and Regulatory Motifs of the Untranslated Regions of Eukaryotic MRNAs. *Nucleic Acids Res* **2010**, *38*, D75-80, doi:10.1093/nar/gkp902.

86. Dandare, A.; Rabia, G.; Khan, M.J. In Silico Analysis of Non-Coding RNAs and Putative Target Genes Implicated in Metabolic Syndrome. *Comput Biol Med* **2021**, *130*, 104229, doi:10.1016/j.compbiomed.2021.104229.

87. Alves, L.; Niemeier, S.; Hauenschild, A.; Rehmsmeier, M.; Merkle, T. Comprehensive Prediction of Novel MicroRNA Targets in Arabidopsis Thaliana. *Nucleic Acids Res* **2009**, *37*, 4010–4021, doi:10.1093/nar/gkp272.

88. Conesa, A.; Madrigal, P.; Tarazona, S.; Gomez-Cabrero, D.; Cervera, A.; McPherson, A.; Szczesniak, M.W.; Gaffney, D.J.; Elo, L.L.; Zhang, X.; et al. A Survey of Best Practices for RNA-Seq Data Analysis. *Genome Biol* **2016**, *17*, 13, doi:10.1186/s13059-016-0881-8.

89. Kronenberg, H.M. Developmental Regulation of the Growth Plate. *Nature* **2003**, *423*, 332–336, doi:10.1038/nature01657.

90. Anderson, H.C. Vesicles Associated with Calcification in the Matrix of Epiphyseal Cartilage. *Journal of Cell Biology* **1969**, *41*, 59–72, doi:10.1083/jcb.41.1.59.

91. Boyan, B.D.; Schwartz, Z.; Swain, L.D.; Carnes, D.L.; Zislis, T. Differential Expression of Phenotype by Resting Zone and Growth Region Costochondral Chondrocytes in Vitro. *Bone* **1988**, *9*, 185–194, doi:10.1016/8756-3282(88)90008-7.

92. Dean, D.D.; Boyan, B.D.; Muniz, O.E.; Howell, D.S.; Schwartz, Z. Vitamin D Metabolites Regulate Matrix Vesicle Metalloproteinase Content in a Cell Maturation-Dependent Manner. *Calcified Tissue International* **1996**, *59*, 109–116.

93. Wuthier, R.E.; Chin, J.E.; Hale, J.E.; Register, T.C.; Hale, L. v; Ishikawa, Y. Isolation and Characterization of Calcium-Accumulating Matrix Vesicles from Chondrocytes of Chicken Epiphyseal Growth Plate Cartilage in Primary Culture. *Journal of Biological Chemistry* **1985**, *260*, 15972–15979.

94. Glaser, J.H.; Conrad, H.E. Formation of Matrix Vesicles by Cultured Chick Embryo Chondrocytes. *J Biol Chem* **1981**, *256*, 12607–12611, doi:10.1016/s0021-9258(18)43318-2.

95. Pawlowski, A.; Makower, A.M.; Madsen, K.; Wroblewski, J.; Friberg, U. Cell Fractions from Rat Rib Growth Cartilage. Biochemical Characterization of Matrix Molecules. *Exp Cell Res* **1986**, *164*, 211–222, doi:10.1016/0014-4827(86)90468-4.

96. Nemere, I.; Schwartz, Z.; Pedrozo, H.; Sylvia, V.L.; Dean, D.D.; Boyan, B.D. Identification of a Membrane Receptor for 1,25-Dihydroxyvitamin D3 Which Mediates Rapid Activation of Protein Kinase C. *Journal of bone and mineral research* **1998**, *13*, 1353–1359, doi:10.1359/jbmr.1998.13.9.1353.

97. Pedrozo, H. a; Schwartz, Z.; Rimes, S.; Sylvia, V.L.; Nemere, I.; Posner, G.H.; Dean, D.D.; Boyan, B.D. Physiological Importance of the 1,25(OH)2D3 Membrane Receptor and Evidence for a Membrane Receptor Specific for 24,25(OH)2D3. *Journal of bone and mineral research* **1999**, *14*, 856–867, doi:10.1359/jbmr.1999.14.6.856.

98. Shapiro, I.M.; Landis, W.J.; Risbud, M. v. Matrix Vesicles: Are They Anchored Exosomes? *Bone* **2015**, *79*, 29–36, doi:10.1016/j.bone.2015.05.013.

99. Schwartz, Z.; Langston, G.G.; Swain, L.D.; Boyan, B.D. Inhibition of 1,25-(OH)2D3- and 24,25-(OH)2D3-Dependent Stimulation of Alkaline Phosphatase Activity by A23187 Suggests a Role for Calcium in the Mechanism of Vitamin D Regulation of Chondrocyte

Cultures. *Journal of Bone and Mineral Research* **1991**, *6*, 709–718, doi:https://doi.org/10.1002/jbmr.5650060708.

100. Langston, G.G.; Swain, L.D.; Schwartz, Z.; del Toro, F.; Gomez, R.; Boyan, B.D. Effect of 1,25(OH)2D3 and 24,25(OH)2D3 on Calcium Ion Fluxes in Costochondral Chondrocyte Cultures. *Calcif Tissue Int* **1990**, *47*, 230–236, doi:10.1007/BF02555924.

101. Schwartz, Z.; Schlader, D.L.; Swain, L.D.; Boyan, B.D. Direct Effects of 1,25-Dihydroxyvitamin D3 and 24,25-Dihydroxyvitamin D3 on Growth Zone and Resting Zone Chondrocyte Membrane Alkaline Phosphatase and Phospholipase-A2 Specific Activities. *Endocrinology* **1988**, *123*, 2878–2884, doi:10.1210/endo-123-6-2878.

102. Schwartz, Z.; Swain, L.D.; Kelly, D.W.; Brooks, B.; Boyan, B.D. Regulation of Prostaglandin E2 Production by Vitamin D Metabolites in Growth Zone and Resting Zone Chondrocyte Cultures Is Dependent on Cell Maturation. *Bone* **1992**, *13*, 395–401, doi:https://doi.org/10.1016/8756-3282(92)90456-7.

103. Schwartz, Z.; Nasatzky, E.; Ornoy, A.; Brooks, B.P.; Soskolne, W.A.; Boyan, B.D. Gender-Specific, Maturation-Dependent Effects of Testosterone on Chondrocytes in Culture. *Endocrinology* **1994**, *134*, 1640–1647, doi:10.1210/endo.134.4.8137726.

104. Schwartz, Z.; Bonewald, L.F.; Caulfield, K.; Brooks, B.; Boyan, B.D. Direct Effects of Transforming Growth Factor-Beta on Chondrocytes Are Modulated by Vitamin D Metabolites in a Cell Maturation-Specific Manner. *Endocrinology* **1993**, *132*, 1544–1552, doi:10.1210/endo.132.4.8462452.

105. Schwartz, Z.; Sylvia, V.L.; Liu, Y.; Dean, D.D.; Boyan, B.D. Treatment of Resting Zone Chondrocytes with Bone Morphogenetic Protein-2 Induces Maturation into a Phenotype Characteristic of Growth Zone Chondrocytes by Downregulating Responsiveness to 24,25(OH)2D3 and Upregulating Responsiveness to 1,25-(OH)2D3. *Endocrine* **1998**, *9*, 273–280, doi:10.1385/ENDO:9:3:273.

106. Dean, D.D.; Schwartz, Z.; Schmitz, J.; Muniz, O.E.; Lu, Y.; Calderon, F.; Howell, D.S.; Boyan, B.D. Vitamin D Regulation of Metalloproteinase Activity in Matrix Vesicles. *Connect Tissue Res* **1996**, *35*, 331–336, doi:10.3109/03008209609029208.

107. Schwartz, Z.; Sylvia, V.L.; del Toro, F.; Hardin, R.R.; Dean, D.D.; Boyan, B.D. 24R,25-(OH)(2)D(3) Mediates Its Membrane Receptor-Dependent Effects on Protein Kinase C and Alkaline Phosphatase via Phospholipase A(2) and Cyclooxygenase-1 but Not Cyclooxygenase-2 in Growth Plate Chondrocytes. *J Cell Physiol* **2000**, *182*, 390–401, doi:10.1002/(SICI)1097-4652(200003)182:3<390::AID-JCP10>3.0.CO;2-T.

108. Sylvia, V.L.; Schwartz, Z.; Schuman, L.; Morgan, R.T.; Mackey, S.; Gomez, R.; Boyan, B.D. Maturation-Dependent Regulation of Protein Kinase C Activity by Vitamin D3 Metabolites in Chondrocyte Cultures. *J Cell Physiol* **1993**, *157*, 271–278, doi:10.1002/jcp.1041570209.

109. Boskey, A.L.; Boyan, B.D.; Doty, S.B.; Feliciano, A.; Greer, K.; Weiland, D.; Swain, L.D.; Schwartz, Z. Studies of Matrix Vesicle-Induced Mineralization in a Gelatin Gel. *Bone and Mineral* **1992**, *17*, 257–262, doi:10.1016/0169-6009(92)90747-2.

110. Boskey, A.L.; Boyan, B.D.; Schwartz, Z. Matrix Vesicles Promote Mineralization in a Gelatin Gel. *Calcif Tissue Int* **1997**, *60*, 309–315, doi:10.1007/s002239900234.

111. Lian, J.B.; Stein, G.S.; van Wijnen, A.J.; Stein, J.L.; Hassan, M.Q.; Gaur, T.; Zhang, Y. MicroRNA Control of Bone Formation and Homeostasis. *Nat Rev Endocrinol* **2012**, *8*, 212–227, doi:10.1038/nrendo.2011.234.

112. Yang, B.; Guo, H.; Zhang, Y.; Chen, L.; Ying, D.; Dong, S. MicroRNA-145 Regulates Chondrogenic Differentiation of Mesenchymal Stem Cells by Targeting Sox9. *PLoS One* **2011**, *6*, e21679, doi:10.1371/journal.pone.0021679.

113. Papaioannou, G.; Mirzamohammadi, F.; Lisse, T.S.; Nishimori, S.; Wein, M.N.; Kobayashi, T. MicroRNA-140 Provides Robustness to the Regulation of Hypertrophic Chondrocyte Differentiation by the PTHrP-HDAC4 Pathway. *J Bone Miner Res* **2015**, *30*, 1044–1052, doi:10.1002/jbmr.2438.

114. Li, P.; Wei, X.; Guan, Y.; Chen, Q.; Zhao, T.; Sun, C.; Wei, L. MicroRNA-1 Regulates Chondrocyte Phenotype by Repressing Histone Deacetylase 4 during Growth Plate Development. *FASEB journal* **2014**, *28*, 3930–3941, doi:10.1096/fj.13-249318.

115. Creemers, E.E.; Tijsen, A.J.; Pinto, Y.M. Circulating MicroRNAs: Novel Biomarkers and Extracellular Communicators in Cardiovascular Disease? *Circ Res* **2012**, *110*, 483–495, doi:10.1161/CIRCRESAHA.111.247452.

116. Tkach, M.; Théry, C. Communication by Extracellular Vesicles: Where We Are and Where We Need to Go. *Cell* **2016**, *164*, 1226–1232, doi:10.1016/j.cell.2016.01.043.

117. Sharma, U.; Conine, C.C.; Shea, J.M.; Boskovic, A.; Derr, A.G.; Bing, X.Y.; Belleannee, C.; Kucukural, A.; Serra, R.W.; Sun, F.; et al. Biogenesis and Function of TRNA Fragments during Sperm Maturation and Fertilization in Mammals. *Science* **2016**, *351*, 391–396, doi:10.1126/science.aad6780.

118. Aydelotte, M.B.; Greenhill, R.R.; Kuettner, K.E. Differences between Sub-Populations of Cultured Bovine Articular Chondrocytes. II. Proteoglycan Metabolism. *Connective Tissue Research* **1988**, *18*, 223–234, doi:10.3109/03008208809016809.

119. Aydelotte, M.B.; Kuettner, K.E. Differences between Sub-Populations of Cultured Bovine Articular Chondrocytes. I. Morphology and Cartilage Matrix Production. *Connective Tissue Research* **1988**, *18*, 205–222, doi:10.3109/03008208809016808.

120. Radhakrishnan, P.; Lewis, N.T.; Mao, J.J. Zone-Specific Micromechanical Properties of the Extracellular Matrices of Growth Plate Cartilage. *Ann Biomed Eng* **2004**, *32*, 284–291, doi:10.1023/b:abme.0000012748.41851.b4.

121. Boyan, B.D.; Sylvia, V.L.; McKinney, N.; Schwartz, Z. Membrane Actions of Vitamin D Metabolites 1α,25(OH)2D3 and 24R,25(OH)2D3 Are Retained in Growth Plate Cartilage Cells from Vitamin D Receptor Knockout Mice. *Journal of Cellular Biochemistry* **2003**, *90*, 1207–1223, doi:10.1002/jcb.10716.

122. Kakuta, S.; Malamud, D.; Golub, E.E.; Shapiro, I.M. Isolation of Matrix Vesicles by Isoelectric Focusing in Pevikon-Sephadex. *Bone* **1985**, *6*, 187–191, doi:10.1016/8756-3282(85)90052-3.

123. Huleihel, L.; Hussey, G.S.; Naranjo, J.D.; Zhang, L.; Dziki, J.L.; Turner, N.J.; Stolz, D.B.; Badylak, S.F. Matrix-Bound Nanovesicles within ECM Bioscaffolds. *Sci Adv* **2016**, *2*, e1600502, doi:10.1126/sciadv.1600502.

124. Leach, R.J.; Schwartz, Z.; Johnson-Pais, T.L.; Dean, D.D.; Luna, M.; Boyan, B.D. Osteosarcoma Hybrids Can Preferentially Target Alkaline Phosphatase Activity to Matrix Vesicles: Evidence for Independent Membrane Biogenesis. *J Bone Miner Res* **1995**, *10*, 1614–1624, doi:10.1002/jbmr.5650101103.

125. Lai, R.C.; Tan, S.S.; Yeo, R.W.Y.; Choo, A.B.H.; Reiner, A.T.; Su, Y.; Shen, Y.; Fu, Z.; Alexander, L.; Sze, S.K.; et al. MSC Secretes at Least 3 EV Types Each with a Unique Permutation of Membrane Lipid, Protein and RNA. *J Extracell Vesicles* **2016**, *5*, 29828, doi:10.3402/jev.v5.29828.

126. Thakral, S.; Ghoshal, K. MiR-122 Is a Unique Molecule with Great Potential in Diagnosis, Prognosis of Liver Disease, and Therapy Both as MiRNA Mimic and Antimir. *Curr Gene Ther* **2015**, *15*, 142–150, doi:10.2174/1566523214666141224095610.

127. Wang, B.; Wang, H.; Yang, Z. MiR-122 Inhibits Cell Proliferation and Tumorigenesis of Breast Cancer by Targeting IGF1R. *PLoS ONE* **2012**, *7*, 1–9, doi:10.1371/journal.pone.0047053.

128. Li, T.; Xie, J.; Shen, C.; Cheng, D.; Shi, Y.; Wu, Z.; Zhan, Q.; Deng, X.; Chen, H.; Shen, B.; et al. MiR-150-5p Inhibits Hepatoma Cell Migration and Invasion by Targeting MMP14. *PLoS One* **2014**, *9*, e115577, doi:10.1371/journal.pone.0115577.

129. Sakr, M.; Takino, T.; Sabit, H.; Nakada, M.; Li, Z.; Sato, H. MiR-150-5p and MiR-133a Suppress Glioma Cell Proliferation and Migration through Targeting Membrane-Type-1 Matrix Metalloproteinase. *Gene* **2016**, *587*, 155–162, doi:https://doi.org/10.1016/j.gene.2016.04.058.

130. Rilla, K.; Mustonen, A.-M.; Arasu, U.T.; Härkönen, K.; Matilainen, J.; Nieminen, P. Extracellular Vesicles Are Integral and Functional Components of the Extracellular Matrix. *Matrix Biol* **2017**, doi:10.1016/j.matbio.2017.10.003.

131. Kirsch, T.; Wuthier, R.E. Stimulation of Calcification of Growth Plate Cartilage Matrix Vesicles by Binding to Type II and X Collagens. *Journal of Biological Chemistry* **1994**, *269*, 11462–11469.

132. Krane, S.M.; Inada, M. Matrix Metalloproteinases and Bone. *Bone* **2008**, *43*, 7–18, doi:10.1016/j.bone.2008.03.020.

133. Boyan, B.D.; Schwartz, Z.; Carnes, D.L.; Ramirez, V. The Effects of Vitamin D Metabolites on the Plasma and Matrix Vesicle Membranes of Growth and Resting Cartilage Cells in Vitro. *Endocrinology* **1988**, *122*, 2851–2860, doi:10.1210/endo-122-6-2851.

134. Schwartz, Z.; Swain, L.D.; Ramirez, V.; Boyan, B.D. Regulation of Arachidonic Acid Turnover by 1,25-(OH)2D3 and 24,25-(OH)2D3 in Growth Zone and Resting Zone Chondrocyte Cultures. *Biochim Biophys Acta* **1990**, *1027*, 278–286, doi:10.1016/0005-2736(90)90319-j.

135. Kobayashi, T.; Chung, U.; Schipani, E.; Starbuck, M.; Karsenty, G.; Katagiri, T.; Goad, D.L.; Lanske, B.; Kronenberg, H.M. PTHrP and Indian Hedgehog Control Differentiation of Growth Plate Chondrocytes at Multiple Steps. *Development* **2002**, *129*, 2977–2986.

136. Mak, K.K.; Kronenberg, H.M.; Chuang, P.-T.; Mackem, S.; Yang, Y. Indian Hedgehog Signals Independently of PTHrP to Promote Chondrocyte Hypertrophy. *Development* **2008**, *135*, 1947–1956, doi:10.1242/dev.018044.

137. van der Eerden, B.C.J.; Karperien, M.; Wit, J.M. Systemic and Local Regulation of the Growth Plate. *Endocrine Reviews* **2003**, *24*, 782–801, doi:10.1210/er.2002-0033.

138. Burdan, F.; Szumiło, J.; Korobowicz, A.; Farooquee, R.; Patel, S.; Patel, A.; Dave, A.; Szumiło, M.; Solecki, M.; Klepacz, R.; et al. Morphology and Physiology of the Epiphyseal Growth Plate. *Folia Histochem Cytobiol* **2009**, *47*, 5–16, doi:10.2478/v10042-009-0007-1.

139. Schwartz, Z.; Sylvia, V.L.; Dean, D.D.; Boyan, B.D. The Synergistic Effects of Vitamin D Metabolites and Transforming Growth Factor-Beta on Costochondral Chondrocytes Are Mediated by Increases in Protein Kinase C Activity Involving Two Separate Pathways. *Endocrinology* **1998**, *139*, 534–545, doi:10.1210/endo.139.2.5753.

140. Ortega, N.; Wang, K.; Ferrara, N.; Werb, Z.; Vu, T.H. Complementary Interplay between Matrix Metalloproteinase-9, Vascular Endothelial Growth Factor and Osteoclast Function Drives Endochondral Bone Formation. *Dis Model Mech* **2010**, *3*, 224–235, doi:10.1242/dmm.004226.

141. Bi, W.; Deng, J.M.; Zhang, Z.; Behringer, R.R.; de Crombrugghe, B. Sox9 Is Required for Cartilage Formation. *Nat Genet* **1999**, *22*, 85–89, doi:10.1038/8792.

142. Ballock, R.T.; O'Keefe, R.J. The Biology of the Growth Plate. *J Bone Joint Surg Am* **2003**, *85-A*, 715–726.

143. Komori, T. Regulation of Bone Development and Extracellular Matrix Protein Genes by RUNX2. *Cell and Tissue Research* **2010**, *339*, 189–195, doi:10.1007/s00441-009-0832-8.

144. Lui, J.C. Regulation of Body Growth by MicroRNAs. *Mol Cell Endocrinol* **2017**, *456*, 2–8, doi:10.1016/j.mce.2016.10.024.

145. Jee, Y.H.; Wang, J.; Yue, S.; Jennings, M.; Clokie, S.J.; Nilsson, O.; Lui, J.C.; Baron, J. Mir-374-5p, Mir-379-5p, and Mir-503-5p Regulate Proliferation and Hypertrophic Differentiation of Growth Plate Chondrocytes in Male Rats. *Endocrinology* **2018**, *159*, 1469–1478, doi:10.1210/en.2017-00780.

146. Nalluri, J.J.; Kamapantula, B.K.; Barh, D.; Jain, N.; Bhattacharya, A.; Almeida, S.S. De; Ramos, R.T.J.; Silva, A.; Azevedo, V.; Ghosh, P. DISMIRA: Prioritization of Disease Candidates in MiRNA-Disease Associations Based on Maximum Weighted Matching Inference Model and Motif-Based Analysis. *BMC Genomics* **2015**, *16 Suppl 5*, S12, doi:10.1186/1471-2164-16-S5-S12.

147. Scott, K.M.; Cohen, D.J.; Hays, M.; Nielson, D.W.; Grinstaff, M.W.; Lawson, T.B.; Snyder, B.D.; Boyan, B.D.; Schwartz, Z. Regulation of Inflammatory and Catabolic Responses to IL-1β in Rat Articular Chondrocytes by MicroRNAs MiR-122 and MiR-451. *Osteoarthritis Cartilage* **2021**, *29*, 113–123, doi:10.1016/j.joca.2020.09.004.

148. Godoy, P.M.; Barczak, A.J.; DeHoff, P.; Srinivasan, S.; Etheridge, A.; Galas, D.; Das, S.; Erle, D.J.; Laurent, L.C. Comparison of Reproducibility, Accuracy, Sensitivity, and Specificity of MiRNA Quantification Platforms. *Cell Rep* **2019**, *29*, 4212-4222.e5, doi:10.1016/j.celrep.2019.11.078.

149. Andrés-León, E.; Núñez-Torres, R.; Rojas, A.M. MiARma-Seq: A Comprehensive Tool for MiRNA, MRNA and CircRNA Analysis. *Sci Rep* **2016**, *6*, 25749, doi:10.1038/srep25749.

150. Robinson, M.D.; McCarthy, D.J.; Smyth, G.K. EdgeR: A Bioconductor Package for Differential Expression Analysis of Digital Gene Expression Data. *Bioinformatics* **2010**, *26*, 139–140, doi:10.1093/bioinformatics/btp616.

151. Core Team, R. R: A Language and Environment for Statistical Computing 2019, https://www.R-project.org/.

152. Auguie, B. Egg: Extensions for “Ggplot2”: Custom Geom, Custom Themes, Plot Alignment, Labelled Panels, Symmetric Scales, and Fixed Panel Size 2019, https://CRAN.R-project.org/package=egg.

153. Auguie, B. GridExtra: Miscellaneous Functions for “Grid” Graphics 2017, https://CRAN.R-project.org/package=gridExtra.

154. Wickham, H. Ggplot2: Elegant Graphics for Data Analysis 2016, https://ggplot2.tidyverse.org.

155. Ahlmann-Eltze, C. Ggsignif: Significance Brackets for “Ggplot2” 2019, https://CRAN.R-project.org/package=ggsignif.

156. Bache, S.M.; Wickham, H. Magrittr: A Forward-Pipe Operator for R 2014, https://CRAN.R-project.org/package=magrittr.

157. Graves, S.; Piepho, H.-P.; Selzer, L.; Dorai-Raj, S. MultcompView: Visualizations of Paired Comparisons 2015, https://CRAN.R-project.org/package=multcompView.

158. Komsta, L. Outliers: Tests for Outliers 2011, https://CRAN.R-project.org/package=outliers.

159. Wickham, H. The Split-Apply-Combine Strategy for Data Analysis. *Journal of Statistical Software* **2011**, *40*, 1–29, doi:10.18637/jss.v040.i01.

160. Maechler, M. Sfsmisc: Utilities from “seminar Fuer Statistik” ETH Zurich 2019, https://CRAN.R-project.org/package=sfsmisc.

161. Haimov, H.; Shimoni, E.; Brumfeld, V.; Shemesh, M.; Varsano, N.; Addadi, L.; Weiner, S. Mineralization Pathways in the Active Murine Epiphyseal Growth Plate. *Bone* **2020**, *130*, 115086, doi:10.1016/j.bone.2019.115086.

162. Christakos, S.; Ajibade, D. v.; Dhawan, P.; Fechner, A.J.; Mady, L.J. Vitamin D: Metabolism. *Endocrinology And Metabolism* **2010**, *39*, 243–253, doi:10.1016/j.ecl.2010.02.002.Vitamin.

163. Boyan, B.D.; Sylvia, V.L.; Dean, D.D.; Schwartz, Z. Vitamin D and Cartilage. In *Encyclopedia of Hormones*; Academic Press, 2003; pp. 592–598 ISBN 978-0-12-341103-7.

164. Sirajudeen, S.; Shah, I.; al Menhali, A. A Narrative Role of Vitamin D and Its Receptor: With Current Evidence on the Gastric Tissues. *Int J Mol Sci* **2019**, *20*, 3832, doi:10.3390/ijms20153832.

165. Maestro, M.A.; Molnár, F.; Mouriño, A.; Carlberg, C. Vitamin D Receptor 2016: Novel Ligands and Structural Insights. *Expert Opin Ther Pat* **2016**, *26*, 1291–1306, doi:10.1080/13543776.2016.1216547.

166. Masuyama, R.; Stockmans, I.; Torrekens, S.; van Looveren, R.; Maes, C.; Carmeliet, P.; Bouillon, R.; Carmeliet, G. Vitamin D Receptor in Chondrocytes Promotes Osteoclastogenesis and Regulates FGF23 Production in Osteoblasts. *Journal of Clinical Investigation* **2006**, *116*, 3150–3159, doi:10.1172/JCI29463.

167. Schwartz, N.; Verma, A.; Bivens, C.B.; Schwartz, Z.; Boyan, B.D. Rapid Steroid Hormone Actions via Membrane Receptors. *BBA - Molecular Cell Research* **2016**, *1863*, 2289–2298, doi:10.1016/j.bbamcr.2016.06.004.

168. Fleet, J.C. Vitamin D Receptors: Not Just in the Nucleus Anymore. *Nutr Rev* **1999**, *57*, 60–62, doi:10.1111/j.1753-4887.1999.tb01779.x.

169. Schwartz, Z.; Shaked, D.; Hardin, R.R.; Gruwell, S.; Dean, D.D.; Sylvia, V.L.; Boyan, B.D. 1alpha,25(OH)2D3 Causes a Rapid Increase in Phosphatidylinositol-Specific PLC-Beta Activity via Phospholipase A2-Dependent Production of Lysophospholipid. *Steroids* **2003**, *68*, 423–437, doi:10.1016/s0039-128x(03)00044-8.

170. Lisse, T.S.; Adams, J.S.; Hewison, M. Vitamin D and MicroRNAs in Bone. *Crit Rev Eukaryot Gene Expr* **2013**, *23*, 195–214, doi:10.1615/CritRevEukaryotGeneExpr.2013007147.

171. Boyan, B.D.; Schwartz, Z. 1,25-Dihydroxy Vitamin D3 Is an Autocrine Regulator of Extracellular Matrix Turnover and Growth Factor Release via ERp60-Activated Matrix Vesicle Matrix Metalloproteinases. *Cells Tissues Organs* **2009**, *189*, 70–74, doi:10.1159/000152916.

172. Rutter, L.; Moran Lauter, A.N.; Graham, M.A.; Cook, D. Visualization Methods for Differential Expression Analysis. *BMC Bioinformatics* **2019**, *20*, 458, doi:10.1186/s12859-019-2968-1.

173. McQuin, C.; Goodman, A.; Chernyshev, V.; Kamentsky, L.; Cimini, B.A.; Karhohs, K.W.; Doan, M.; Ding, L.; Rafelski, S.M.; Thirstrup, D.; et al. CellProfiler 3.0: Next-Generation Image Processing for Biology. *PLoS Biol* **2018**, *16*, e2005970, doi:10.1371/journal.pbio.2005970.

174. Kirsch, T.; Harrison, G.; Golub, E.E.; Nah, H.D. The Roles of Annexins and Types II and X Collagen in Matrix Vesicle-Mediated Mineralization of Growth Plate Cartilage. *J Biol Chem* **2000**, *275*, 35577–35583, doi:10.1074/jbc.M005648200.

175. Wuthier, R.E. Lipid Composition of Isolated Epiphyseal Cartilage Cells, Membranes and Matrix Vesicles. *BBA - Lipids and Lipid Metabolism* **1975**, *409*, 128–143, doi:10.1016/0005-2760(75)90087-9.

176. Dash, S.; Balasubramaniam, M.; Dash, C.; Pandhare, J. Biotin-Based Pulldown Assay to Validate MRNA Targets of Cellular MiRNAs. *Journal of Visualized Experiments* **2018**, doi:10.3791/57786.

177. Patro, R.; Duggal, G.; Love, M.I.; Irizarry, R.A.; Kingsford, C. Salmon Provides Fast and Bias-Aware Quantification of Transcript Expression. *Nat Methods* **2017**, *14*, 417–419, doi:10.1038/nmeth.4197.

178. Li, H. Minimap2: Pairwise Alignment for Nucleotide Sequences. *Bioinformatics* **2018**, *34*, 3094–3100, doi:10.1093/bioinformatics/bty191.

179. Love, M.I.; Huber, W.; Anders, S. Moderated Estimation of Fold Change and Dispersion for RNA-Seq Data with DESeq2. *Genome Biol* **2014**, *15*, 550, doi:10.1186/s13059-014-0550-8.

180. Weiner, J. Pca3d: Three Dimensional PCA Plots 2020.

181. Blighe, K.; Lun, A. PCAtools: Everything Principal Components Analysis 2021.

182. Chen, H. VennDiagram: Generate High-Resolution Venn and Euler Plots 2018.

183. Mi, H.; Ebert, D.; Muruganujan, A.; Mills, C.; Albou, L.P.; Mushayamaha, T.; Thomas, P.D. PANTHER Version 16: A Revised Family Classification, Tree-Based Classification Tool, Enhancer Regions and Extensive API. *Nucleic Acids Research* **2021**, *49*, D394–D403, doi:10.1093/nar/gkaa1106.